

NUREG/CR-2127  
PNL-3801-1  
Vol. 1

---

---

# Reactor Safety Research Programs

Quarterly Report  
January - March 1981



---

Prepared by S. K. Edler, Ed.

Pacific Northwest Laboratory  
Operated by  
Battelle Memorial Institute

Prepared for  
U.S. Nuclear Regulatory  
Commission

8107310549 810731  
PDR NUREG  
CR-2127 R PDR

NOTICE

This report was prepared as an account of work sponsored by an agency of the United States Government. Neither the United States Government nor any agency thereof, or any of their employees, makes any warranty, expressed or implied, or assumes any legal liability or responsibility for any third party's use, or the results of such use, of any information, apparatus product or process disclosed in this report, or represents that its use by such third party would not infringe privately owned rights.

Available from

GPO Sales Program  
Division of Technical Information and Document Control  
U. S. Nuclear Regulatory Commission  
Washington, D. C. 20555

Printed copy price: \$4.75

and

National Technical Information Service  
Springfield, Virginia 22161

---

# Reactor Safety Research Programs

Quarterly Report  
January - March 1981

---

Manuscript Completed: May 1981  
Date Published: July 1981

Prepared by  
S. K. Edler, Ed.

Pacific Northwest Laboratory  
P. O. Box 999  
Richland, WA 99352

Prepared for  
Division of Accident Evaluation  
Division of Engineering Technology  
Office of Nuclear Regulatory Research  
U.S. Nuclear Regulatory Commission  
Washington, D.C. 20555  
NRC FINs B2101, B2088, B2289  
B2043, B2383, B2084, B2372  
B2084, B2041, B2277, B2097

## ABSTRACT

This document summarizes the work performed by Pacific Northwest Laboratory (PNL) from January 1 through March 31, 1981, for the Division of Reactor Safety Research within the U.S. Nuclear Regulatory Commission (NRC). Evaluations of nondestructive examination (NDE) techniques and instrumentation are reported; areas of investigation include demonstrating the feasibility of determining the strength of structural graphite, evaluating the feasibility of detecting and analyzing flaw growth in reactor pressure boundary systems, examining NDE reliability and probabilistic fracture mechanics, and assessing the integrity of pressurized water reactor (PWR) steam generator tubes where service-induced degradation has been indicated. Experimental data and analytical models are being provided to aid in decision-making regarding pipe-to-pipe impacts following postulated breaks in high-energy fluid system piping. Core thermal models are being developed to provide better digital codes to compute the behavior of full-scale reactor systems under postulated accident conditions. Fuel assemblies and analytical support are being provided for experimental programs at other facilities. These programs include loss-of-coolant accident (LOCA) simulation tests at the NRU reactor, Chalk River, Canada; fuel rod deformation, severe fuel damage, and postaccident coolability tests for the ESSOR reactor Super Sara Test Program, Ispra, Italy; the instrumented fuel assembly irradiation program at Halden, Norway; and experimental programs at the Power Burst Facility, Idaho National Engineering Laboratory (INEL). These programs will provide data for computer modeling of reactor system and fuel performance during various abnormal operating conditions.



## CONTENTS

ABSTRACT . . . . .	iii
GRAPHITE NONDESTRUCTIVE TESTING . . . . .	1
ACOUSTIC EMISSION/FLAW RELATIONSHIP FOR IN-SERVICE MONITORING OF NUCLEAR PRESSURE VESSELS . . . . .	5
INTEGRATION OF NONDESTRUCTIVE EXAMINATION RELIABILITY AND FRACTURE MECHANICS . . . . .	17
EXPERIMENTAL SUPPORT AND DEVELOPMENT OF SINGLE-ROD FUEL CODES: TASK A - IRRADIATION EXPERIMENTS . . . . .	33
EXPERIMENTAL SUPPORT AND DEVELOPMENT OF SINGLE-ROD FUEL CODES: TASK B - DATA QUALIFICATION AND ANALYSIS . . . . .	39
EXPERIMENTAL SUPPORT AND DEVELOPMENT OF SINGLE-ROD FUEL CODES: TASK C - CODE COORDINATION AND EX-REACTOR TESTING . . . . .	45
EXPERIMENTAL SUPPORT AND DEVELOPMENT OF SINGLE-ROD FUEL CODES: TASK D - PELLET-CLADDING INTERACTION EXPERIMENTS . . . . .	49
PIPE-TO-PIPE IMPACT . . . . .	53
SEVERE CORE DAMAGE TEST SUBASSEMBLY PROCUREMENT PROGRAM - PBF SEVERE FUEL DAMAGE PROJECT . . . . .	59
SEVERE CORE DAMAGE TEST SUBASSEMBLY PROCUREMENT PROGRAM - ESSOR PROJECT . . . . .	75
SEVERE CORE DAMAGE TEST SUBASSEMBLY PROCUREMENT PROGRAM - NINE-ROD TEST TRAIN FOR OPTRAN 1-3 PROJECT . . . . .	77
CORE THERMAL MODEL DEVELOPMENT . . . . .	87
LOCA SIMULATION IN NRS . . . . .	101
STEAM GENERATOR TUBE INTEGRITY . . . . .	103

## FIGURES

### ACOUSTIC EMISSION/FLAW RELATIONSHIP FOR IN-SERVICE MONITORING OF NUCLEAR PRESSURE VESSELS

1	Test Specimen - KS07 Degraded Steel . . . . .	8
2	Sensor Layout for ZB-1 Test Vessel . . . . .	9
3	Sensor Layout for A533B Insert in ZB-1 Test Vessel . . . . .	10
4	Acoustic Emission Results from Irradiated Fracture Specimen 61-W . . . . .	14

### INTEGRATION OF NONDESTRUCTIVE EXAMINATION RELIABILITY AND FRACTURE MECHANICS

1	Fatigue Crack Growth Rate Data for Ferritic Steel as Compiled in Reference 1 . . . . .	21
2	Fatigue Crack Growth Rate Data for Stainless Steel as Compiled in Reference 1 . . . . .	22
3	Fatigue Crack Growth Rate Data for Stainless Steel as Compiled in Reference 2 . . . . .	23
4	Effect of Vibrational Frequency on Critical Flaw Size . . . . .	25
5	Effect of Aspect Ratio of ID Surface Flaw on Critical Flaw Size for Vibrational Stresses . . . . .	26
6	Effect of Threshold $\Delta K$ Behavior on Critical Flaw Size for Vibrational Stress . . . . .	27
7	Comparison of Ferritic and Stainless Steel Threshold $\Delta K$ Behavior on Critical Flaw Size for Vibrational Stress . . . . .	28

### EXPERIMENTAL SUPPORT AND DEVELOPMENT OF SINGLE-ROD CODES:

#### TASK A - IRRADIATION EXPERIMENTS

1	Pressures for Rods 1, 2, and 3 of Instrumented Fuel Assembly (IFA)-527 from December 12-22, 1980 . . . . .	35
2	Lower Centerline Temperatures for Rods 1, 2, and 3 of Instrumented Fuel Assembly (IFA)-527 from December 12-22, 1980 . . . . .	36

EXPERIMENTAL SUPPORT AND DEVELOPMENT OF SINGLE-ROD FUEL CODES:  
 TASK B - DATA QUALIFICATION AND ANALYSIS

1	Comparison of Data Scatter and Calculated Centerline Temperature Bounds for Instrumented Fuel Assembly (IFA)-527 . . . . .	43
---	--	----

PIPE-TO-PIPE IMPACT

1	Pneumatic-Powered Pipe Accelerator Conceptual Design . . . . .	57
---	--	----

SEVERE CORE DAMAGE TEST SUBASSEMBLY PROCUREMENT PROGRAM - PBF SEVERE FUEL DAMAGE TEST PROJECT

1	Sealed Shroud System Utilizing ZrO <sub>2</sub> Fiberboard Insulation and ZrO <sub>2</sub> Tube Supports . . . . .	64
2	Sealed Shroud System with ZrO <sub>2</sub> Fiberboard Insulator and Pressure Equalization System . . . . .	65
3	Peak Assembly Temperature Versus Power for the Low Thermal Conductivity Shroud . . . . .	67
4	Peak Assembly Temperature Versus Power for the High Thermal Conductivity Shroud . . . . .	68
5	Assembly Peak Temperature and Metal-Water Reaction Heating Rate Versus Time for the Baker-Just Correlation . . . . .	71
6	Assembly Peak Temperature and Metal-Water Reaction Heating Rate Versus Time for the Cathcart Correlation . . . . .	72

SEVERE CORE DAMAGE TEST SUBASSEMBLY PROCUREMENT PROGRAM - NINE-ROD TEST TRAIN FOR OPTRAN 1-3 PROJECT

1	Modular Design of the Nine-Rod Fuel Bundle Assembly . . . . .	78
2	Lower Part of Test Train . . . . .	79
3	Upper Part of Test Train . . . . .	79
4	Remote Assembly of Test Train Using Strongback . . . . .	80
5	Lower End of Strongback with Partially Assembled Test Train . . . . .	80
6	Exploded View of Flow Restrictor Seal . . . . .	81

7	Zircaloy Shroud Clamped in Shroud Fixture . . . . .	82
8	Close-Up of C-Seal in Dovetail Corner Joint of Shroud . . . . .	83
9	Lower End of Core Region of Test Train . . . . .	83
10	Catch Screen in Position Near Top of Test Train . . . . .	84

CORE THERMAL MODEL DEVELOPMENT

1	Liquid Mass Velocity Versus Time . . . . .	91
2	Collapsed Liquid Level Versus Time . . . . .	92
3	Steam Generation Rate Versus Time . . . . .	93
4	Westinghouse Drain Test No. 5, Upper Head Fluid Level Versus Time . . . . .	94
5	Computed and Experimental Temperature Versus Time Plot at an Axial Level of 74 in. . . . .	97
6	Computed and Experimental Temperature Versus Time Plot at an Axial Level of 96 in. . . . .	97
7	Lower Plenum Liquid Volume Versus Time Plot for Test 501 . . . . .	99
8	Lower Plenum Liquid Volume Versus Time Plot for Test 404 . . . . .	100

STEAM GENERATOR TUBE INTEGRITY

1	Cast-in-Place Tower Portion of Steam Generating Examination Facility . . . . .	106
2	View of Tower Showing Foundation Forms for Support Building Portion of Facility . . . . .	107
3	View into Tower Showing Depth of Excavation and Generator Support Pad . . . . .	108

TABLES

GRAPHITE NONDESTRUCTIVE TESTING

1 Elemental Composition of Graphite Ash in Atomic Percent . . . .	4
---	---

INTEGRATION OF NONDESTRUCTIVE EXAMINATION RELIABILITY AND FRACTURE MECHANICS

1 Assessment of Crack Growth Rates and Vibrational Frequencies . . . . .	20
--	----

EXPERIMENTAL SUPPORT AND DEVELOPMENT OF SINGLE-ROD FUEL CODES:  
TASK B - DATA QUALIFICATION AND ANALYSIS

1 burnup for Instrumented Fuel Assembly (IFA)-432 as of February 7, 1981 . . . . .	41
--	----

PIPE-TO-PIPE IMPACT

1 Pipe-to-Pipe Impact Program Initial Test Matrix . . . . .	55
---	----

SEVERE CORE DAMAGE TEST SUBASSEMBLY PROCUREMENT PROGRAM - PBF SEVERE FUEL  
DAMAGE TEST PROJECT

1 Evaluation of Various Candidate Shroud Insulation Types . . . . .	63
---	----

CORE THERMAL MODEL DEVELOPMENT

1 Battelle Columbus Downcomer Test Conditions . . . . .	98
---	----

## GRAPHITE NONDESTRUCTIVE TESTING(a)

W. C. Morgan, Project Manager  
T. J. Davis, Project Manager

M. T. Thomas

### SUMMARY

During this quarter the new computer program, ZFIT, was tested and refined using eddy current measurements from samples with known oxidation; the results are quite encouraging. The frequency range for use of the ultrasonic backscattering technique in PGX graphite was determined, design criteria were established for the sensors, and procurement of two types of sensor elements was initiated.

### INTRODUCTION

This is a continuation of previous work at Pacific Northwest Laboratory (PNL) that demonstrated the feasibility of monitoring changes in the compressive strength of oxidized graphite by measuring changes in the velocity of an ultrasonic wave propagated through the graphite. The fiscal year (FY)-1981 scope of this project is to

- develop eddy current techniques for near-surface profiling of oxidation in the Fort St. Vrain PGX core support blocks, including initiation of a prototype system development leading to interpretable indications of graphite strength
- complete assessment of ability to profile oxidation using ultrasonic surface waves; determine technical feasibility of using ultrasonic backscattering techniques to find in-depth oxidation profiles; continue evaluation of high-power ultrasonic tests and acoustic imaging techniques for bulk oxidation measurements as appropriate

---

(a) RSR FIN Budget No.: 62101-1; RSR Contact: R. B. Foulds.

- as funds permit, outline development of predictive techniques for oxidation depth profiles under reactor environments to provide strength indications for large graphite components.

The objective of this investigation is to demonstrate the feasibility of nondestructive testing (NDT) techniques for in-service monitoring of structural graphite strength to be applied initially to the Fort St. Vrain reactor.

### TECHNICAL PROGRESS

#### EDDY CURRENT TESTING

Work during the reporting period centered upon evaluation and refinement of our computer algorithm, ZFIT, for estimating near-surface graphite oxidation from multifrequency eddy current data.

Simulated oxidation profiles were formed by stacking thin graphite plates of known oxidation. Eddy current data were taken at test frequencies of 100 kHz, 1 MHz, and 4 MHz using both single plates and stacks of up to four plates. The program began by calculating conductivities of single plates from the multifrequency measurement data. This best-fit conductivity was then used to back-calculate the eddy current data for each frequency that would be expected from the individual plates. An average error of 10% was observed between calculated and measured values with one worst-case error of 34%. We feel that these are reasonable levels of error for initial attempts; but efforts are continuing to identify the source of the errors.

This specialized use of eddy current instrumentation has required that some new technical ground be covered because it is necessary for the instrument to output precise values for resistive and reactive impedances of the search coil. These impedances must be calibrated for each frequency so that the data may be fed directly to the ZFIT program. In contrast, conventional eddy current instrumentation deals with relating output voltages to various calibration specimens; moreover, substantial errors in linearity and orthogonality of the instrument can be tolerated. Our present work on the instrument covers the following areas:

- verifying linearity
- verifying orthogonality (independence, or  $90^{\circ}$  separation, between resistance and reactance)
- obtaining samples of graphite with known conductivity so that an error correction program can be developed and used in the computer.

#### ULTRASONIC TESTING

Tests were conducted to arrive at an initial design for an ultrasonic sensor to perform backscatter measurements in graphite. The tests indicated that a frequency range of 200 to 800 kHz will be required for backscatter measurements in PGX graphite. Above 600 kHz attenuation of ultrasonic energy in unoxidized PGX increases rapidly as the frequency increases. The upper transmission frequency response of oxidized graphite is substantially less. Procurement was initiated on two types of piezoelectric sensors, both of which can be used with or without ultrasonic delay lines. The delay lines would aid in assessing near-surface oxidation.

Both types of piezoelectric sensor elements (barium titanate and lead metaniobate) will be evaluated to determine which is best suited for backscatter testing. One or both of the sensors will then be used to establish a final correlation between ultrasonic backscattering measurements and oxidation.

#### OXIDATION

The elemental compositions of ash remaining after oxidation of samples of five grades of graphite were determined by x-ray photoelectron spectroscopy (XPS). The compositions, shown in Table 1, vary considerably between grades. This is consistent with the wide variation in visual appearance, texture, and color of the ash. A paper based on this work will be submitted for presentation at the Fifteenth Conference on Carbon (June 22-26, 1981).



TABLE 1. Elemental Composition of Graphite Ash in Atomic Percent

Sample	Total Ash, ppm	Si	Ca	Ba	Fe	Sn	P	K	Al	S	Ti	Na
2020	970	18.5	18.8	1.0	-	0.1	2.8	1.3	1.3	0.8	0.3	-
S1090	1030	9.4	15.4	0.4	-	0.1	1.0	0.8	-	14.6	-	-
PGX	3820	1.1	6.6	0.5	3.0	0.1	0.6	2.4	23.0	5.7	0.9	1.2
ATJ	880	13.3	23.6	1.5	-	0.1	2.4	0.8	-	0.8	-	-
P3W	2410	33.5	3.8	0.2	2.7	0.1	0.8	0.9	-	-	-	-

#### FUTURE WORK

##### EDDY CURRENT TESTING

- complete development of the profiling algorithm
- test the algorithm using large oxidized samples.

##### ULTRASONIC TESTING

- combine new sensors with ultrasonic waveform averaging instrumentation to obtain backscatter measurements
- evaluate the ability of ultrasonic backscattering to accurately quantify graphite oxidation.

ACOUSTIC EMISSION/FLAW RELATIONSHIP FOR IN-SERVICE  
MONITORING OF NUCLEAR PRESSURE VESSELS<sup>(a)</sup>

P. H. Hutton, Project Manager  
R. J. Kurtz, Assistant Project Manager

T. T. Taylor  
J. R. Skorpik  
P. G. Doctor  
D. K. Lemon  
R. B. Melton

SUMMARY

Fabrication of the A533B insert for the ZB-1 German vessel test is about 50% completed and is no longer a critical path item. Testing of the degraded KS07 steel that will be inserted in the ZB-1 vessel shows that the acoustic noise under cyclic load is significant but not prohibitive for effective monitoring of the A533B insert. An acoustic emission (AE) sensor location diagram has been supplied to Materialprüfungsanstalt (MPA), Stuttgart, West Germany, for incorporation in the overall ZB-1 vessel instrumentation plan; and electronic simulation of reactor background noise from inside the ZB-1 vessel is being investigated.

A planning meeting for installing an AE system on the Watts Bar, Unit 1 reactor was held with the Tennessee Valley Authority (TVA). A detailed installation plan is in process.

A differential wave-guide sensor/preamplifier combination has been tested and can function up to 250<sup>0</sup>F, which should be adequate for reactor monitoring.

The AE system for monitoring the German ZB-1 vessel test and for reactor monitoring was assembled; system testing has begun.

---

(a) RSR FIN Budget No.: B2088; RSR Contact: J. Muscara.

Detection of flaws during welding using AE has been successfully demonstrated at Oberhausen, Germany. Evaluation of AE results versus conventional nondestructive testing (NDT) and destructive examination is in progress.

AE monitoring of the first 4T irradiated fracture specimen test at the Naval Research Laboratory (NRL) showed reasonable correlation between AE and crack growth. Thorough analysis of the data is yet to be done.

### INTRODUCTION

The purpose of this Pacific Northwest Laboratory (PNL) program is to provide an experimental evaluation of the feasibility of detecting and analyzing flaw growth in reactor pressure boundaries on a continuous basis using AE. Type A533B, Class 1 steel is being used in all experimental testing. Objectives of this program are to:

- develop a method to identify crack growth AE signals in the presence of other acoustic signals
- develop a relationship to estimate flaw significance from AE data
- develop an instrument system to implement these techniques
- demonstrate the total concept off-reactor and on-reactor.

Progress relative to these objectives is discussed in the following sections on off-reactor vessel test, reactor installation, AE monitor system development, sensor development, weld monitor demonstration, irradiated fracture specimen tests, and reports. The final section describes work planned for the next quarter.

### TECHNICAL PROGRESS

#### OFF-REACTOR VESSEL TEST

Fabrication of the A533B steel insert for the ZB-1 vessel test began in late December 1980 under a contract with MPA. Stress relief heat treatment and

machining of the insert to shape from material supplied by PNL has been completed. One outside and two inside flaws still have to be machined and fatigue precracked. The A533B insert is no longer a critical path item for vessel preparation since fabrication work on the ZB-1 vessel has been delayed awaiting Bundesministerium fuer Forschung und Technologie (BMFT) authorization.

A 30-3/4 x 6 x 4 in. sample of the intentionally degraded German KS07 steel insert for the ZB-1 vessel was obtained from MPA for AE characterization tests. The sample was cut into three subplates: two were 30-3/4 x 6 x 1 in. and the third was 30-3/4 x 6 x 1.6 in. Figure 1 shows a scale drawing of the top and bottom surfaces of subplate KS07 CBCABBB. The dotted lines in the drawing outline the plate tension test specimen that was machined from the subplate. The central portion of the plate was heavily cracked, but the last 5-1/2 in. on each end showed a much lower defect density. The plate tension specimen in Figure 1 was approximately 1 in. thick by 2.5 in. wide in the gage section region. Two size 2T compact tension specimens were machined from the low-defect ends of the other 1-in. thick subplate to study the AE response of the KS07 material when only one macroscopic crack is present. The last subplate was machined to a 1.5 in. thickness for later testing.

The plate tension specimen was tested in tension-tension fatigue loading at a frequency of 10 cpm, an R-ratio of 0.1, and in room temperature laboratory air. A three-sensor AE system (one sensor at each end and one in the middle of the test section) was used to monitor the specimen. With this arrangement, the test section could be divided into two isolation zones. Since the objective of the test was to investigate the amount of acoustic output from the cracks under cyclic load, no effort was made to focus on a single crack. In practice, only one-half of the section could be monitored because signals would not propagate the full length of the section effectively due to the abundance of cracks. The area that was monitored contained the crack that caused specimen failure.

Using the AE test results for fatigue cycling over the nominal gross stress range of 7.47 ksi and allowing for volumetric considerations, the predicted event rate for the KS07 vessel insert would be about 13 events/sec. Although this would represent an interference with monitoring the A533B insert, it does not appear prohibitive. Source location/source isolation should allow



FIGURE 1. Test Specimen - KS07 Degraded Steel

separating the acoustic signals from the KS07 insert and that data rate would not saturate the AE monitor system. MPA is also considering using a less seriously degraded material for the insert.

Sensor location diagrams for AE monitoring of the ZB-1 vessel have been supplied to MPA (see Figures 2 and 3) and will be used to prepare an instrumentation plan that will include the needs of all test participants.

Electronic simulation of reactor background noise using transducers on the inside of the vessel is being investigated. If the appropriate noise spectrum can be achieved at the outer surface of the vessel, it will provide a less costly and more controllable means of simulating reactor noise.

#### REACTOR MONITORING

Agreement has been reached with TVA to install an AE system on the Watts Bar, Unit 1 reactor by September 1981. PNL and U.S. Nuclear Regulatory Commission (NRC) personnel visited the site on January 20-22, 1981, to make

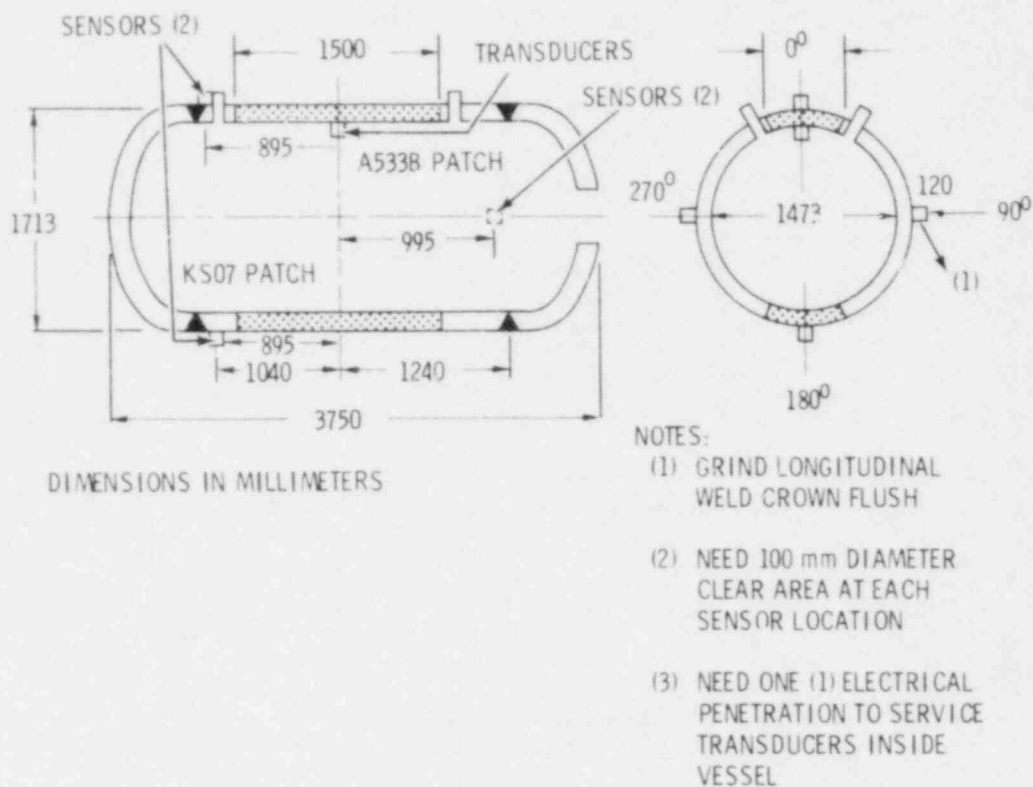


FIGURE 2. Sensor Layout for ZB-1 Test Vessel

preliminary determinations on locations to monitor, identify problem areas, and determine timing requirements. The following locations were selected for monitoring:

- #2 inlet nozzle
- #2 cold leg pipe
- a 10-in. accumulator line that tees in a #2 cold leg; some type of crack growth specimen will be installed on the surface of the 10-in. pipe
- a segment of the vessel cylinder with the included portion of the fabrication girth weld.

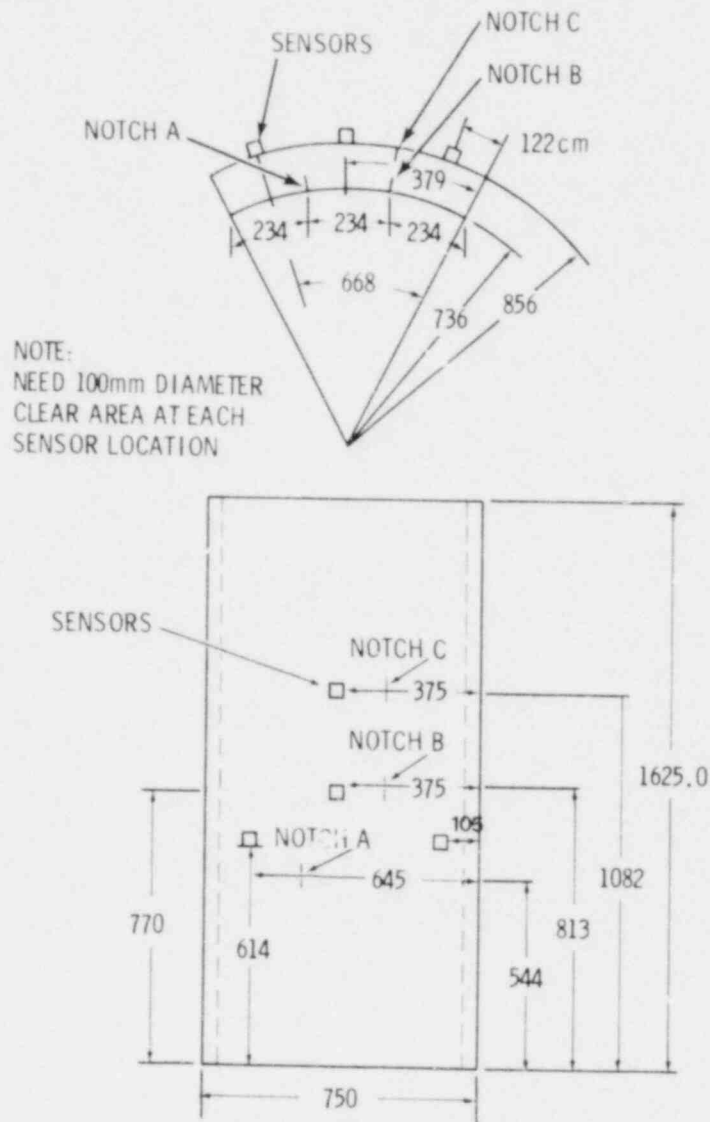


FIGURE 3. Sensor Layout for A533B Insert in ZB-1 Test Vessel (dimensions in millimeters)

Current work is concentrating on preparing a test plan (including specific sensor locations and sensor mounting methods) and on resolving questions concerning containment penetrations for signal leads and compatibility of system components for use in containment.

### SENSOR SYSTEM IMPROVEMENTS

A differential sensor/preamplifier combination that will improve common-mode noise (electromagnetic and ground loop generated) rejection has been designed and tested in the laboratory. This work is pertinent to both the ZB-1 vessel test and reactor monitoring.

The effect of high temperature on the sensor/amplifier system has been evaluated. The amplifier experienced only a 5% drop in output voltages between 70 and 250°F, but at 300°F the amplifier ceased working. In subsequent temperature tests, the amplifier functioned properly between 70 and 200°F.

The sensors showed some change in spectral response between 70 and 300°F although the variations are acceptable. All three sensors tested withstood repeated thermal cycling. In one case, the oven was opened and pressure was applied to the hot PZT element to determine that it was still securely bonded to the alumina disk.

In summary, the present sensor/amplifier combination can operate safely to 250°F. If temperatures of 300°F are experienced, the performance of these amplifiers will be degraded. Although present amplifiers use standard transistors, mil-spec transistors will be used in the future to improve high-temperature performance.

### AE MONITOR SYSTEM

The AE monitor system for vessel testing and reactor monitoring has been assembled and is ready for testing.

Implementation of pattern recognition software on the PDP 11/03 computer was completed. The wave-guide data from the heavy section cylindrical bend test were analyzed, and a set of feature weights was computed to separate valid AE from noise. The features used to calculate these weights were taken from the power spectral density estimate and include the mean power and its standard deviation along with the relative power and first two statistical moments in



100-kHz bands from 200 to 800 kHz. Thus, a total of 20 features are currently being used. These weights resulted in the classification matrix shown below:

			COMPUTED CLASS	
			1	2
T R U E	C L A S S	1	213 93.0%	16 7.0%
		2	53 19.6%	217 80.4%

where class 1 is valid AE and class 2 is noise from all sources. The software is now in place on the PDP 11/03; data can be transferred from the D/E 1032 system data files to the 11/03, waveform tapes and data files can be processed, or waveform tapes alone can be processed. A user's manual has been written for this software.

A signal identification or numbering method is yet to be installed although it has been designed, and selection of a graphics output is yet to be completed. These items do not preclude performance testing of the system, which has begun and includes:

- testing system operation on 110-V, 50-Hz power
- introducing signals into the system from tape to verify that the sub-systems function as an integrated system
- installing the system on a cylindrical vessel where AE signals as well as artificial signals can be generated to verify system performance.

#### DEMONSTRATION OF WELD MONITORING USING AE

The weld flaw AE detection/analysis system developed by GARD, Inc., for NRC has been demonstrated to the German technical community under the auspices of this program. The test was performed the week of February 16 at Oberhausen, West Germany. Initial results indicate that the demonstration was very successful; 16 flaws (small cracks, large cracks, porosity, and slag inclusions) were induced in the submerged arc weld, which was 1350 mm long by 250 mm thick. The material was German KS15 pressure vessel steel. The AE system apparently

detected and correctly classified all crack and slag inclusion flaws; porosity was detected, but classification was not as consistent as with the other flaws.

The total weld will be inspected by radiography and ultrasonic methods for comparison of flaw indications with AE results. A section of the weld about 300 mm long will be destructively examined at MPA for positive determination of flaw description and location. Evaluation of this portion of the test is expected to be completed by the end of June 1981. The balance of the weld (approximately 1000 mm) will become one of the specimens to be examined under the PISC II Program. Results from this program will not be available for two to three years.

#### HEAVY SECTION STEEL TECHNOLOGY (HSST) IRRADIATED FRACTURE SPECIMENS

Fracture testing of unirradiated and irradiated weld specimens under the HSST program provides a rare opportunity to gain insight on the effect of irradiation on AE during crack growth. Testing of a dummy specimen at NRL has been AE monitored to verify the technique and identify problems. This test showed that the basic technique was satisfactory; however, there is a severe transient noise problem associated with the test facility. Modification of the monitor system to use differential sensors alleviated the problem significantly.

The first irradiated 4T specimen test (61-W) was conducted on February 22, 1981, and produced the AE results shown in Figure 4. Although some problems were experienced with the differential preamplifiers used on this test, the AE data show reasonable consistency with crack growth. A more thorough analysis will be done to relate AE to fracture mechanics parameters.

Current plans are to monitor a minimum of two more 4T irradiated specimens and companion unirradiated specimens.

#### REPORTS

- quarterly progress report for the period October 1-December 31, 1980
- midyear review report - February 25, 1981.

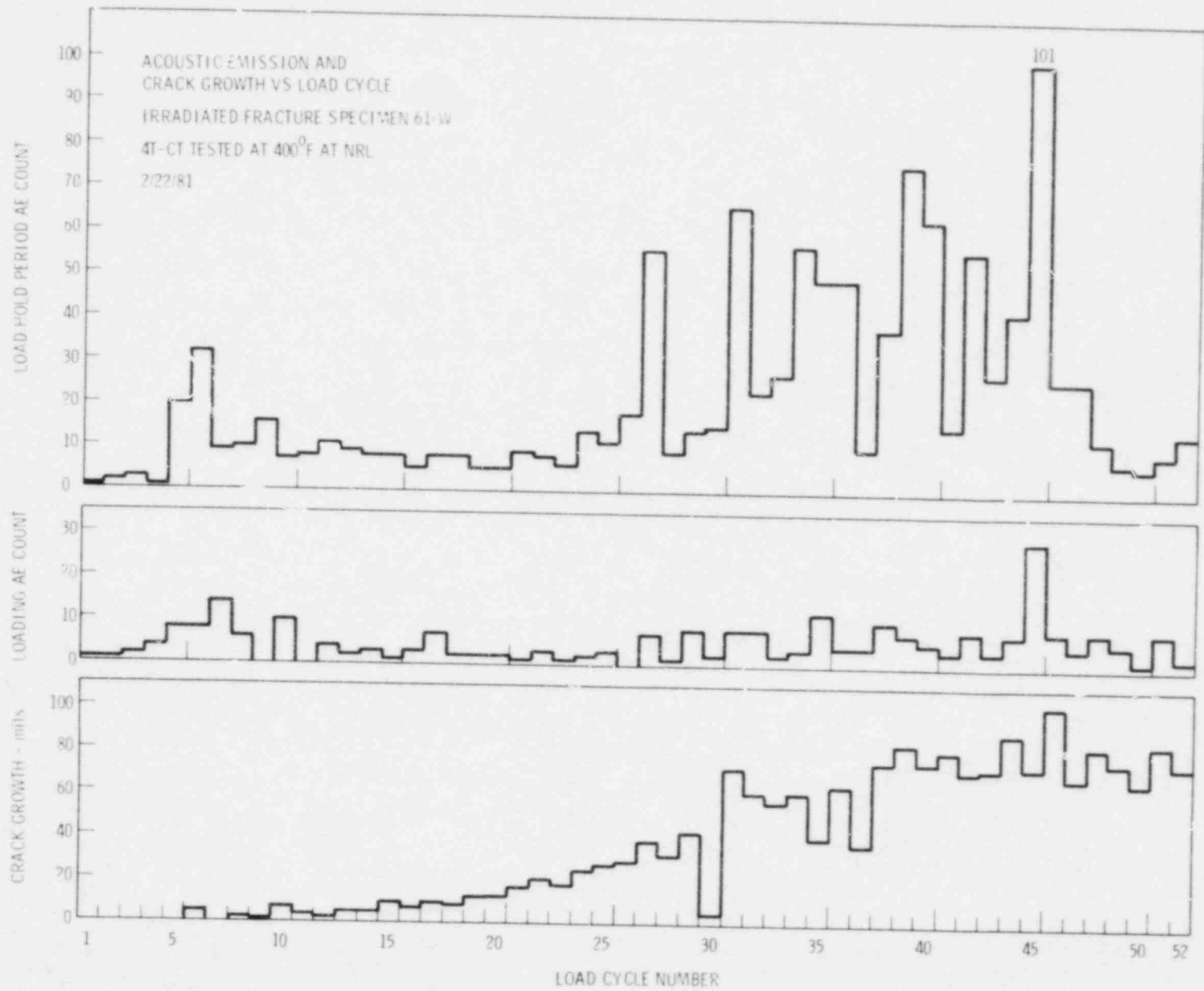


FIGURE 4. Acoustic Emission Results from Irradiated Fracture Specimen 61-W

### FUTURE WORK

Plans for the period from April 1 to June 30, 1981, are to:

- complete the vessel test plan and hold a test planning meeting with MPA, Stuttgart
- complete the Watts Bar, Unit 1 AE instrumentation plan and review it with TVA
- continue monitoring HSST irradiated fracture test specimens
- complete testing of AE monitor system
- complete first-phase evaluation of AE/weld monitor demonstration results.

INTEGRATION OF NONDESTRUCTIVE EXAMINATION  
RELIABILITY AND FRACTURE MECHANICS<sup>(a)</sup>

F. L. Becker, Program Manager  
S. H. Bush, Project Manager  
F. A. Simonen, Project Manager

S. R. Doctor  
G. B. Dudder  
P. G. Heasler  
G. P. Selby

SUMMARY

Principal accomplishments during the past quarter have included a fracture mechanics evaluation of the influence of vibrational stresses, completion and evaluation of 90% of the crack samples required for the round robin, and completion of several instrument evaluation tasks. All of the crack samples required for the upcoming round robin have been completed with the exception of the smallest flaw sizes for the intergranular stress corrosion cracks (IGSCC).

INTRODUCTION

The primary piping systems of nuclear power plants are inspected in-service according to the rules of the ASME Boiler and Pressure Vessel Code, Section XI (Rules for In-Service Inspection of Nuclear Power Plant Components). Ultrasonic techniques are normally used for these inspections, which are periodically performed on a sampling of pipe joints.

The Integration of Nondestructive Examination (NDE) Reliability and Fracture Mechanics Program at Pacific Northwest Laboratory (PNL) has been established to determine the reliability of current in-service inspection (ISI) techniques and to develop recommendations that will assure a suitably high inspection reliability. The objectives of this program are to:

---

(a) RSR FIN Budget No.: 82289-0; RSR Contact: J. Muscara.

- determine the reliability of ultrasonic ISI performed on commercial light water reactor (LWR) primary piping systems
- using fracture mechanics analysis, determine the impact of NDE unreliability on system safety and determine the level of inspection reliability required to assure a suitably low failure probability
- evaluate the degree of reliability improvement that could be achieved using improved and advanced NDE techniques
- based on material, service, and NDE uncertainties, formulate recommended revisions to ASME Code, Section XI, and Regulatory Requirements needed to assure suitably low failure probabilities.

The scope of this program is limited to ISI of primary piping systems, and the results and recommendations are also applicable to Class II piping systems. Programs currently in progress concerning inspection reliability of pressure vessels are also being monitored and evaluated.

#### TECHNICAL PROGRESS

The progress and accomplishments of the past quarter are described below by task.

#### TASK 4 - FRACTURE MECHANICS: EVALUATION OF VIBRATIONAL STRESSES ON PIPING INTEGRITY

The presence of even relatively low levels of vibrational stresses can have potentially serious consequences on piping integrity. Results of the Battelle Columbus Laboratories (BCL) cold leg integrity study were in many respects governed by vibrational stress levels.<sup>(1)</sup> In the BCL work a vibrational stress of 1.0 ksi at 1000 cycles per minute (cpm) was assumed to be present in all cases. Study of their crack growth rate predictions suggests that vibrational stresses have an "all or nothing" type of effect. Once an inside diameter (ID) surface defect grew to a critical depth (this growth being due to other loading transients), the vibrational stress resulted in a very rapid failure of the pipe at the location of concern. The analysis described

below is an attempt to explain the results of the BCL study and to develop an alternate method of treating crack growth due to vibrational stresses.

Lacking data from the reactor system vendors, BCL assumed the 1.0-ksi cyclic stress at 1000 cpm. Subsequent comments from vendors have indicated that although such a stress may not be a common occurrence it is not an unrealistic condition corresponding, for example, to operation of a pump with a bad bearing. Another questionable aspect of the BCL work is the treatment of fatigue crack growth (FCG) in the low  $\Delta K$  regime and possible errors in the treatment of threshold  $\Delta K$  crack growth behavior.

#### Frequencies and Growth Rates of Interest

It is of interest to consider the implications of BCL's 1000-cpm vibrational stress frequency and crack growth rate of  $10^{-8}$  in./cycle (ferritic steel) at the threshold  $\Delta K$  values of 2.58 ksi  $\sqrt{\text{in}}$ . The time to grow a crack a significant increment in the wall of a primary coolant pipe (e.g., 2.5 in. thick) can be estimated: for example, the time for a 1.0-in. increment in crack growth at 1000 cpm and  $10^{-8}$  in./cycle is

$$\text{Time} \leq \frac{a}{da/dN} \left( \frac{1}{f} \right) = \frac{1.0 \text{ in.}}{10^{-8} \text{ in./cycle}} \times \frac{1}{1000 \text{ cpm}}$$

$$\text{Time} \leq 10^5 \text{ min (2.3 months)}$$

This clearly shows that the BCL calculations by the nature of their assumptions will predict rapid failure by vibration once the fatigue threshold is exceeded.

It is also of interest to establish other combinations of vibrational frequencies and threshold crack growth rates that will lead to rapid pipe failure. Rapid failure is viewed as failure in a time period that is brief relative to the ASME Section XI 10-yr inspection interval. Table 1 shows the time to grow a crack 1.0 in. for frequencies ranging from 100 to 10,000 cpm (1.7 to 1700 Hz) and crack growth rates of  $10^{-10}$  to  $10^{-6}$  in./cycle.

TABLE 1. Assessment of Crack Growth Rates and Vibrational Frequencies

Crack Growth Rate, in./cycle	Time to Grow 1.0-in. Crack, yr		
	100 cpm	1,000 cpm	10,000 cpm
$10^{-10}$	200.0	20.0	2.0
$10^{-9}$	20.0	2.0	0.2
$10^{-8}$	2.0	0.2	0.02
$10^{-7}$	0.2	0.02	0.002
$10^{-6}$	0.02	0.002	0.0002

Table 1 indicates that crack growth rates much below  $10^{-9}$  in./cycle are unlikely to lead to significant crack growth. Thus, in developing FCG data one needs to establish the minimum  $\Delta K$  required to grow a crack at a rate of say  $10^{-9}$  to  $10^{-8}$  in./cycle and treat this value as a threshold  $\Delta K$ , even though it may not truly be a threshold. Vibrations at low frequencies (100 cpm or about 2 Hz) can quickly give a sufficient number of stress cycles to result in failure in a time period less than the ASME ISI interval (see Table 1).

#### Crack Growth Data

To apply a "critical flaw" size concept for failure due to vibrational stresses in piping it is first necessary to establish crack growth rates at low propagation rates and low  $\Delta K$  levels. An extensive search for such data on ferritic and stainless steels was performed by BCL.<sup>(1)</sup> A similar compilation was made for stainless steel (SS) data by Lawrence Livermore Laboratory (LLL),<sup>(2)</sup> and another recent compilation of data on piping steels has been published by the Naval Research Laboratory (NRL).<sup>(3)</sup> However, none of the data in Reference 3 would increase the upper bounds on the crack growth rates shown in Figures 1 through 3.

As is made quite clear in the NRL report, the crack growth rates and fatigue threshold behavior are governed by such factors as environment, cycling rates, waveform, and mean stress level (R-ratio). Much of the data displayed in Figures 1 through 3 was selected to reflect upper bound crack growth rate behavior. In the calculations described below, critical crack sizes will be



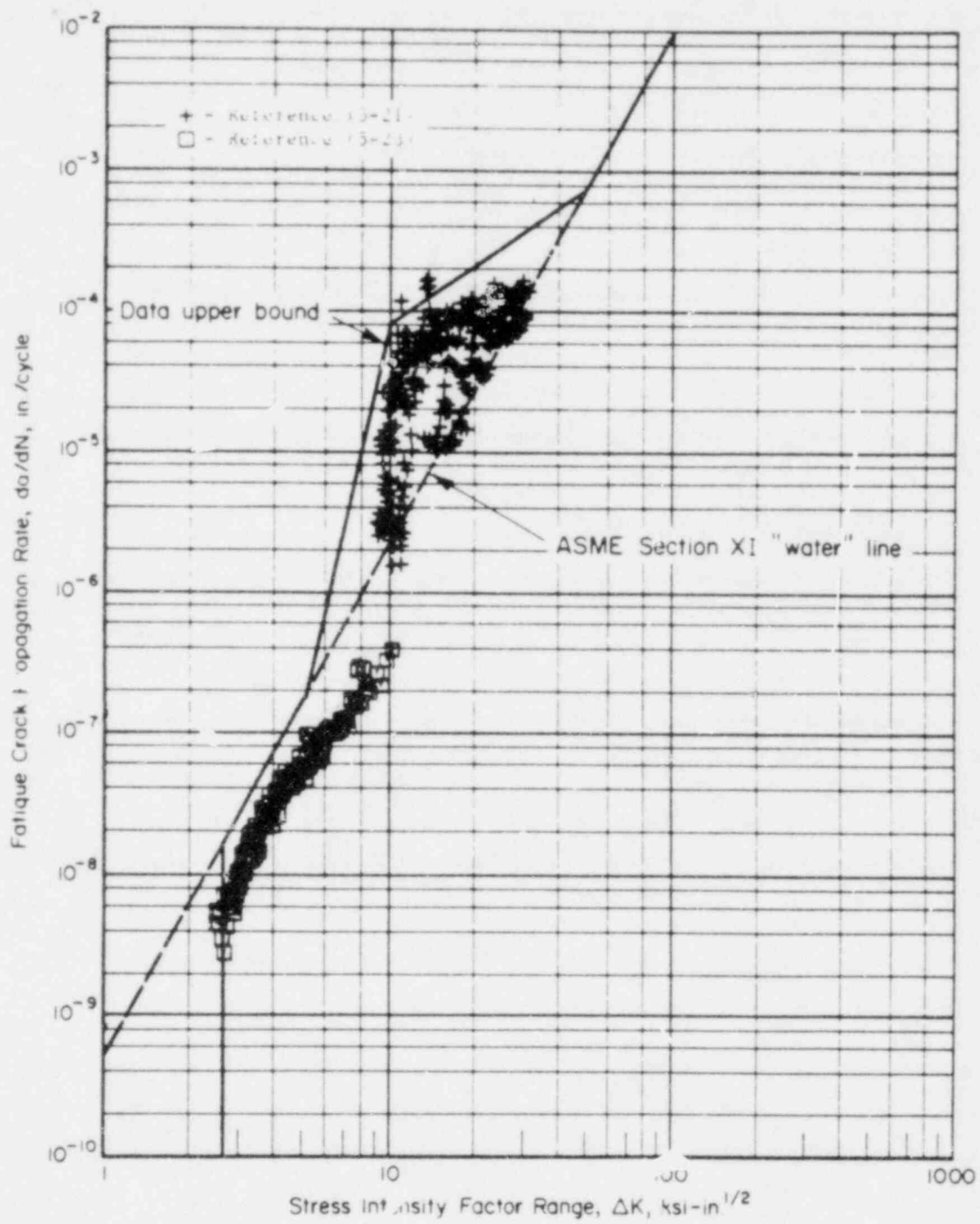


FIGURE 1. Fatigue Crack Growth Rate Data for Ferritic Steel as Compiled in Reference 1

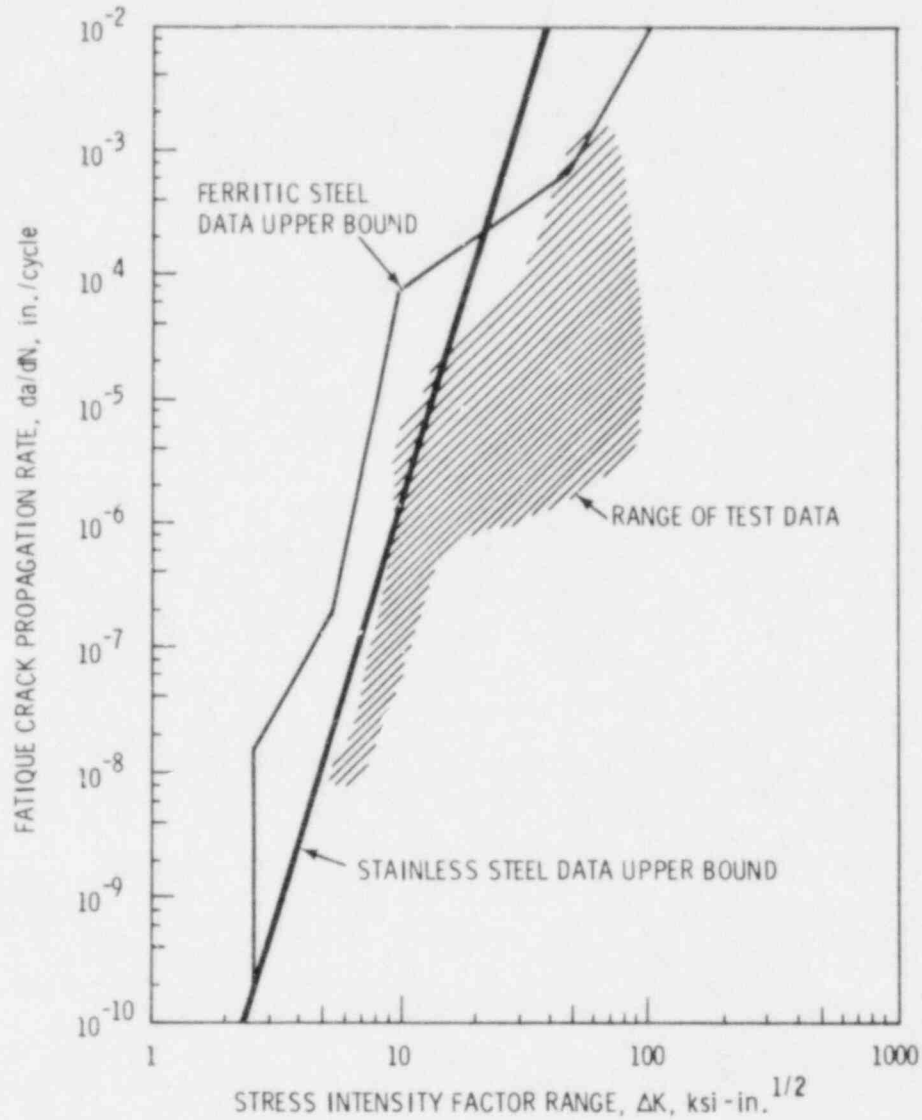


FIGURE 2. Fatigue Crack Growth Rate Data for Stainless Steel as Compiled in Reference 1

estimated on the basis of these upper bound curves. It should be recognized that on most occasions the proper conditions will not be present in a flawed pipe to give rise to the upper bound growth rates. Nevertheless, the estimates will be based on real data--that is, crack growth rates that have actually been measured and reported in the literature. Attempts to extrapolate behavior beyond actual data will be avoided.

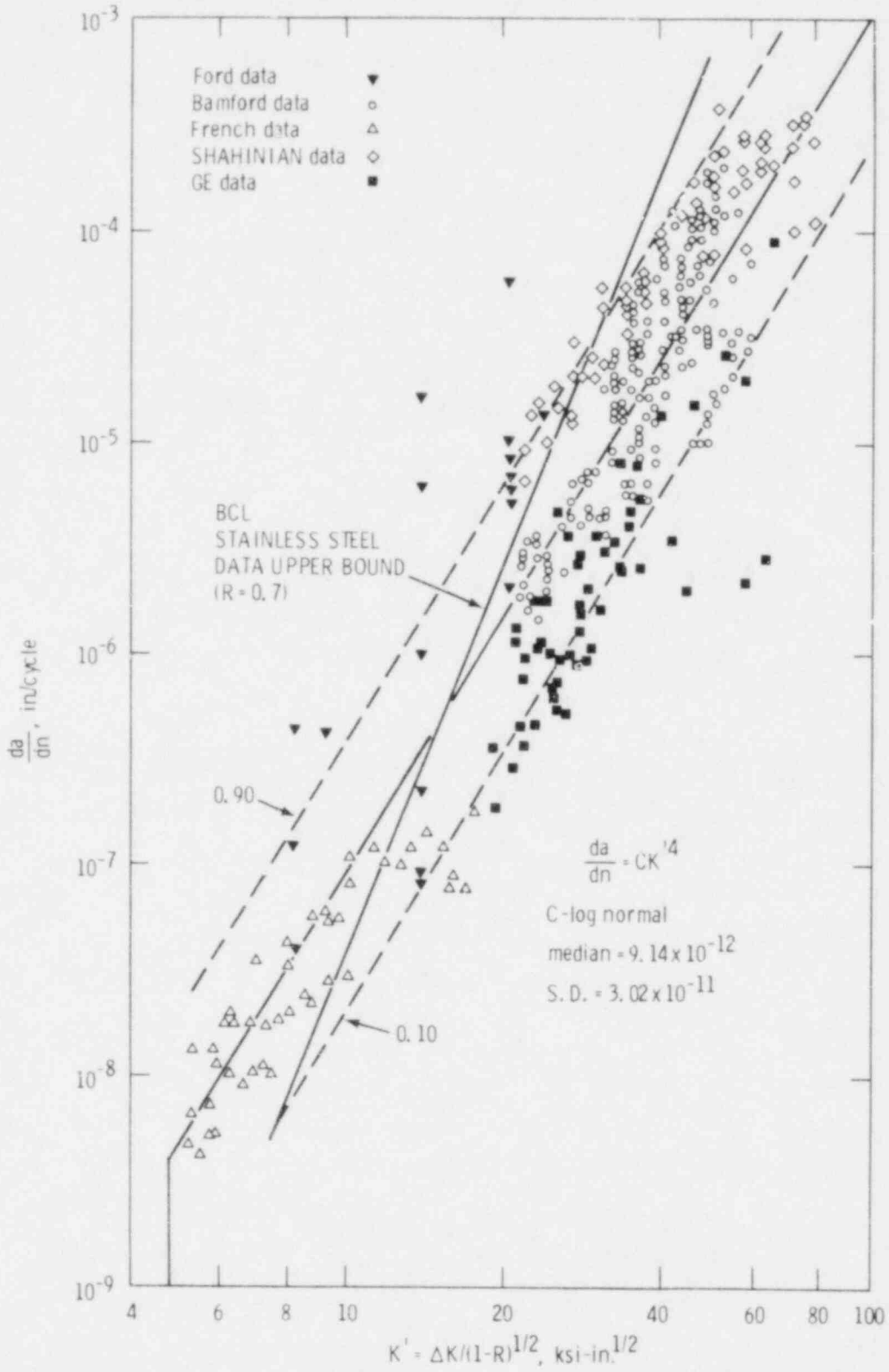


FIGURE 3. Fatigue Crack Growth Rate Data for Stainless Steel as Compiled in Reference 2

It can be seen from the data of Figures 1 through 3 that measurable crack growth rates in the  $10^{-8}$  in./cycle range can in fact occur at a  $\Delta K$  of about 2.58 ksi  $\sqrt{\text{in.}}$  in ferritic steels and at 5 ksi  $\sqrt{\text{in.}}$  in stainless steel.

The crack growth rates in the high  $\Delta K$  range (say, greater than 20 ksi  $\sqrt{\text{in.}}$ ) are outside the range of interest for vibrational fatigue. Nevertheless, we wish to note concerns related to the curves of Figures 2 and 3. In particular, the BCL data upper bound line lies above the actual data in this range and is also above the median line of the LLL data shown in Figure 3. A review of calculations in Reference 1 for the Westinghouse Farley plant showed that as a consequence of the large assumed initial flaws for stainless piping (a/t = 50%), the predicted crack growth was dominated by  $\Delta K$  values in excess of 20 ksi  $\sqrt{\text{in.}}$ . The crack growth rates of the BCL curves in this  $\Delta K$  range were about a factor of 30 greater than corresponding experimental data. It is recommended that revisions to the BCL calculations for SS piping be considered.

#### Critical Flaw Size Estimates

A flaw will be defined to be of a critical size in this discussion if it can grow through the wall of the pipe in a time that would be considered small when compared to the inspection interval; a flaw is somewhat arbitrarily defined as critical if its growth rate under vibrational stress attains a magnitude of  $da/dt \geq 1.0$  in./yr. In the evaluations below, a pipe wall thickness of 2.5 in. is taken as typical of a PWR primary cooling loop; thus, the criterion of 1.0 in./yr implies a year or less before an ID surface flaw becomes a through-wall crack.

A number of calculations have been performed using the FCG rates of Figures 1 and 2. The effects of vibrational frequency, ferritic versus stainless steel, threshold  $\Delta K$ , and flaw aspect ratio have been considered.

Surface defects were assumed to be elliptical with the specific aspect ratios of  $a/2c = 0.1$  and  $0.5$ . The state of stress through the pipe wall was taken to be uniform, which could approximate stresses for internal pressure or bending moment loads to the pipe. Back surface effects as a function of a/t were included in calculations of crack tip stress intensity factors. No plastic zone size effects were considered.

### Frequency Effect

Figure 4 shows the critical depths for surface flaws that will give a 1.0 in./yr growth rate in a ferritic steel pipe as a function of cycle stress level at various frequencies. The upper bound crack growth curve of Figure 1 was applied with the threshold  $\Delta K$  of 2.6 ksi  $\sqrt{\text{in.}}$ . Once the frequency exceeds 120 cpm, there are a sufficient number of cycles accumulated in 1 year at the threshold growth rate of  $1.58 \times 10^{-8}$  in./cycle to grow the crack the required 1 in./yr. At relatively low frequencies, the stress must be increased somewhat to give a sufficient growth per cycle for 1.0 in. of growth a year. Since vibration frequencies will usually exceed 120 cpm, it appears that they do not govern critical flaw size estimates. Rather, when any flaw growth occurs under vibration stress, the number of cycles is so large that the flaw will grow at a rapid rate.

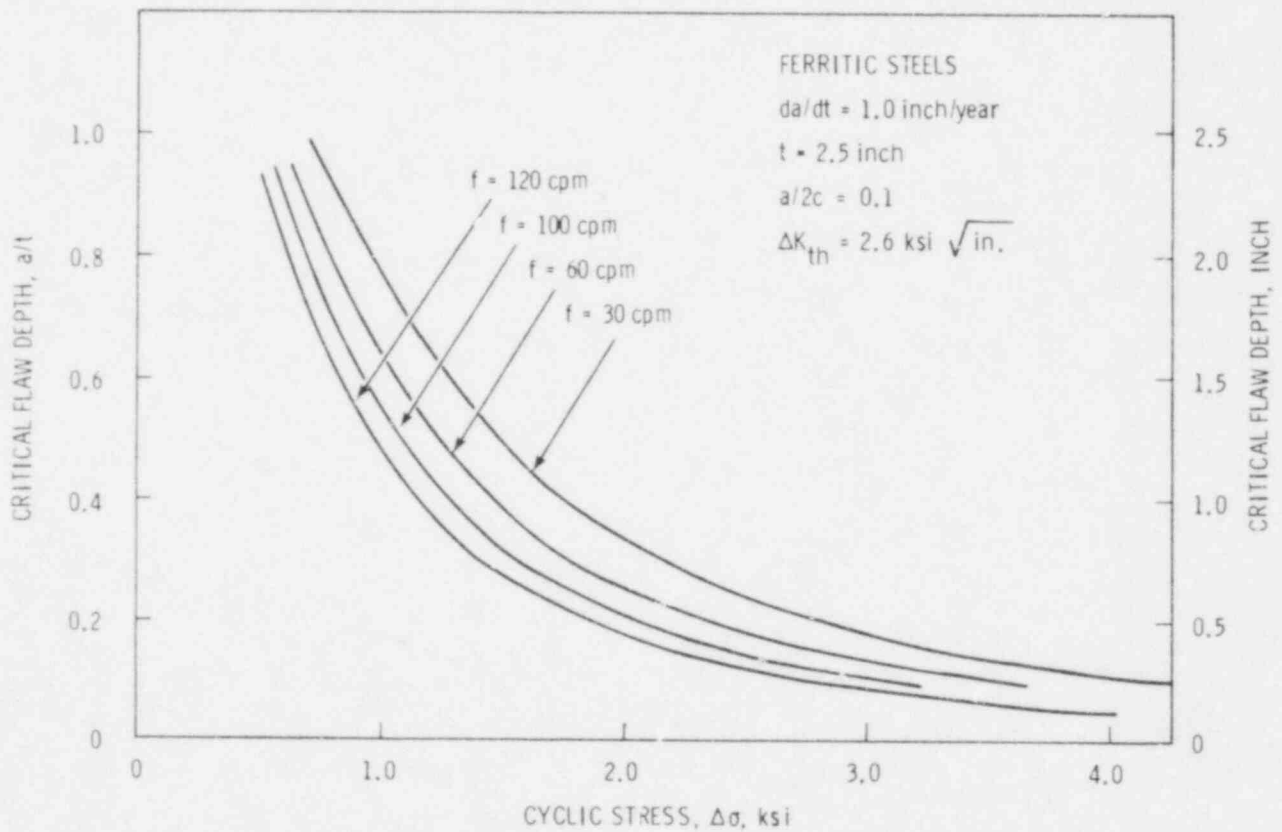


FIGURE 4. Effect of Vibrational Frequency on Critical Flaw Size

### Aspect Ratio Effect

Figure 5 shows the effect of flaw aspect ratio with  $a/2c$  first being a long surface flaw and then being the case of a half-penny surface flaw. These results were selected to correspond to the BCL analysis of the St. Lucie cold leg. In the BCL study a  $\Delta\sigma$  of 1.0 ksi was assumed, for which the critical flaw depths of Figure 5 for vibrational stress are 1.2 in. for  $a/2c = 0.1$  and 2.25 in. for  $a/2c = 0.5$ . This compares favorably with the BCL results, which indicated rapid growth of the  $a/2c = 0.1$  flaw once a depth of about 1 in. was attained (Figure 8-1c of Reference 1).

### Effect of Threshold Behavior

BCL calculations were based on crack growth data at low cyclic stresses, which indicated a threshold-type behavior at  $\Delta K = 2.6 \text{ ksi} \sqrt{\text{in.}}$ . Figure 6 shows

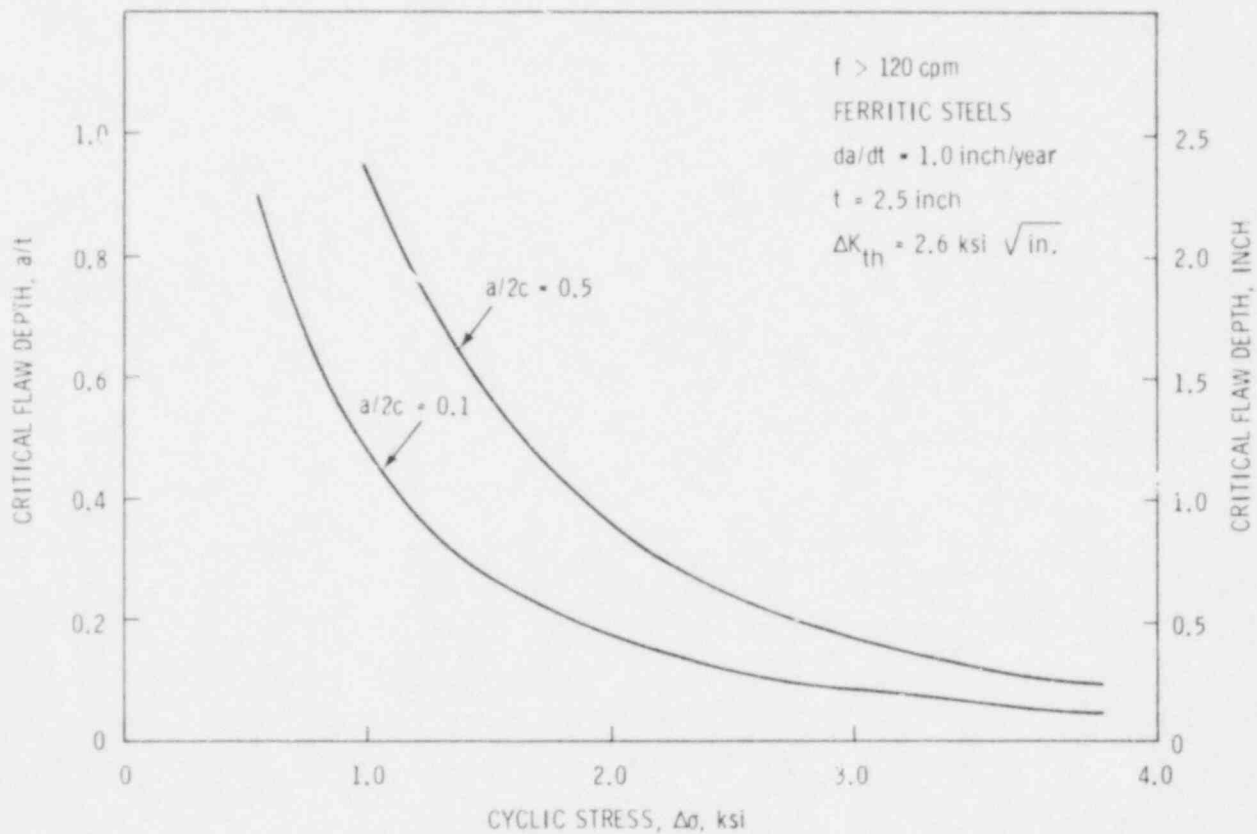


FIGURE 5. Effect of Aspect Ratio of ID Surf Flaw on Critical Flaw Size for Vibrational Stresse.

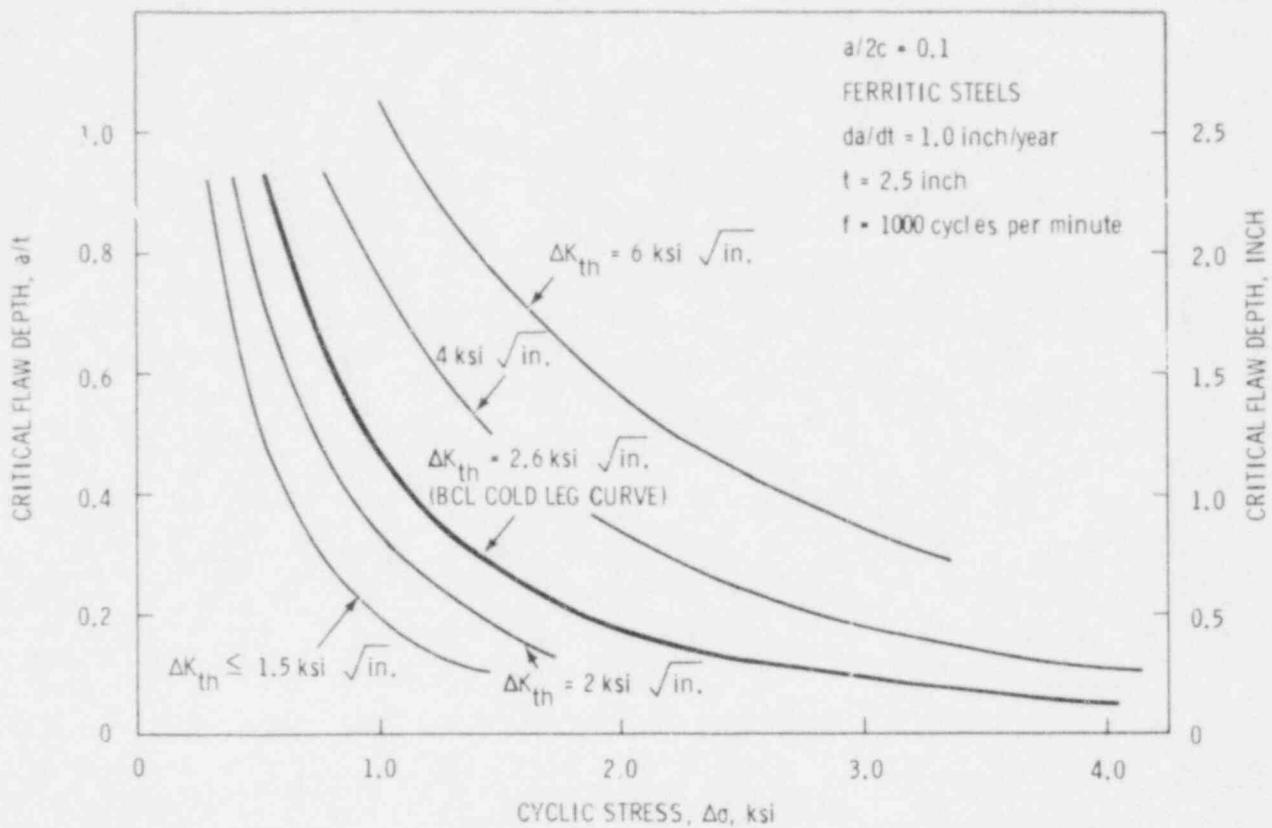


FIGURE 6. Effect of Threshold  $\Delta K$  Behavior on Critical Flaw Size for Vibrational Stress

predicted critical flaw sizes for other possible threshold crack growth levels. The crack growth curve was in each case the same as in Figure 1, except for the  $\Delta K$  corresponding to the vertical segment of the curve at low  $\Delta K$ . Based on available data, the BCL curve is clearly a reasonable upper bound representation of a threshold behavior. Nevertheless, the critical flaw depths are also clearly affected by the exact value of the threshold  $\Delta K$  used in the calculations. It should also be noted that  $\Delta K_{th} \leq 1.4$  ksi  $\sqrt{\text{in.}}$  corresponds to a growth rate sufficiently slow that 1 in. of growth does not accumulate (at a 1000-cpm frequency) in 1 year (see Figure 6).

#### Stainless Versus Ferritic Steel

Figure 7 shows results for stainless steel based on the crack growth rate data of Figures 2 and 3. Stainless steel appears to be affected by vibrational stresses (larger critical flaw depths) when compared to ferritic steels. While

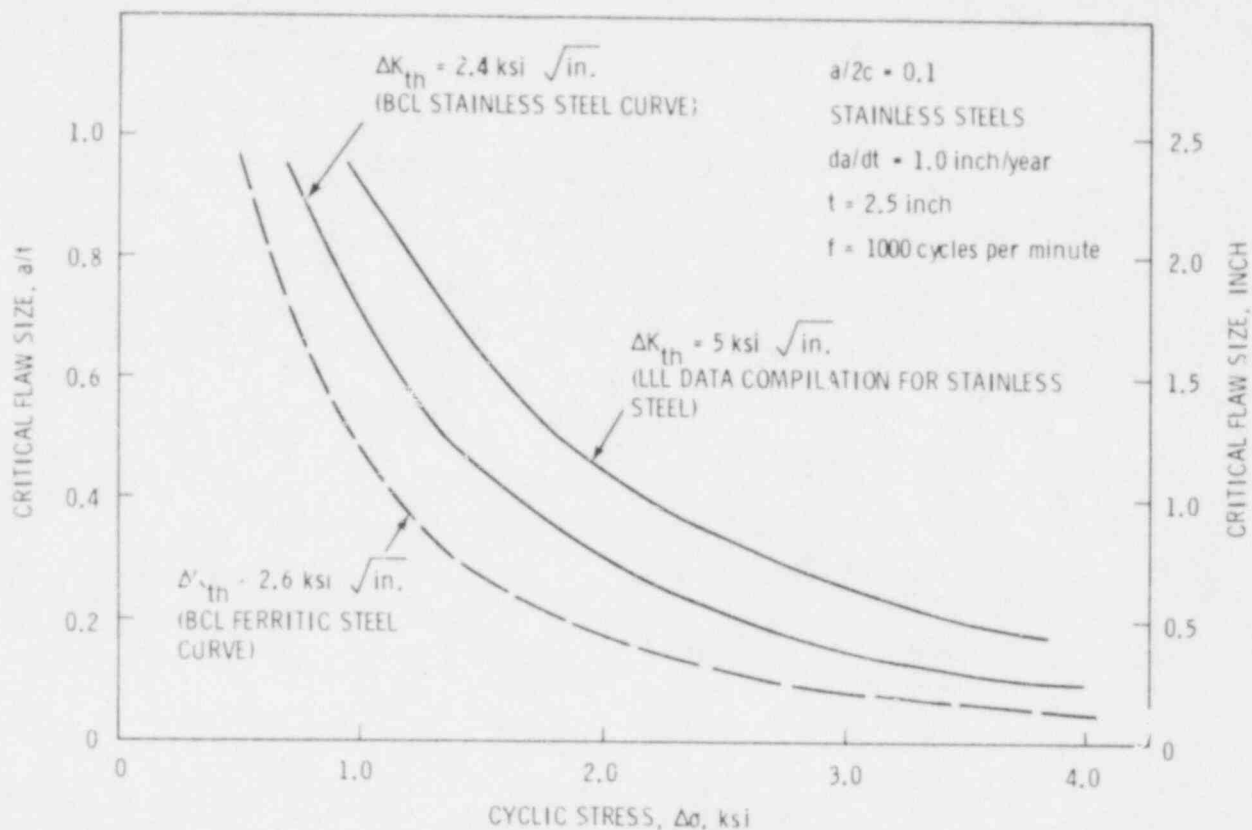


FIGURE 7. Comparison of Ferritic and Stainless Steel Threshold  $\Delta K$  Behavior on Critical Flaw Size for Vibrational Stress

BCL's estimate of the threshold  $\Delta K$  for stainless is slightly lower than for ferritic steels, the much slower growth rates at the threshold results in larger critical flaw sizes. This trend is reflected in BCL results for the Farley SS piping in which vibration plays a less dominant role than for ferritic piping.<sup>(1)</sup> In Figure 7, results for a threshold  $\Delta K$  of  $5 \text{ ksi } \sqrt{\text{in.}}$  are also shown. The data of Figure 3 computed by LLL suggest a  $5 \text{ ksi } \sqrt{\text{in.}}$  threshold, rather than BCL's  $2.5 \text{ ksi } \sqrt{\text{in.}}$  value. The BCL estimate was based on extrapolation of a curve to an arbitrarily low crack growth rate rather than a threshold behavior indicated by actual data.

### Conclusions

The effects of vibrational stresses on flaw growth in piping can be treated as a critical flaw size effect. Critical flaw sizes are primarily a



function of the vibrational stress level and the threshold crack growth behavior of the piping material. Vibrational frequency is a relatively unimportant factor.

The critical flaw size treatment allows decoupling of predictions of crack growth due to vibration from growth due to reactor operating transients. The upcoming BCL cold leg calculations can be performed only for operating transients, and consequences of various assumed vibration conditions can be clearly delineated.

The fatigue crack threshold behavior for ferritic steels used in the BCL study appears reasonable (not overly conservative); furthermore, it is supported by actual laboratory data. However, the BCL threshold behavior for stainless steel is somewhat conservative when compared with available data. In addition, the BCL-extrapolated curve for stainless steel at high  $\Delta K$  (greater than 20 ksi  $\sqrt{\text{in.}}$ ) is quite conservative when compared with available data in this  $\Delta K$  range. The predicted crack growth rates and lives of defected SS pipe (Farley cold leg) have been found to be significantly affected by this conservatism.

#### TASK 6 - SAMPLE FABRICATION

Sample fabrication of 33-in. clad ferritic, 32-in. cast stainless steel, and 10-in. Schedule 80S SS pipe samples with thermal fatigue cracks for the round robin was completed. Fabrication of IGSCC in 10-in. Schedule 80 pipe is 75% complete. IGSCC flaws in the range of 20 to 40% have been fabricated; flaws of approximately 10% depth are required to complete the test matrix. Fabrication of these flaws is in progress.

#### TASK 7 - MEASUREMENT AND EVALUATION

The major effort of the past quarter, characterization of pipe crack samples to be used in the round robin, is largely complete for all samples with the exception of the IGSCC specimens, which are still in fabrication. Measurements currently in progress are indicating the unlikelihood of detecting flaws in or near austenitic SS pipe welds when inspecting from the far side of the

weld. The instrument and search unit characterization system that will evaluate systems used in the round robin is approximately 90% complete.

#### Sample Characterization

In order to implement the proper statistical mix of inspection types during the round robin, the depth category of each crack must be known ahead of time. A great deal of effort has gone into the sizing of the cracks. Because no single flaw sizing technique was found to be effective for all cases, a combination of techniques (ultrasonics and electrical resistance) was used to achieve a higher degree of confidence in the actual flaw sizes. Very few actual data are presented here so that round robin participants do not gain foreknowledge of the samples they will be inspecting.

Crack depth measurement is complete for the clad ferritic, cast stainless, and 10-in. Schedule 80S thermal fatigue samples. They have been satisfactorily broken down into distinct size categories for preparation of round robin inspection schedules.

To date, four pipe samples have been cracked by IGSCC. Although these samples have not yet reached their final form (the crowns are being removed), preliminary data taken at a long metal path indicate that the cracks are from 20 to 40% through-wall.

#### Through-Weld Inspection of 10-in. Schedule 80S SS Pipe

Several electric discharge machined (EDM) notches were fabricated in the ID weld region of two 10-in. Schedule 80S SS pipes to aid in efforts to size thermal fatigue cracks as well as to measure sensitivity loss due to attenuation and beam diversion by the weld grain structure.

Although this experiment has just begun, significant data have been taken using a broad band 2.25-MHz pulse echo transducer at 45° and 60° shear wave angles. The reflectors used were a set of eight EDM notches 0.12 in. deep (25% through-wall) and 0.6 in. long that were located on the pipe ID at varying axial positions in the root and counterbore regions.

With the  $45^{\circ}$  shear beam, most of these notches respond with signals above DAC (reportable) when inspected from the near side. From the far side of the weld, only those in or adjacent to the root could be detected. Notches further away from the root (for example, in the far side counterbore region) were lost in root geometry indications. Their response amplitudes, if the notch signals could be singled out, would be at least 20 dB below DAC.

Near-side inspection with the  $60^{\circ}$  shear beam produced signals from 7 to 14 dB above DAC. All were detectable from the far side but much attenuated. The amplitude loss, which increased with notch distance from the weld root, ranged from 7 to 21 dB. Even so, those notches within 0.150-in. of the root edge produced recordable signals.

The relative success of  $60^{\circ}$  shear waves as opposed to  $45^{\circ}$  waves can be understood if the characteristics of the weld and the location of the reflectors are considered. The weld is a single vee-open butt with a preparation angle of  $37^{\circ}$ . The first three passes were applied by the gas tungsten arc (GTAW or TIG) technique with the remainder done by the shielded metal arc weld (SMAW) method. The TIG root passes on the lower 25% of the weld are fine grained with little or no dendritic structure while the SMAW passes exhibit pronounced dendritic structure. For the reflectors listed above, the more oblique  $60^{\circ}$  wave passes through less of the dendritic SMAW portion of the weld than does the  $45^{\circ}$  wave. For the reflectors nearest the root, the  $60^{\circ}$  beam passes through only the TIG portion of the weld. In addition, the 1977 ASME calibration reflector (end-mill notch) causes the  $60^{\circ}$  inspection to be inherently more sensitive because of the loss of signal strength due to mode conversion at the notch face.

This experiment will be repeated with other search units and beam angles, including such large grain penetrators as  $45^{\circ}$  longitudinal waves and low-frequency dual probes. It will indicate how well this type of inspection is currently being done and how it may be improved through Code modification.

#### Instrument and Search Unit Characterization

Systems techniques and computer programs for the characterization of ultrasonic pulsers, receivers, and search unit frequency and bandwidth have

been completed. The system for measuring ultrasonic beam profiles of angle beam search units is completed and is currently being evaluated.

#### TASK 8 - ROUND ROBIN PREPARATION

Final preparations for the round robin are in progress. The tests are scheduled to begin in early May, barring any unforeseen delays in sample preparation and documentation.

#### FUTURE WORK

The major objective of the coming quarter is completion of the preparations for the round robin and initiation of testing.

#### REFERENCES

1. Mayfield, M. E., et al. February 1980. Cold Leg Integrity Evaluation, Final Report. NUREG/CR-1319, Battelle Columbus Laboratories, Columbus, Ohio. \*
2. Chou, C. K., et al. July 1980. Load Combination Program Progress Report No. 5. NUREG/CR-1624, Lawrence Livermore Laboratory, Livermore, California. \*
3. Cullen, W. A., and K. Torronen. September 1980. A Review of Fatigue Crack Growth of Pressure Vessel and Piping Steels in High-Temperature, Pressurized Reactor-Grade Water. NUREG/CR-1576, Naval Research Laboratory, Washington, D.C. \*

\*Available for purchase from the NRC/GPO Sales Program, U.S. Nuclear Regulatory Commission, Washington, DC 20555, and/or the National Technical Information Service, Springfield, VA 22161.

EXPERIMENTAL SUPPORT AND DEVELOPMENT OF SINGLE-ROD CODES:

TASK A - IRRADIATION EXPERIMENTS<sup>(a)</sup>

D. D. Lanning, Program Manager  
D. D. Lanning, Task Leader

M. E. Cunningham  
R. E. Williford

SUMMARY

This task is concerned with the irradiation of instrumented fuel assemblies (IFAs) for the U.S. Nuclear Regulatory Commission (NRC) at Halden, Norway. The purpose of these tests is to obtain reliable independent data on fuel thermal and mechanical behavior for development of fuel rod modeling computer codes.

Irradiation test IFA-431 is completed. Two other tests (IFA-432 and IFA-513) are still under irradiation as is the final test, IFA-527. All the IFAs are heavily instrumented six-rod clusters.

The Halden Project, NRC, and Pacific Northwest Laboratory (PNL) mutually agreed to allow further operation of IFA-527 even though at least three of its six rods have suffered failure of the pressure boundary (i.e., cladding or end closure) and have some inleakage of water. The assembly was successfully brought from cold shutdown to full power in December 1980 with no detectable fission product leakage. However, rod 2 definitely went to failed status during this startup.

Postirradiation examinations (PIEs) of rod 8 of IFA-432 being conducted at Harwell, U.K., were delayed to perform checkout tests on steatite stand-in pellets. These latter tests proved informative and encouraging.

---

(a) RSR FIN Budget No.: B2043; RSR Contact: G. P. Marino.

## INTRODUCTION

The objectives of the Experimental Support and Development of Single-Rod Fuel Codes Program at PNL are now fourfold:

- collect and analyze in-reactor data on fuel rod thermal/mechanical behavior, especially as a function of burnup
- correlate in-reactor data with postirradiation data and with ex-reactor tests on mechanical and thermal parameters of fuel rods
- integrate the above information into the FRAPCON and FRAP-1 series of computer codes
- study the occurrence and mechanisms of fuel cladding failure using controlled experiments with centrally heated simulated fuel pins in a PNL pressurized water loop.

The Halden Boiling Water Reactor (HBWR) in Norway is currently the sole site used by this program for irradiation tests. PIE will be carried out at both Kjeller, Norway, and Harwell, U.K. Task A of the program is concerned with the conduct of the tests and coordination of test design, test fabrication, shipping, PIE, and sample disposal. The test matrix now spans the full range of expected BWR conditions for pelletized  $UO_2$  fuel, including

- powers up to 50 kW/m (16 kW/ft)
- diametral gap sizes of 50-380  $\mu\text{m}$  (0.002-0.015 in.)
- gas compositions ranging from pure helium to pure xenon
- fuel densities of 95% and 92% theoretical density (TD), the latter both stable and unstable regarding in-reactor densification.

IFA-527 is specifically designed to study the progress and variability of fuel cracking and relocation and features xenon-filled rods to magnify thermal effects.

## TECHNICAL PROGRESS

The HBWR was restarted on December 12, 1980, with IFA-527 containing fuel rods known to have failed. No fission product leakage was detected; however, contrary to statements in the previous quarterly report further fuel failure occurred: Rod 2 temperatures and pressures at startup definitely point to pressure boundary failure and water ingress. This is shown in Figures 1 and 2, where the startup rod pressures and lower end fuel temperatures from rod 1 (failed), rod 2 (resealed, now failed), and rod 3 (unfailed) are compared.

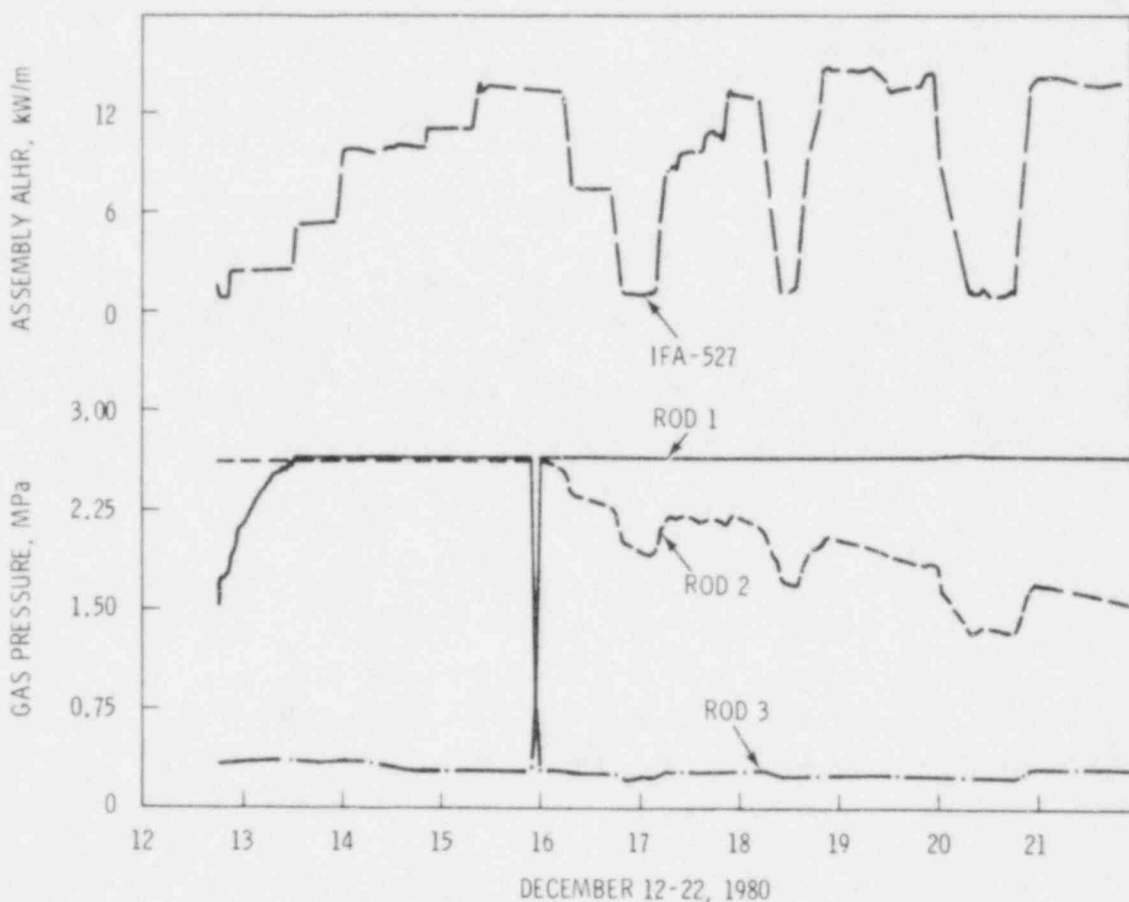


FIGURE 1. Pressures for Rods 1, 2, and 3 of Instrumented Fuel Assembly (IFA)-527 from December 12-22, 1980

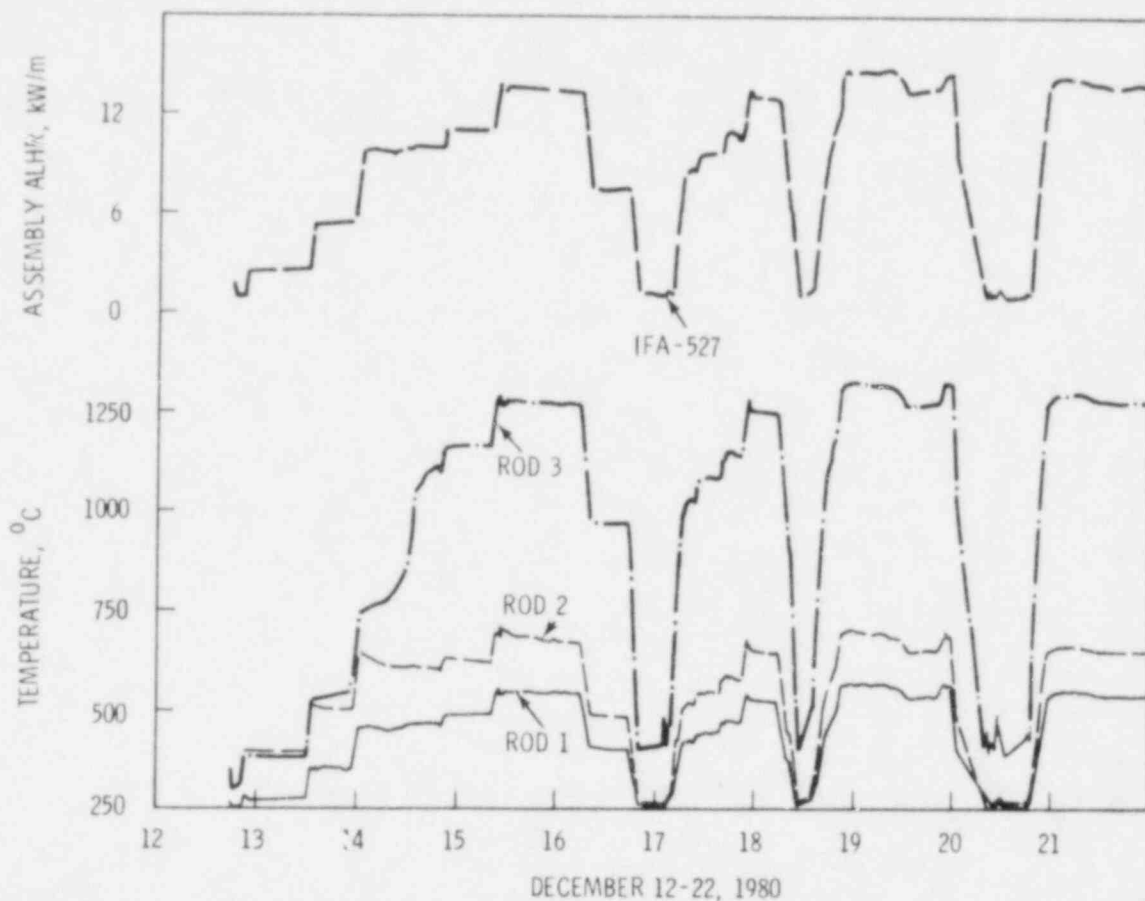


FIGURE 2. Lower Centerline Temperatures for Rods 1, 2, and 3 of Instrumented Fuel Assembly (IFA)-527 from December 12-22, 1980

It is interesting to note that the pressures for rods 1 and 2 follow the system pressure even before startup, indicating full pressure boundary failure; however, rod 2 fuel temperatures initially track the unfailed rod temperatures and then suddenly degrade toward the failed rod temperatures, as if the water took some time (2 days) to reach and affect the thermocouple location. The fall in rod 2 pressures may indicate some resealing.

Pressure transducers in rods 1, 4, and 5 reveal erratic behavior during the operating period from December 12 to February 8; sometimes following system pressure and sometimes falling off at constant power similar to rod 2 behavior (see Figure 1). This may be due to alternate sealing and unsealing of the rods.



IFA-432 performance continued uneventfully over the period. The thermocouple in the lower end of rod 6 (TF 10) definitely failed and was removed from service; the pressure transducer for this rod is also suspect. The lower thermocouple for rod 1 (TF 1) demonstrated some erratic behavior during the last part of the current operating cycle.

Rod 1 of IFA-527 was removed during the February 8 to March 31 shutdown to provide an estimate of the progression of damage in the failed rods. No unusual appearance of the rod was noted during the removal.

#### FUTURE WORK

The data that were gathered from the simulated rods in the compliance test at Harwell, U.K., compared favorably to similar data from tests at PNL in late January 1981. Harwell will test the compliance of rod 7 (unirradiated) and rod 8 (irradiated) in April and May, respectively.

All assemblies should restart in April and continue operation until August or September 1981, at which time they will be permanently discharged to meet cooling and PIE requirements before the mandated close of the program in September 1982.

EXPERIMENTAL SUPPORT AND DEVELOPMENT OF SINGLE-ROD FUEL CODES:

TASK B - DATA QUALIFICATION AND ANALYSIS(a)

D. D. Lanning, Program Manager  
M. E. Cunningham, Task Leader

E. R. Bradley  
W. N. Rausch  
R. E. Williford

SUMMARY

A major objective of the Experimental Support and Development of Single-Rod Fuel Codes Program is the irradiation of instrumented fuel assemblies (IFAs) to obtain well-characterized data. Task B of this program is responsible for qualifying and analyzing that data. During this quarter data for the operating period from December 12, 1980, through February 7, 1981, were received, corrected, and made available for analysis. A data report for IFA-432 covering the period from April 1978 through May 1980 was forwarded to the U.S. Nuclear Regulatory Commission (NRC) for publication while reports discussing the precharacterization of IFA-527, the irradiation behavior of IFA-527, and the irradiation behavior of rod 6 of IFA-431 are nearing completion.

INTRODUCTION

The Experimental Support and Development of Single-Rod Fuel Codes Program is a continuation of the Experimental Support and Verification of Steady-State Codes Program (begun in 1974) and is conducted by Pacific Northwest Laboratory (PNL). This program now has the general objectives of collecting and analyzing in-reactor data on fuel rod temperatures, fission gas release, and cladding elongation as a function of irradiation history; correlating postirradiation examination (PIE) with in-reactor data; utilizing ex-reactor testing for a better understanding of fuel rod mechanical behavior; and integrating this

---

(a) RSR FIN Budget No.: B2043; RSR Contact: G. P. Marino.

information into the FRAPCON computer code series. The qualification and analysis of the data obtained from in-reactor testing of fuel rods is the responsibility of Task B, which has been divided into three subtasks:

- Subtask B-1 - Data Processing: This subtask is responsible for receiving, correcting, characterizing, and presenting the data obtained from the fuel assemblies.
- Subtask B-2 - Data Reports: This subtask is responsible for preparing reports on the precharacterization of the fuel assemblies, the data obtained from the assemblies, and the postirradiation analysis of the assemblies.
- Subtask B-3 - Data Analysis: This subtask is responsible for providing in-depth analysis of the in-reactor fuel rod data. Specific areas of interest for fiscal year (FY)-1981 are analysis of data for inferring fuel relocation and its effect, use of transient temperature data to better understand fuel behavior, analysis of statistical variations and error propagation, and analysis of fuel rod fill gas pressure data for inferring fission gas release.

### TECHNICAL PROGRESS

This quarter's activities are discussed below by subtask.

#### SUBTASK B-1 - DATA PROCESSING

During the last quarter, a test fuel data report (TFDR) tape was received for IFA-432, -513, and -527 for the period from December 12, 1980, to February 7, 1981. Burnup for IFA-432 as of February 7, 1981, is shown in Table 1.

#### SUBTASK B-2 - DATA REPORTS

Efforts this quarter have concentrated on the preparation and publication of several reports on the irradiation of the test assemblies as detailed below:

TABLE 1. Burnup for Instrumented Fuel Assembly (IFA)-432 as of February 7, 1981

Rod Number	Burnup, Mwd/MTM		Rod Average
	Upper Thermocouple	Lower Thermocouple	
1	32,233	23,974	28,104
2	31,180	23,582	27,381
3	31,088	23,973	27,531
9	4,246	3,496	3,871
5	32,191	24,722	28,457
6	32,526	24,525	28,526

- "Data Report for the NRC/PNL Halden Assembly IFA-432: April 1978 through May 1980," NUREG/CR-1950; forwarded to NRC for printing and distribution. This report presents centerline temperature, cladding elongation, and internal gas pressure data for the assembly.
- "Observation of Porosity Reduction in a Densification-Prone Test Fuel Rod: Data and Analysis," NUREG/CR-2042; internal review and final writing in progress. This report will present the data obtained from rod 6 of IFA-431 (92% theoretical density fuel that densified to 96.5% TD), an analysis of the observed in-reactor behavior, and an analysis of pre- and postirradiation fuel microstructural changes.
- "Precharacterization Report for IFA-527"; internal review now in progress. IFA-527 was principally designed to study fuel cracking and relocation. This report presents the design and rationale for the assembly.
- "Beginning-of-Life Irradiation Report for IFA-527"; draft now nearing completion. This report will present data and analysis covering the period from startup of IFA-527 in July 1980 to October 1980. A discussion will be included of the behavior of the assembly following failure of four of the rods during the September 1980 startup.

## SUBTASK B-3 - DATA ANALYSIS

During this quarter, analysis continued in the areas of fuel cracking, and relocation, error and uncertainty analysis, and the general behavior of fuel rods.

### Fuel Cracking and Relocation Analysis

A journal article on fuel cracking and relocation was written and forwarded to Nuclear Technology for review. The article is principally based on the work reported in Reference 1.

The relocation analysis that was previously presented is based on data from early in life. Work has now begun on extending that analysis to higher burnup data. Initial analysis of temperatures and elongation data from rod 2 of IFA-432 (large-gap rod) indicates that crack roughness increases with burnup.

### Error and Uncertainty Analysis

One question to be examined by the irradiation of IFA-527 is the variability between nominally identical rods irradiated under nearly identical conditions. Five of the six rods in the assembly are identical, within tolerances; thus, comparing the variance of their behavior to predicted uncertainties is of interest.

Centerline temperature versus power data from rods 1 through 5 are shown in Figure 1 as is an uncertainty estimate for a computer code (STORE) calculation that matched the data.<sup>(2)</sup> The observed scatter of the temperature data is approximately  $\pm 50\text{K}$ , independent of power; and the predicted uncertainty, based on observed manufacturing variances and estimated modeling uncertainties, is greater than the observed data scatter.<sup>(a)</sup> This means that the predicted variation in fuel rod behavior is greater than the observed variation.

---

(a) The major modeling uncertainties assumed were  $\pm 10\%$  for both the linear heat rate and the fuel thermal conductivity.

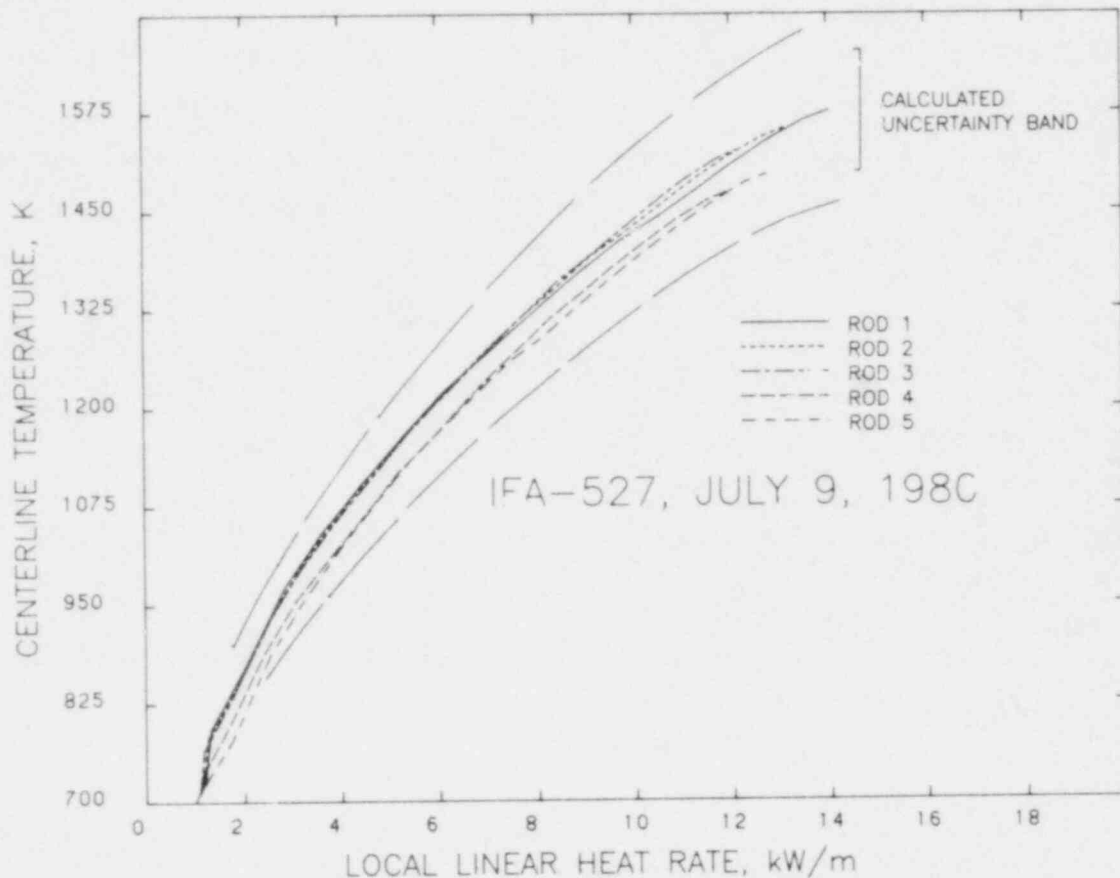


FIGURE 1. Comparison of Data Scatter and Calculated Centerline Temperature Bounds for Instrumented Fuel Assembly (IFA)-527

### Fission Gas Release Analysis

Internal pressure data from rods 1 and 5 of IFA-432 through September 1981 have been examined and used to estimate fission gas release fractions, which as of September 1980 ranged from 4 to 8% for rod 1 and from 7 to 11% for rod 5. These rods have now achieved peak burnups in excess of 2600 GJ/kgU (30,000 MWd/MTM) with no definite evidence of burnup-enhanced fission gas release.

The internal pressure in rod 1 has remained fairly constant for the past 900 GJ/kgU (8,000 MWd/MTM) of exposure; however, pressure increases have been observed in rod 5 during the same irradiation period. Fuel temperature data

show that rod 1 operated at slightly higher temperatures ( 25K) than rod 5 during this period, which suggests that either the lower density fuel in rod 5 is releasing more fission gas at equivalent temperatures or the pressure transducer in rod 1 is no longer operating correctly. Future pressure data and the results from the PIE of these rods are required to determine the definite cause of the difference in gas release between rods 1 and 5.

#### FUTURE WORK

Data processing for next quarter will continue as required. The reports on porosity changes, IFA-527 precharacterization, and IFA-527 irradiation will be completed and forwarded to NRC for printing and distribution. Analysis of fuel cracking and relocation, errors and uncertainties, fission gas release, and related subjects will continue.

#### REFERENCES

1. Williford, R. E., et al. April 1980. Interim Report: The Analysis of Fuel Relocation for the NRC/PNL Halden Assemblies IFA-431, IFA-432, and IFA-513. NUREG/CR-0588, PNL-2709, Pacific Northwest Laboratory, Richland, Washington.\*
2. Cunningham, M. E., et al. October 1980. Application of Linear Propagation of Errors to Fuel Rod Temperature and Stored Energy Calculations. NUREG/CR-1753, PNL-3539, Pacific Northwest Laboratory, Richland, Washington.\*

\*Available for purchase from the NRC/GPO Sales Program, U.S. Nuclear Regulatory Commission, Washington, DC 20555, and/or the National Technical Information Service, Springfield, VA 22161.

EXPERIMENTAL SUPPORT AND DEVELOPMENT OF SINGLE-ROD FUEL CODES:

TASK C - CODE COORDINATION AND EX-REACTOR TESTING(a)

D. D. Lanning, Program Manager  
R. E. Williford, Task Leader

M. E. Cunningham  
W. N. Rausch

SUMMARY

The FRAPCON-2 developmental assessment document is undergoing extensive reorganization by Pacific Northwest Laboratory (PNL) before publication; and Version 1, Mod. 2 (VIM2) of the code is being prepared for transmittal to the Argonne Code Center. Some experimental verification data for the cracked fuel model parameters were reported, and Harwell conducted the first long rod mechanical compliance test with good results. Work continued on the three-dimensional (3-D) cracked fuel mechanical behavior model.

INTRODUCTION

The primary objectives of the code maintenance and experimental support efforts are the documentation, maintenance, and improvement of the FRAPCON-2 licensing audit code. Code documentation will result in code description and developmental assessment documents in coordination with the Idaho National Engineering Laboratory (INEL). Code improvement includes providing experimentally verified models to describe the mechanical interaction between the cracked fuel and the cladding and the quantification of operating conditions that lead to fuel failures with a specified probability.

In fiscal years (FY)-1979 and -1980 thermal-mechanical models were developed that describe the behavior of cracked fuel and those models were implemented in FRAPCON-2. Fuel cracking causes reduced thermal conductivity and elastic moduli and is presently described by three primary parameters--crack

---

(a) RSR FIN Budget No.: B2043; RSR Contact: G. P. Marino.



roughness, gap roughness, and crack pattern--that were inferred from in-reactor data. In FY-1980, ex-reactor data were collected to confirm these parameters. In FY-1981, these experimental efforts will continue in concert with improvement of the cracked fuel model, which represents the driving component for the fuel failure model.

Task C efforts include the following subtasks: code maintenance, fuel mechanics experiments, and pellet-cladding interaction (PCI) model development.

### TECHNICAL PROGRESS

Progress that has been made in each subtask during this quarter is summarized below.

#### SUBTASK C-1 - FRAPCON-2 CONTROL AND MAINTENANCE

A draft of the FRAPCON-2 Developmental Assessment was completed by EG&G Idaho, Inc., and sent to PNL for review; however, publication has been delayed because the document is being reorganized by PNL for clarity and completeness. This document is a joint effort by PNL and EG&G.

In response to a U.S. Nuclear Regulatory Commission (NRC) request, PNL attempted to run the FRAPCON-2 code on both the CDC 6600 and 7600 computers at Brookhaven National Laboratory (BNL); however, the code requires too much core space for these computers. Modifications to reduce core requirements have been identified and provided to NRC.

FRAPCON-2 VIM2 is being prepared for transmittal to the Argonne Code Center. This version includes corrections for coding errors that were found in the Beyer-Hann gas release option.

#### SUBTASK C-2 - FUEL MECHANICS EXPERIMENTS

Experimental results concerning the three basic parameters of the 2-D thermal-mechanical fuel relocation model were reported in a paper for the 6th SMiRT Conference, "Compliance Characteristics of Cracked UO<sub>2</sub> Pellets." Agreement was reported between laboratory and in-reactor values for crack

roughness and total crack length, but more work is required to verify the values previously reported for effective gap roughness.

The analysis of PNL ex-reactor fuel rod compliance tests has revealed similarities to in-reactor data, particularly in the early stages of bamboo ridge formation. The first "long rod" (20-in. fuel column) compliance test was performed by Harwell with good results. The data from the long rod compliance test were very similar to the PNL short rod tests, except where rod bowing induced by the cracked fuel column is concerned. The results may indicate an axial variation of cracked fuel column mechanical properties. Azimuthal variation of bamboo ridge heights was also found.

Both the Harwell and PNL tests are simple in principle: The fuel pellet column is loaded axially in steps, and both rod axial elongation and diametral deformation (including ridging) are measured during the load steps.

#### SUBTASK C-3 - PELLET-CLADDING INTERACTION MODEL DEVELOPMENT

Work continued on the 3-D cracked fuel mechanical behavior model, with progress being made in the areas of thermal strain and rigid body motion characteristics of fuel fragments. The basic scheme for a radial-axial model was established, but the hoop direction requires more work.

The 3-D model efforts are being integrated with the analysis of cracked fuel-cladding compliance data in Subtask C-2 to verify some of the modeling parameters. An end objective of this subtask is to provide estimates of localized cladding stresses induced by the asymmetrically cracked fuel. These stress distributions will be used in a fuel failure model to be included in FRAPCON-2.

#### FUTURE WORK

The following activities are planned for next quarter:

- The FRAPCON-2 Developmental Assessment rewriting will be completed, and the report will be sent to NRC for printing and distribution.

- Harwell will complete compliance testing of rod 7 (unirradiated) and rod 8 (irradiated) of IFA-432.
- The PNL and Harwell fuel rod mechanical compliance data analysis will be completed, and report writing will continue.
- The 3-D cracked fuel model should near completion, and report writing will begin.

EXPERIMENTAL SUPPORT AND DEVELOPMENT OF SINGLE-ROD FUEL CODES:

TASK D - PELLET-CLADDING INTERACTION EXPERIMENTS(a)

D. D. Lanning, Program Manager  
R. E. Williford, Task Leader

D. E. Fitzsimmons  
R. K. Marshall

SUMMARY

An instrument concept was chosen for measuring strain over small gage lengths; the detailed design is about 90% complete. The loop pressure boundary (test section) design is in progress for placing a heated fuel rod simulator in a pressurized flowir, water loop.

INTRODUCTION

The primary objective of Task D of the Experimental Support and Development of Single-Rod Fuel Codes Program is to collect fuel rod failure data on irradiated cladding under temperature loading conditions typical of those in-reactor, including asymmetrically cracked pellets and coolant external pressures. The fuel-induced pellet-cladding interaction (PCI) will be simulated with cracked annular pellets and an internal heater rod in a pressurized water loop facility at PNL. This experimental equipment has the capability for controlled power ramping and load cycling schemes and provides great experimental flexibility at a cost much lower than in-reactor experiments. The relationships between power ramp rate, localized cladding strain rate, and fuel rod relaxation rate will be characterized. The localized cladding deformations will be measured by an instrument especially designed and built for this purpose.

---

(a) RSR FIN Budget No.: B2043; RSR Contact: M. L. Picklesimer.

The loop will be proof tested in fiscal year (FY)-1981 with unirradiated cladding, and actual data collection with irradiated cladding will begin in FY-1982. These data complement Task C efforts and provide a means of verifying PCI models.

In Task D-1 a measurement instrument capable of characterizing the elastic deformation of the simulated fuel rod at power within the loop will be designed and produced.

### TECHNICAL PROGRESS

Progress that has been made in each subtask during this quarter is summarized below.

#### SUBTASK D-1 - ROD STRAIN INSTRUMENT DESIGN

A survey of possible concepts resulted in an instrument design based on existing technology. A strain gage cantilever system was chosen that has the capability of recording cladding diameter traces in the axial and azimuthal directions during the tests. Two traces are recorded simultaneously in each case. Strain gages and thermocouples have been ordered. The detailed design of the instrument is about 90% complete.

#### SUBTASK D-2 - LOOP EXPERIMENTS

Detailed design of the pressure boundary (test section) for the pressurized loop experiments began. Efforts have focused on the instrument-pressure boundary interface, the pressure vessel code requirements, and a means to calibrate the strain-measuring instrument.

### FUTURE WORK

The following activities are planned for next quarter:

- Instrument fabrication and assembly will be completed.

- Proof testing and calibration of the instrument will begin.
- The loop pressure boundary design will be completed, and fabrication is scheduled to begin.

## PIPE-TO-PIPE IMPACT(a)

M.C.C. Bampton, Project Manager

J. M. Alzheimer  
F. A. Simonen

### SUMMARY

Emphasis during the past quarter has been on developing a preliminary test matrix, determining the method to be used to accelerate the impacting pipe, and designing the test facility and instrumentation system.

### INTRODUCTION

The objective of the Pipe-to-Pipe Impact Program is to provide the U.S. Nuclear Regulatory Commission (NRC) with experimental data and analytic models for making licensing decisions regarding pipe-to-pipe impact following postulated breaks in high-energy fluid system piping. Current licensing criteria--as contained in Standard Review Plan 3.6.2, "Determination of Break Locations and Dynamic Effects Associated with Postulated Rupture of Piping"--will be evaluated. Data will be obtained from a series of tests in which selected pipe specimens with appropriate energies will be impacted against stationary specimens to achieve required damage levels.

This Pacific Northwest Laboratory (PNL) program involves two main areas: obtaining experimental data and developing predictive models. Preliminary analyses to determine significant test parameters and required energies and pipe velocities have been completed. The preliminary test matrix was developed, a system capable of accelerating the pipe was selected, and design of the test facility began. The next phase of the program will encompass construction of the test machines and actual testing. Predictive models will be developed that are analytically based and/or empirical fits of the data. These predictive models will be compared to current licensing criteria.

---

(a) RSR FIN Budget No.: B2383; RSR Contact: M. Vagins.

## TECHNICAL PROGRESS

### PRELIMINARY TEST MATRIX

The preliminary test matrix (see Table 1) is based partially upon current licensing criteria and partially upon analysis to determine significant parameters of interest. A nominal pipe diameter of 6 in. was selected for all impacting pipe specimens to simplify the design of the pipe accelerating system. The target pipe specimen diameters and the wall thicknesses of the two pipes were selected so that the impacting pipe would have various combinations of greater, equal, or lesser diameters and greater, equal, or lesser wall thicknesses. At least two tests will be run from each group in the preliminary matrix; and these tests will be at different impact velocities, which will be selected based upon estimations of damage levels. Initial tests will be performed at modest velocities with target specimens at room temperature and unpressurized; testing will then progress to higher velocities with pressurized target specimens. If it is deemed necessary, the target pipe will also be at elevated temperature.

Initial estimates of the energy requirements of the pipe-to-pipe impact tests were based upon maximum kinetic energies obtained by pipes during various pipe rupture scenarios. Ruptured pipes were allowed to swing through more than 90° before impact. These energy requirements were used to assess the capabilities of several systems for accelerating the impacting pipe. Due to the high energies and velocities required, most concepts for accelerating the pipe proved infeasible. The most promising concept was to use compressed gas to expel a slug of water from inside the pipe through a 90° elbow, which is similar to the actual loading that occurs during a postulated pipe break event.

### SELECTING THE PIPE ACCELERATING SYSTEM

A modest test setup was built to assess the potential of the compressed gas/water concept; a 40-in. long 1-in. Schedule 80 pipe was used. Thrust time histories were obtained for several tests run with various ratios of gas to



TABLE 1. Pipe-to-Pipe Impact Program Initial Test Matrix

Group <sup>(a)</sup>	Test Condition
1	6-in. Schedule 40 striking 6-in. Schedule 40 <sup>(b)</sup>
2	6-in. Schedule 40 striking 6-in. Schedule 40
3	6-in. Schedule 80 striking 6-in. Schedule 80
4a	6-in. Schedule 40 striking 6-in. Schedule 80
4b	6-in. Schedule 80 striking 6-in. Schedule 40
5a	6-in. Schedule 120 striking 12-in. Schedule 60
5b	6-in. Schedule 80 striking 3-in. Schedule 160

(a) At least two tests will be performed from each group. Each test in a group will be at a different velocity to be determined from analysis before the test.

(b) Group 1 target pipe unpressurized; target pipe pressurized to typical pressure for all other groups.

water and various pressures. The data indicated that the impulse generated by this method would be adequate to accelerate the pipe to the desired velocities; however, it was evident that potential safety hazards were present. For larger diameter pipes, the noise would be extremely loud; and the jet impingement effects of the water and gas would have to be taken into account. The swinging specimen would in effect be a pressure vessel that would have to withstand up to 2000 psi. While these safety problems could be overcome, they did detract from the acceptability of the concept.

A reevaluation of the energy requirements was undertaken based not on the energy potential in a pipe break scenario but on the energy requirements to cause "failure" of the impacted pipe. While actual failure of the piping had not been analyzed in detail, estimates of failure energies were made. Pipe failure during a postulated pipe break event can be defined as the loss of the pipe's ability to maintain its safety function, which includes maintaining its structural integrity and not rupturing or leaking. If flow in the pipe is required, loss of cross-sectional flow area could be considered failure. While the tasks were not readily available to analyze the rupture of the pipe wall, conservative estimates could be made of the energy required to crush the pipe

cross section. These energy values were considerably lower than those previously obtained from pipe break scenario analysis.

Once the reevaluation of the energy requirements indicated that lower impact energies would be required, other systems for accelerating the pipe became practical. While the compressed gas/water system was probably practical, it had shortcomings; namely

- potential safety hazards
- extrapolation to larger pipe sizes had not been proven
- determination of desired impact velocities would require trial and error testing
- preparation of the impacting specimen would be costly since it would essentially be a pressure vessel.

Because of these considerations other accelerating systems were investigated, and a system that uses a pneumatic cylinder to power a catapult arm was selected (see Figure 1). The pneumatic cylinder has a 20-in. diameter and a stroke of 36 in. The energy is supplied by the volume of compressed air (up to 250 psi) contained in the rod end of the cylinder prior to release of the catapult arm. No makeup air is needed. After the pipe has been accelerated to the necessary velocity, the catapult arm is stopped by the cushion of air trapped in the head end of the cylinder.

This system has several advantages over the compressed gas/water system. Safety problems are reduced because the impacting pipe specimen is not pressurized; and, therefore, the swinging specimens do not have to be designed to withstand up to 2000 psi. There are no noise or jet impingement problems. The system is also much more analyzable; obtaining fairly precise test velocities should not be a problem.

#### TEST FACILITY AND INSTRUMENTATION SYSTEM DESIGN

All major components of the pneumatic catapult have been designed, and the few remaining details are being finalized. The catapult mechanism will be built while the design for the remainder of the facility is being completed.

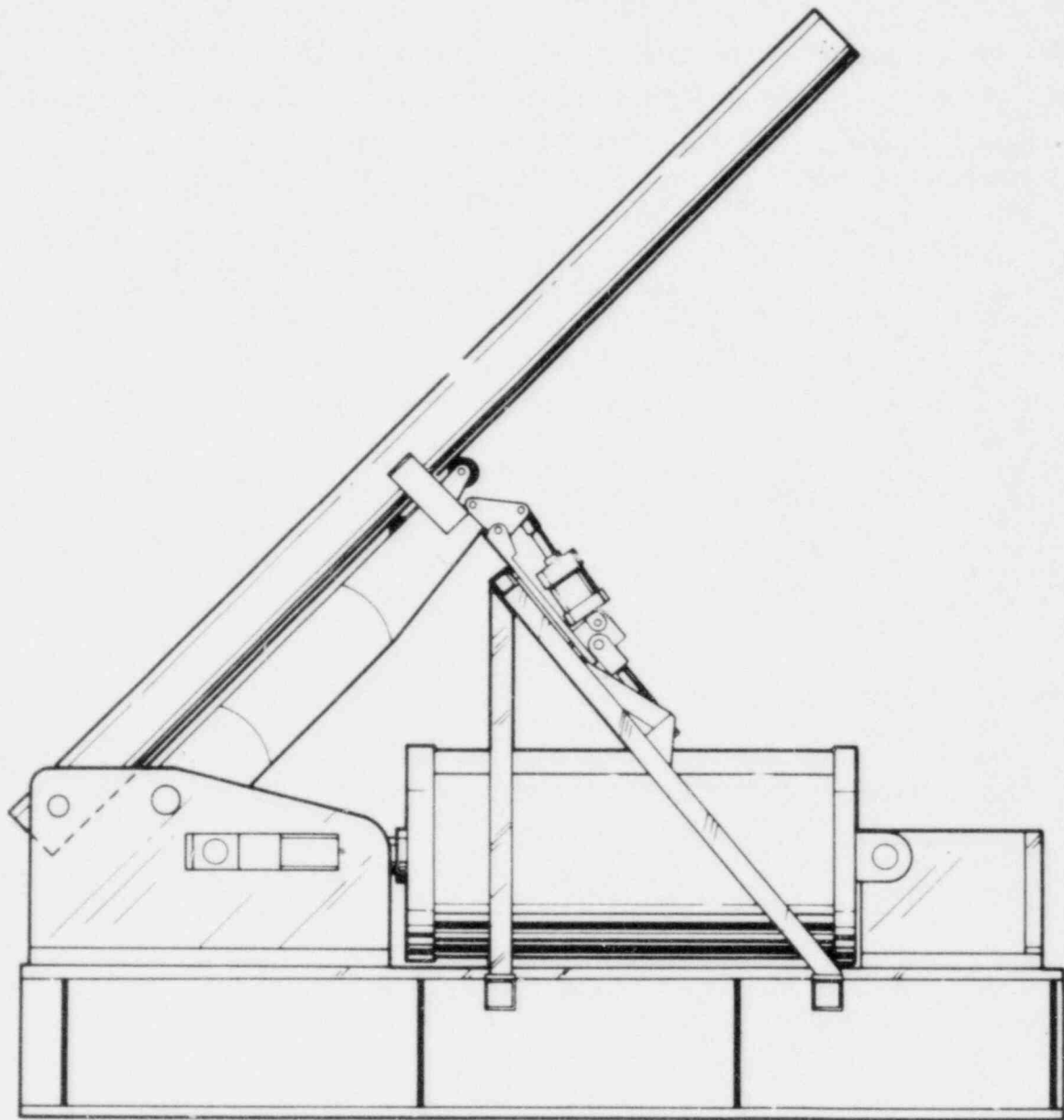


FIGURE 1. Pneumatic-Powered Pipe Accelerator Conceptual Design

A computer program was written to simulate the kinematics and dynamics associated with the catapult. It has been useful in evaluating the loads used in the design of the catapult and will also be useful in selecting pressures and configurations for obtaining the appropriate test velocities without excessive experimentation.

An instrumentation system for the pipe-to-pipe impact tests is being designed. Parameters of primary importance are pipe velocity, target pipe pressure, and final specimen deformations. Secondary parameters of interest are support reaction, material strain time histories, and specimen acceleration.

#### FUTURE WORK

The following activities are planned for next quarter:

- complete design of test facility
- begin construction of test facility
- complete instrumentation system
- prepare test specimens.

SEVERE CORE DAMAGE TEST SUBASSEMBLY PROCUREMENT PROGRAM

PBF SEVERE FUEL DAMAGE TEST PROJECT(a)

E. L. Courtright, Program Manager  
R. L. Goodman, Project Manager

G. S. Allison	S. D. Miller
L. R. Bunnell	L. J. Parchen
T. M. Fish	J. D. Rising
L. L. King	R. D. Tokarz
R. K. Marshall	J. O. Vining
M. A. McKinnon	C. L. Wheeler

SUMMARY

Testing and evaluation of possible insulation materials for the shroud continued; all development testing was done on  $ZrO_2$ -based materials. A rigid felted low-density (~19% theoretical density)  $ZrO_2$  fiberboard is currently favored from the standpoint of low thermal conductivity, good water compatibility, and easy fabricability; the  $ZrO_2$  honeycomb material remains as a backup. If quarter sections of the octagonal insulation can be made by extrusion, the brickwork aspects of fit-up and construction will be easier.

Detailed mechanical design of the spacer grid assemblies, fuel bundle region, and insulated shroud region of the test train assembly have been through formal checking; and drawings were released for final design review approval.

Approved copies of the Quality Assurance Plan (QAP MD-82) and the Quality Control Plan (QCP-3, Revision 0) were released for use on the Power Burst Facility (PBF) Severe Fuel Damage (SFD) test program. These two documents set forth the guidelines that have been developed for planning and monitoring the activities for supporting analytical work and design, fabrication, and assembly of hardware and fuel components to support this Pacific Northwest Laboratory (PNL) program.

---

(a) RSR FIN Budget No.: B2084-1; RSR Contact: R. Van Houten.

Final design of the boil-off test apparatus was completed, and all shop fabrication of hardware components for both the fallback barrier and boil-off test apparatus were finished. Operational tests of the "slugbuster" flow loop and its new control panel were successfully performed, and final assembly of the fallback barrier components into the slugbuster loop is nearing completion.

Additional independent design scoping analyses were completed with the THTD heat transfer computer code to provide an independent evaluation of both PNL calculations with the TRUMP code and EG&G Idaho, Inc., calculations with the TRAC-BDO code.

### INTRODUCTION

This part of the Severe Core Damage (SCD) Test Subassembly Procurement Program--the PBF Severe Fuel Damage Test Project--has been divided into two tasks for fiscal year (FY)-1981.

#### TASK 1 - PBF SEVERE FUEL DAMAGE PROGRAM SUPPORT

The scope of this task includes the design effort, development of appropriate materials and supporting fabrication processes, and complete fabrication of two fully instrumented test train assemblies. Many portions of the PBF work should directly benefit the ESSOR program due to similarities in the experimental objectives, particularly for materials development, instrumentation, and fabrication development. The program is designed to yield important experimental data related to fuel and cladding behavior during small-break accidents as well as provide information on the postaccident coolability of damaged fuel rod clusters after small-break accidents.

#### TASK 2 - SMALL-BREAK WATER LEVEL CONTROL AND BOIL-OFF EXPERIMENTS

A small-scale boil-off experiment will be conducted to investigate the sensitivity of water level control to the absolute water level during simulated small-break conditions. The experiment will also examine the effects of water level on the axial temperature profile of the electrically heated rod bundle.

Electrical heater rods with approximately 1 m of heated length and internal cladding thermocouples will be installed in a 9-rod square array inside a specially designed and fabricated high-pressure test section. The test section will be instrumented to measure inlet and outlet water/steam conditions as well as water level. Water at approximately 295K will be injected into the bottom of the test section at rates sufficient to maintain water levels between 10.2 to 22.9 cm (4 to 9 in.) above the beginning of the heated length. Nominal operating pressure will be about 650 psig, and both water injection rate and heater rod power will be varied over a matrix of test conditions.

#### TECHNICAL PROGRESS

The following paragraphs detail technical progress made during this reporting period by topic.

#### SHROUD DESIGN AND DEVELOPMENT TESTING

Testing and evaluation of candidate insulators for the shroud continued with all work being done on  $ZrO_2$ -based insulation materials. The  $ZrO_2$  honeycomb filled with bubble  $ZrO_2$  that was previously proposed continued to look promising; however, fabrication of the composite shroud size and shapes would be very difficult. The honeycomb units are in the form of 10.2 x 10.2 x 0.64 cm (4 x 4 x 1/4 in.) "bricks"; and cutting and fitting the bricks into the required octagonal shapes would require diamond tooling, which would be very difficult and time consuming.

Another  $ZrO_2$  insulation form--rigid  $ZrO_2$  fiberboard--is available in 30.5 x 30.5 x 1.3 cm (12 x 12 x 1/2 in.) pieces and can be worked with normal hand tools. This material form could be used either wet with a perforated inner shroud liner or dry in a sealed shroud container. In the perforated inner shroud liner concept, the thermal conductivity of the insulation material would be raised by the water when wet; but tests have shown that the insulation would dry out during the early stages of the test and the fiberboard would regain its high thermal resistance value before it was required later in the test.  $ZrO_2$  extruded honeycomb and  $ZrO_2$  rigid fiberboard are both compatible



with high-pressure hot water. For the perforated inner liner wet fiberboard insulation case, the fiberboard must not be eroded by  $\sim 0.61$  m/sec (2 ft/sec) water flow during the preconditioning phase of the test. The resistance of sintered  $ZrO_2$  fiberboard to erosion by water at 0.61 m/sec was evaluated in two autoclave tests at  $350^\circ C$  and 17.2 MPa (2500 psi). The lower density (30 lb/ft<sup>3</sup>) fiberboard eroded severely in a test lasting 15 min; the high-density (60 lb/ft<sup>3</sup>) fiberboard was apparently undamaged by the flowing water. Surface impregnation of boards of both densities with highly sinterable  $ZrO_2$  (rigidizer) also resulted in no noticeable erosion.

However, uncertainties concerning the behavior of a wetted insulation and problems in analytically predicting the behavior of such an insulation resulted in the elimination of the perforated inner liner concept. The insulation evaluation and choice now involves two candidates, both used in the sealed mode:  $ZrO_2$  fiberboard and  $ZrO_2$  extruded honeycomb.

Since the flat sides of the 0.076-cm (0.030-in.) thick octagonal inner liner make it vulnerable to differential pressures, a shroud design that provides a simple pressure equalization system will be required. The crushing strengths of 60 lb/ft<sup>3</sup> fiberboard and  $ZrO_2$  extruded honeycomb were determined to be about 80 and 660 psi, respectively. A summary of the evaluation of various candidate shroud insulation types is presented in Table 1. Collapse of the  $ZrO_2$  fiberboard insulation could be eliminated by using short lengths of  $ZrO_2$  tubing as support columns, as was demonstrated by autoclave testing at pressures to 17.2 MPa. A simple view of the proposed sealed shroud system using the  $ZrO_2$  fiberboard insulation and  $ZrO_2$  tube supports is shown in Figure 1, which indicates the relationship of the inner liner,  $ZrO_2$  fiberboard insulation,  $ZrO_2$  tube supports, and shroud outer Zircaloy liner. It is currently assumed that a simple pressure balance will be used to keep the full system pressure--6.9 MPa (1000 psi)--from possibly crushing the insulation; this pressure balance is presumed to be approximately 200 psi.

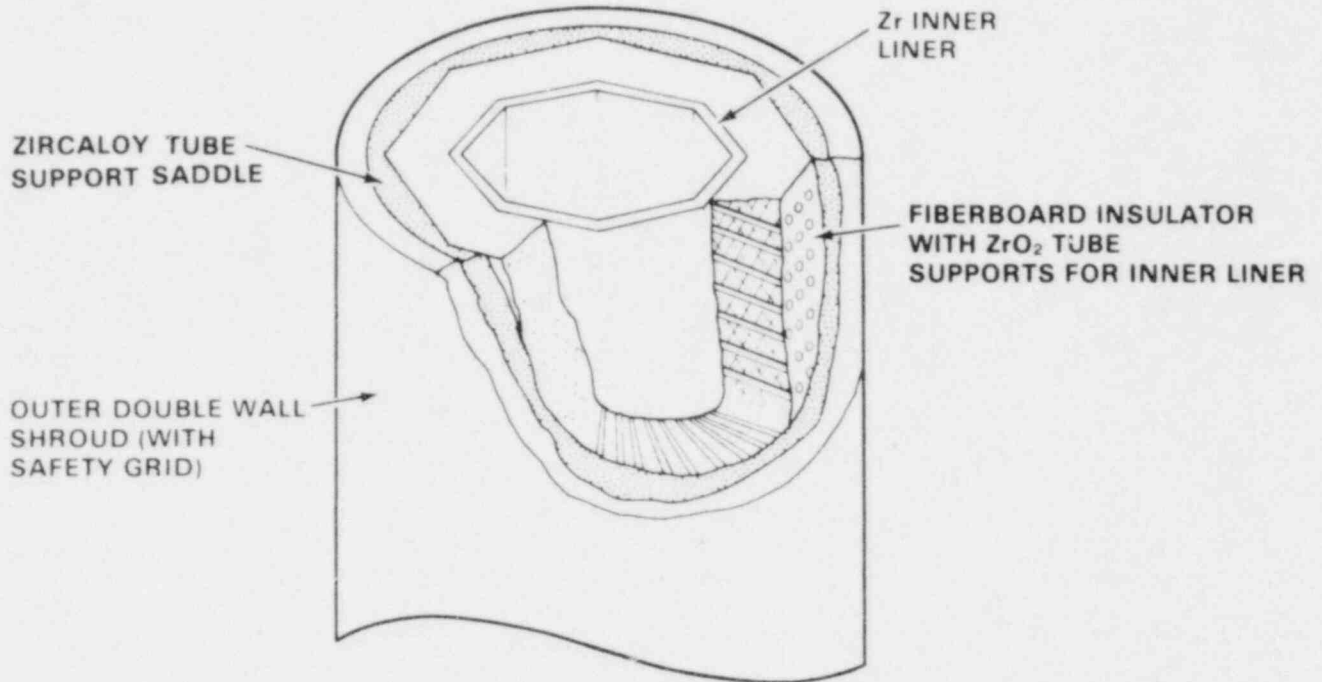
Fiberboard  $ZrO_2$  insulation is now being applied to a full-section insulated shroud mockup of the sealed shroud design that will be autoclave tested to assure that the tube support method will be sufficient and to verify the



TABLE 1. Evaluation of Various Candidate Shroud Insulation Types

	BONDED ZrO <sub>2</sub> FABRIC	ZrO <sub>2</sub> BUBBLE FILLED HONEYCOMB	ZrO <sub>2</sub> FIBERBOARD (NON SUPPORTED)	ZrO <sub>2</sub> FIBERBOARD (SUPPORTED)	ZrO <sub>2</sub> HONEYCOMB EXTRUDED TO SHAPE
1. SEALED SYSTEM					
A. COMPRESSIVE STRENGTH >2000 psi (NO PRESSURE EQUALIZATION)	NO (UNSUPPORTED)	YES	NO	YES	NO
B. COMPRESSIVE STRENGTH >200 psi (PRESSURE EQUALIZATION)	YES	YES	YES	YES	YES
b. INSULATION VALUE	OK (DATA)	OK CALCULATED)	OK (VENDOR DATA)	OK	MARGINAL
D. THERMAL SHOCK RESISTANCE	GOOD	GOOD	GOOD	GOOD	GOOD
2. NON-SEALED SYSTEM					
A. RESISTS H <sub>2</sub> O, 350 C, 2500 psi	DISINTEGRATED	OK	OK	OK	OK
B. RESISTS EROSION BY 2000 psi H <sub>2</sub> O (2 ft/sec)	DISINTEGRATED	OK	FAIRLY SEVERE EROSION	N.A.	OK
3. FABRICABILITY *					
(1 SIMPLE, 10 IMPOSSIBLE)	7	8	2	5	5

\*BUNNELL SCALE



**FIGURE 1.** Sealed Shroud System Utilizing ZrO<sub>2</sub> Fiberboard Insulation and ZrO<sub>2</sub> Tube Supports

inner liner and fiberboard insulation collapse resistance. Figure 2 shows an axial section through the insulated shroud region of the test assembly and a schematic view of the pressure equalization system.

ZrO<sub>2</sub> extruded honeycomb remains as a backup material of higher thermal conductivity but greater crush strength for the shroud insulation. If proposed quarter sections of the octagonal insulation can be made by extrusion, the brickwork aspects of fit-up and construction of the insulated shroud assembly will be lessened. The feasibility of this method will be determined with the manufacturer (Applied Ceramics, Int., Atlanta, Georgia) in the near future.

#### SCOPING DESIGN ANALYSIS

Additional design scoping analyses were completed with the THTD transient heat transfer computer code to provide an independent evaluation of the proposed PBF severe fuel damage experiment thermal performance. The scoping

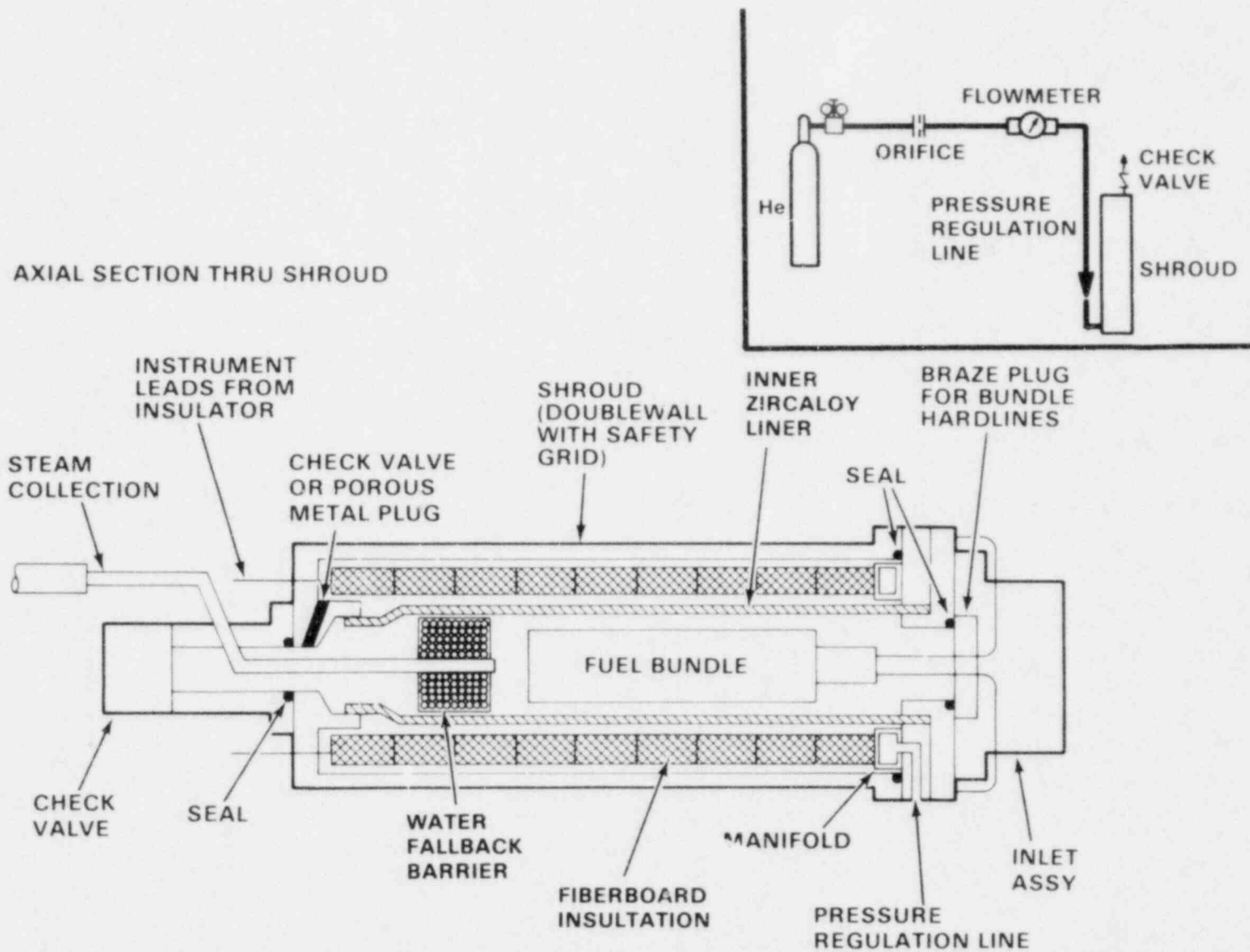


FIGURE 2. Sealed Shroud System with  $ZrO_2$  Fiberboard Insulator and Pressure Equalization System

analyses included the effect of the metal-water reaction occurring at the surface of the Zircaloy fuel cladding at elevated temperatures in a steam environment.

The thermal analysis was performed with an axi-symmetric model that represented the 32 test pins as three radial regions. The steam was also divided into three regions with the interchannel mixing approximated by a convective connection between adjacent fluid regions. The model consisted of 290 nodes in 10 axial layers and was run for two steady-state shroud conditions. The only difference in the model for these cases was the thermal conductivity of the shroud material. The two conditions considered the effect of using two values for the thermal conductivity for the shroud insulation. Assembly peak temperature versus average assembly power curves are shown for the two shroud cases in Figures 3 and 4, which indicate the importance of a low thermal conductivity material for the insulation of the shroud. For the lowest thermal conductivity material examined, the assembly power required to meet the desired test temperature of 2300K is about 13 kW/m (4 kW/ft); for the higher thermal conductivity material, an assembly power of approximately 130 kW/m (40 kW/ft) is required to meet the desired test temperature of 2300K. The importance of the selection of the lowest thermal conductivity material is shown in the order of magnitude differences in assembly powers required to achieve the desired experimental temperatures.

Figures 3 and 4 indicate that the low thermal conductivity shroud gives peak cladding and peak shroud temperatures that are close in magnitude to one another as a function of assembly power. For the low-conductivity case, the weighted average exit steam temperature curve falls below the curve for the peak shroud temperature. In contrast, for the higher thermal conductivity material, the peak shroud temperatures are all below the weighted average exit steam temperatures as a function of assembly power; and the peak shroud temperatures are much lower than the peak cladding temperatures as a function of assembly power. Finally, the cladding-to-shroud differential temperature varies as a function of the thermal conductivity of the shroud insulation material. The higher thermal conductivity material has a larger cladding-to-shroud differential temperature.

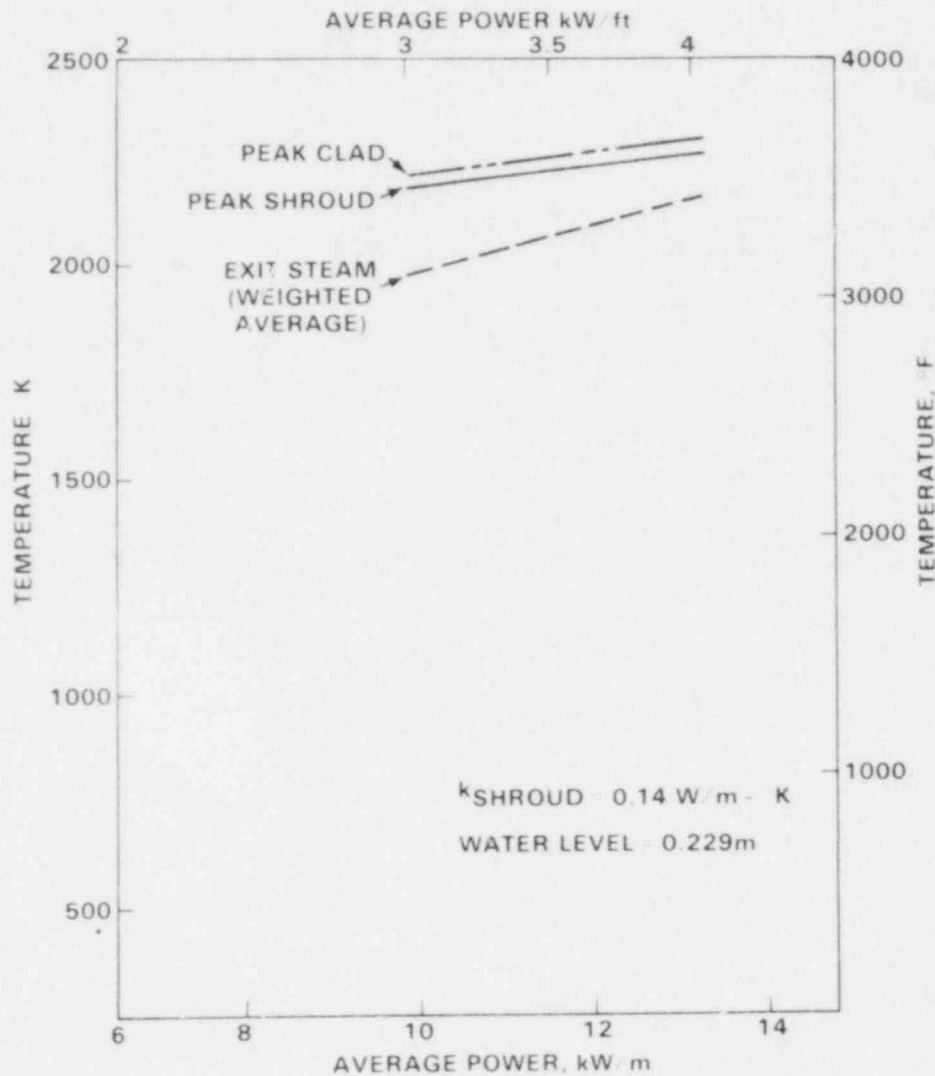


FIGURE 3. Peak Assembly Temperature Versus Power for the Low Thermal Conductivity Shroud

After the steady-state calculations were completed, transient heating analyses, including the effect of the metal-water reaction heating, were run for two correlations (those presented by Baker-Just and Cathcart).<sup>(1,2)</sup> The metal-water reaction process is important to the computation of the fuel temperatures for the small-break loss-of-coolant accident (LOCA) tests because the potential magnitude of the heat generation rate could dominate the experiment performance. This process is thought to have had a significant impact on the core thermal performance during the Three-Mile Island (TMI)-2 accident.

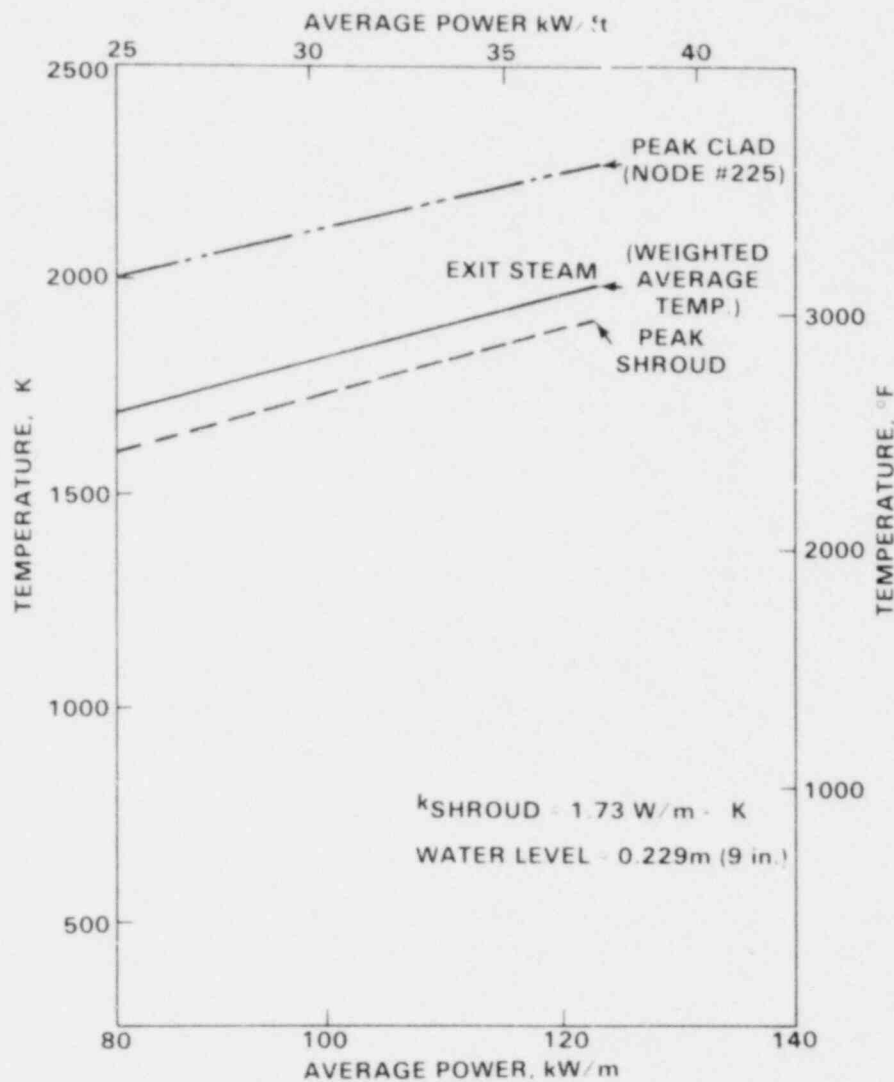


FIGURE 4. Peak Assembly Temperature Versus Power for the High Thermal Conductivity Shroud

The implementation of a metal-water reaction heat generation model in THTD accounts for only the effect of the parabolic rate law on the heat generation rate. The parabolic rate equation is of the form:

$$\left(\frac{W}{A}\right)^2 = K_p(T)\tau$$

where  $W$  = weight of zirconium consumed  
 $A$  = the reaction surface area

$\tau$  = time

$K_p(T)$  = rate constant, which is a function of temperature.

It is more convenient to work with the thickness of the oxide layer. The parabolic rate equation may be evaluated at the beginning and end of a time step to yield the following relationship for oxide thickness.

$$x_2 = \sqrt{x_1^2 + \frac{K_p(\bar{T})\Delta\tau}{2}} \quad (x_2 \leq x_0)$$

where  $x_1$  = initial oxide thickness at the start of the time step

$x_2$  = oxide thickness at the end of the time step

$x_0$  = the total material thickness

$K_p(\bar{T})$  = rate constant evaluated at the average temperature during the time step.

The volumetric heat generation rate based on the initial volume of the material is:

$$\dot{q} = \frac{H(x_2 - x_1)}{x_0 \Delta\tau}$$

where  $H$  = reaction heating per unit weight.

The metal-water reaction analyses were added to the transient heatup of the test section starting from a uniform temperature of 561K (550°F) and with a constant nuclear heating rate and water level. This particular transient does not have any real physical significance as far as any reactor accident or test sequence is concerned; however, it does provide an insight into the potential impact of the metal-water reaction process on the performance of a small-break LOCA test sequence. In addition, it provides shroud and steam temperatures with metal-water reaction process contribution.

which aid in test train assembly and insulated shroud design. The transient heating analyses were all performed for the high thermal conductivity shroud case. The average bundle nuclear heating rate was varied from 45.9 to 59.1 kW/m (14 to 18 kW/ft).

Figure 5 presents the predicted performance of the system for three nuclear power levels using the Baker-Just correlation to predict the metal-water reaction heat generation rate. An uncontrolled temperature rise occurred between 45.9 and 52.5 kW/m. However, a rate-limiting effect due to the availability of steam imposes an upper limit on the metal-water reaction heating rate. For the 22.9-cm (9-in.) water level, the maximum possible metal-water reaction heating rate assuming consumption of all available oxygen is 45.9 kW and 51.5 kW for the first two cases. This steam depletion limit would have significantly altered the rate of the temperature rise but probably would not have avoided the uncontrolled temperature rise in the bundle.

Results for three cases at 65.6, 72.2, and 78.7 kW/m average nuclear heating using the Cathcart correlation are presented in Figure 6. The three cases examined do not exhibit the uncontrolled temperature rise in the bundle because the rate constant in the 1922K range is a factor of five less than the Baker-Just correlation. It should be noted, however, that the rate constant is strongly temperature dependent and will very likely still produce the same uncontrolled temperature rise in the bundle as the nuclear power is increased.

The transients performed using the Baker-Just and Cathcart correlations did not include metal-water reaction heating at the surface of the Zircaloy liner of the shroud. The extra heat generation due to the shroud metal-water reaction appears to have a negligible effect on peak cladding temperatures. For the uncontrolled temperature rise cases, the shroud metal-water heat generation will be on the order of 10 to 25% of the total metal-water reaction heating.

The current modeling involves two significant deficiencies. First, it does not compute the steam-hydrogen composition and thus permits the



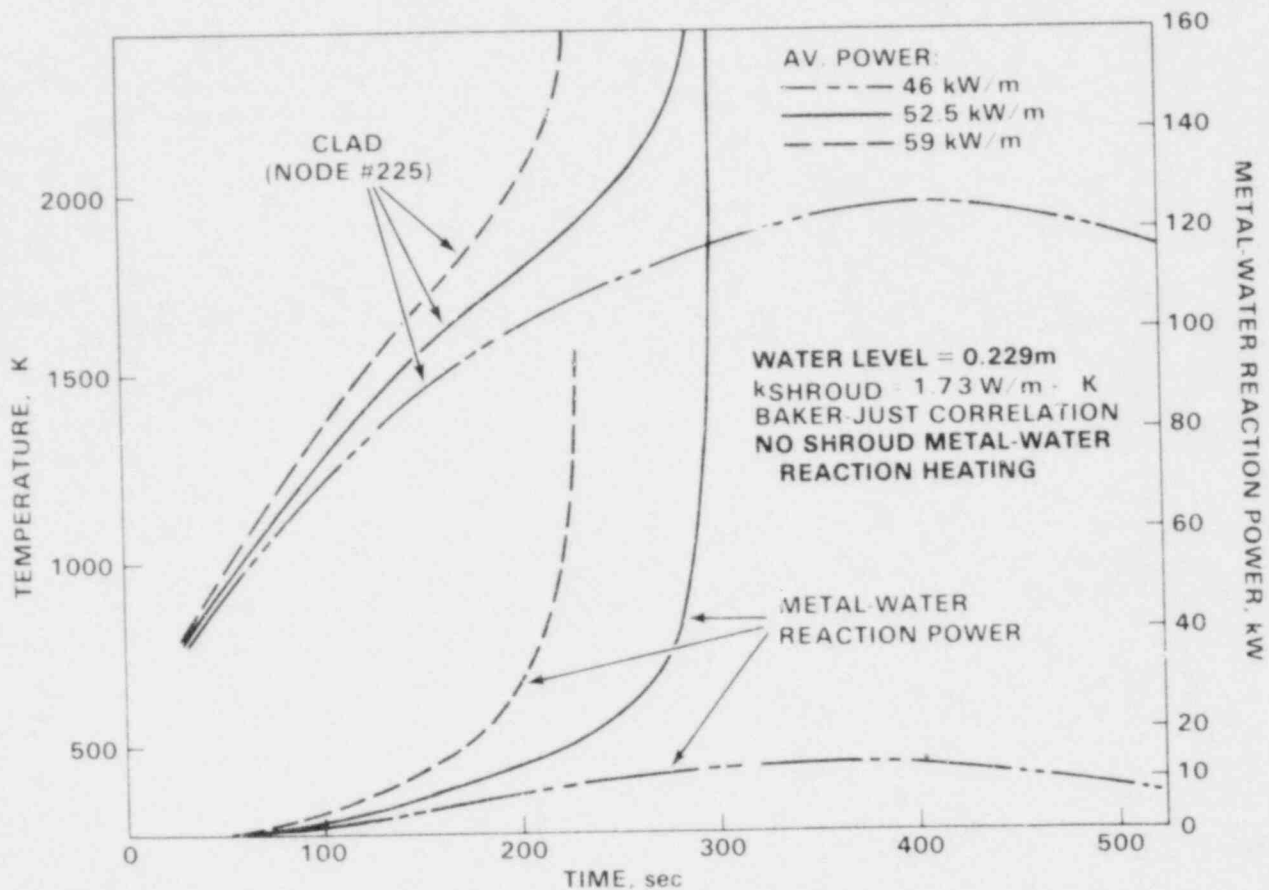


FIGURE 5. Assembly Peak Temperature and Metal-Water Reaction Heating Rate Versus Time for the Baker-Just Correlation

computation of oxidation heating rates beyond that possible on a simple inventory basis. Second, the effects of the mass transfer process have been neglected entirely. These additions are being considered and will be included in further model calculations for the test assemblies. The last area requiring closer evaluation is the matter of selecting the reaction rate constant since substantially different results were obtained with the two correlations.

#### BOIL-OFF EXPERIMENTS

Final design of the boil-off test apparatus was completed, and all shop fabrication of hardware components for both the fallback barrier and boil-off test apparatus were completed. Operational tests of the "slugbuster" flow

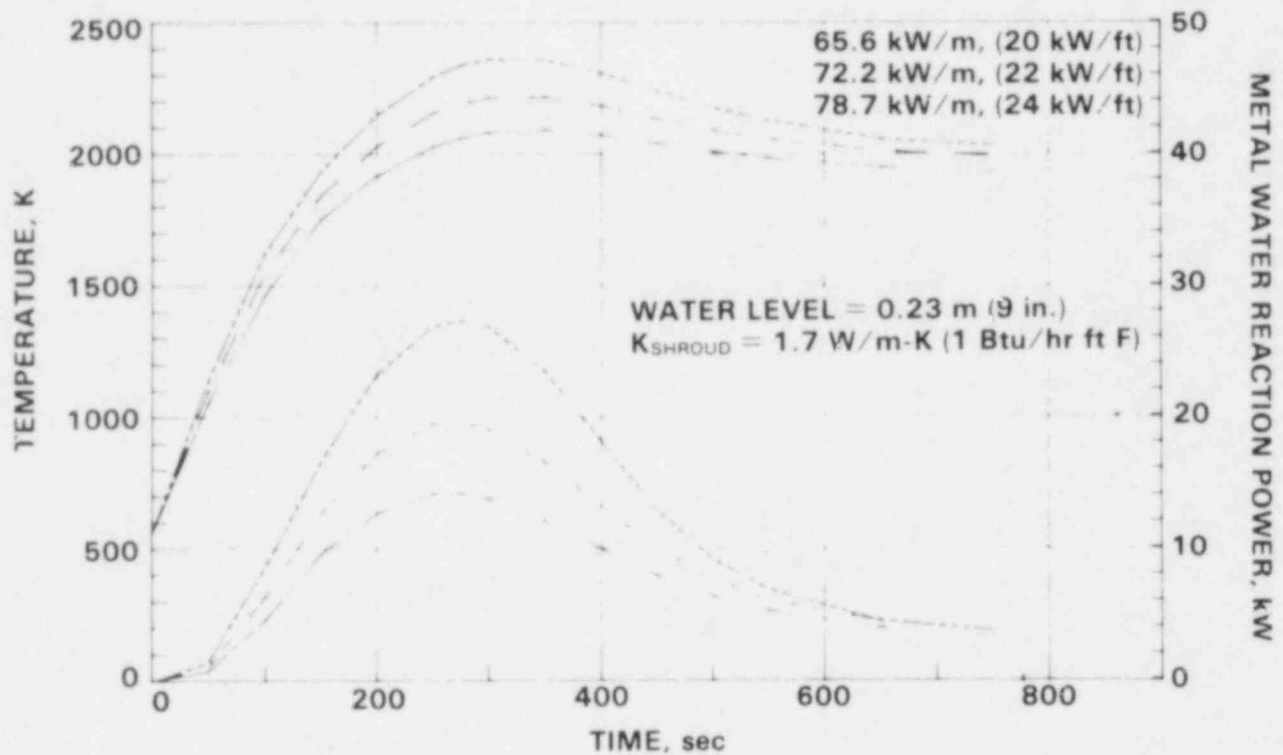


FIGURE 6. Assembly Peak Temperature and Metal-Water Reaction Heating Rate Versus Time for the Cathcart Correlation

loop and its new control panel were successfully completed, and final assembly of the fallback barrier components into the slugbuster loop is nearing completion.

#### FUTURE WORK

Detailed design of test train assembly No. 1 will be completed and released for fabrication. Design, fabrication, and testing of prototypes for the molten fuel penetration detector (MFPD) for the insulated shroud will continue. Pressure drop testing of the proposed fallback barrier components will be completed for a range of typical preconditioning water flow rates. Detailed design for the in-pile liner tube for the PBF pressure tube required to support the SFD tests will be started.

## REFERENCES

1. Baker, L., and L. C. Just. May 1962. Studies of Metal-Water Reactions at High Temperatures; III. Experimental and Theoretical Studies of the Zirconium-Water Reaction. ANL-6548, Argonne National Laboratory, Argonne, Illinois.
2. Cathcart, J. V., et al. August 1977. Zirconium Metal-Water Oxidation Kinetics; IV. Reaction Rate Studies. ORNL/NUREG-17, Oak Ridge National Laboratory, Oak Ridge, Tennessee.

SEVERE CORE DAMAGE TEST SUBASSEMBLY PROCUREMENT PROGRAM

ESSOR PROJECT(a)

E. L. Courtright, Program Manager  
F. E. Panisko, Project Manager

J. E. Tanner  
R. D. Tokar  
C. L. Wheeler

SUMMARY

No contribution was submitted for this quarterly report.

INTRODUCTION

The Super Sara Test Program (SSTP) is a major European community effort to study reactor safety during rapid or large-break and slow or small-break loss-of-coolant (LOC) events. The program will use the SUPER SARA high-temperature, high-pressure loop in the ESSOR reactor at Ispra, Italy. The SSTP is designed to yield important experimental data on fuel rod deformation and postaccident coolability of damaged fuel assemblies after they experience a loss of coolant. The complete testing program currently includes 21 tests to simulate various large- and small-break conditions in PWRs and boiling water reactors (BWRs). Pacific Northwest Laboratory (PNL) will supply three fully instrumented and fueled test assemblies, analytical services, and engineering support for the SSTP.

---

(a) RSR FIN Budget No.: B2372-1; RSR Contact: R. Van Houten.

SEVERE CORE DAMAGE TEST SUBASSEMBLY PROCUREMENT PROGRAM

NINE-ROD TEST TRAIN FOR OPTRAN 1-3 PROJECT(a)

E. L. Courtright, Program Manager

R. E. Schreiber, Project Manager

R. E. Falkoski

D. E. Hurley

L. L. King

SUMMARY

The nine-rod test train hardware and remote handling fixtures were shipped to the Idaho National Engineering Laboratory (INEL) at the end of the quarter. The test train hardware (see Figure 1) was described in the report for the first quarter of 1980, and the remote handling fixtures were described in the report for the last quarter of 1980. Final assembly of the preirradiated rods, the rod bundle, and the test train will be done by EG&G Idaho, Inc., in the hot cell and basin facilities associated with the Materials Testing Reactor (MTR).

INTRODUCTION

The purpose of this Pacific Northwest Laboratory (PNL) project is to provide instrumented test train hardware for Power Burst Facility (PBF) experimental programs. A nine-rod test array was chosen for the abnormal operating transient simulation (OPTRAN 1-3).

In support of this experiment, a test train has been designed with a replaceable core region and shroud to allow other tests of a similar nature to be performed with the basic assembly. The design allows for insertion and removal of one rod following the preconditioning phase and has built-in features to facilitate disassembly and repair.

---

(a) RSR FIN Budget No.: B2084-1; RSR Contact: R. Van Houten.

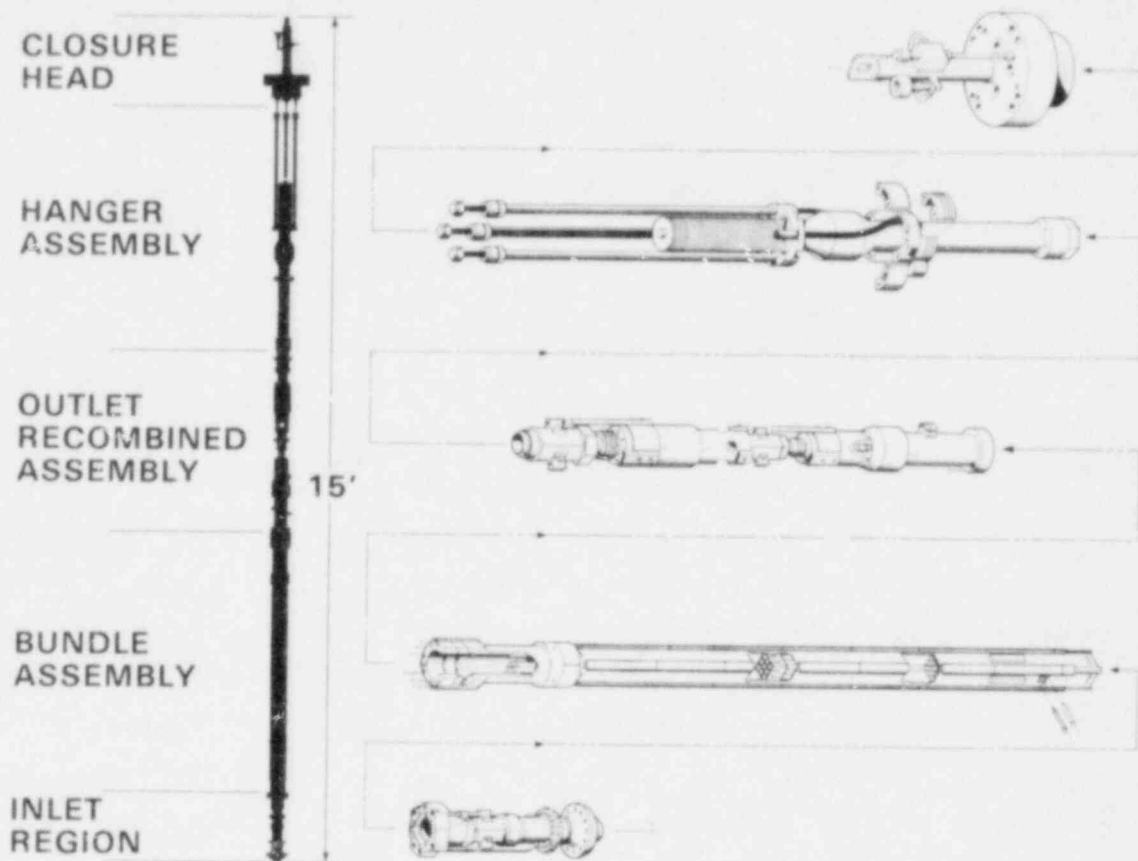


FIGURE 1. Modular Design of the Nine-Rod Fuel Bundle Assembly

The inlet, core, and outlet regions of the test train are shown in Figure 2. In the photograph, the darker portion of the assembly is the Zircaloy shroud that surrounds the nine-rod bundle; and dummy thermocouple leads may be seen exiting the shroud outlet housing (short wires just above the man's left hand). The upper portion of the test train extending from the outlet region to the closure head is shown in Figure 3; and in Figure 4, the closure head is supported in the strongback that is to be used in the MTR canal. The means of manipulating the lower portions of the train during remote assembly is illustrated. The lower end of the strongback and the associated clamps are shown in Figure 5; the core region of the test train is being packed for shipment.

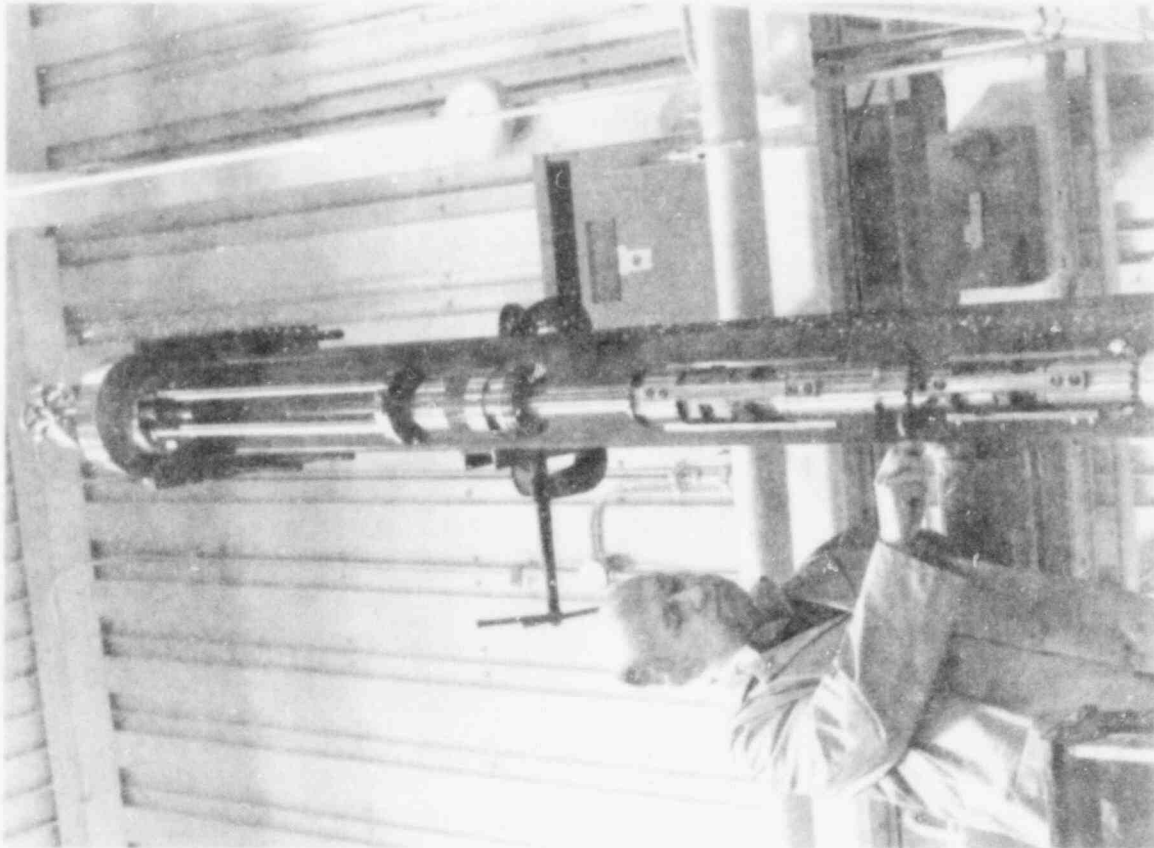


FIGURE 3. Upper Part of Test Train

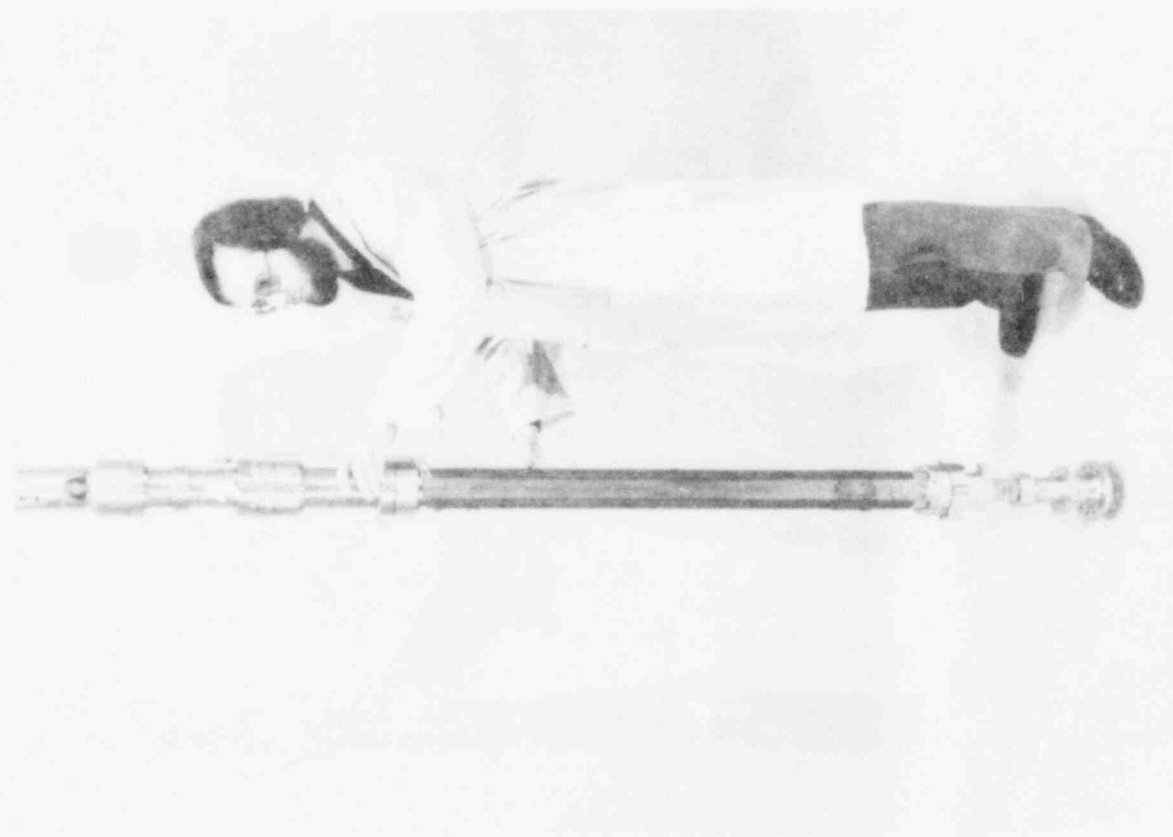


FIGURE 2. Lower Part of Test Train

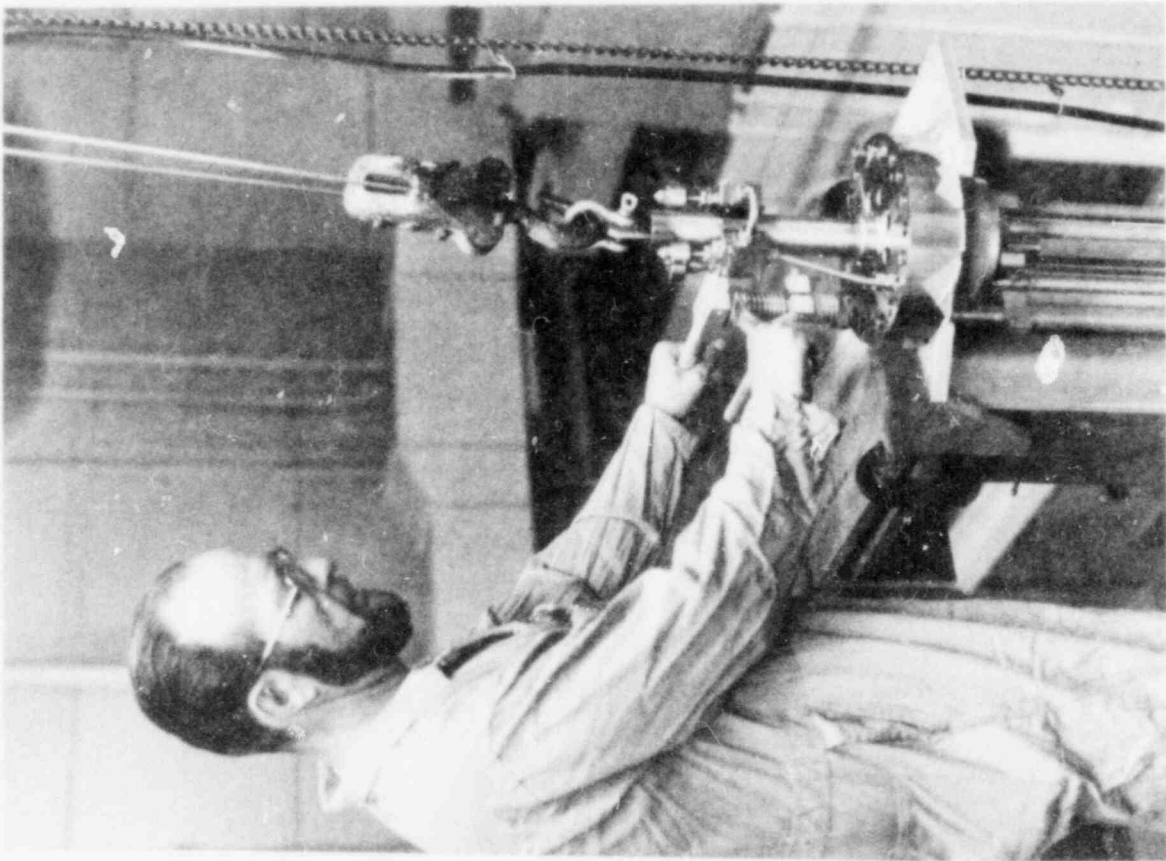


FIGURE 4. Remote Assembly of Test Train Using Strongback

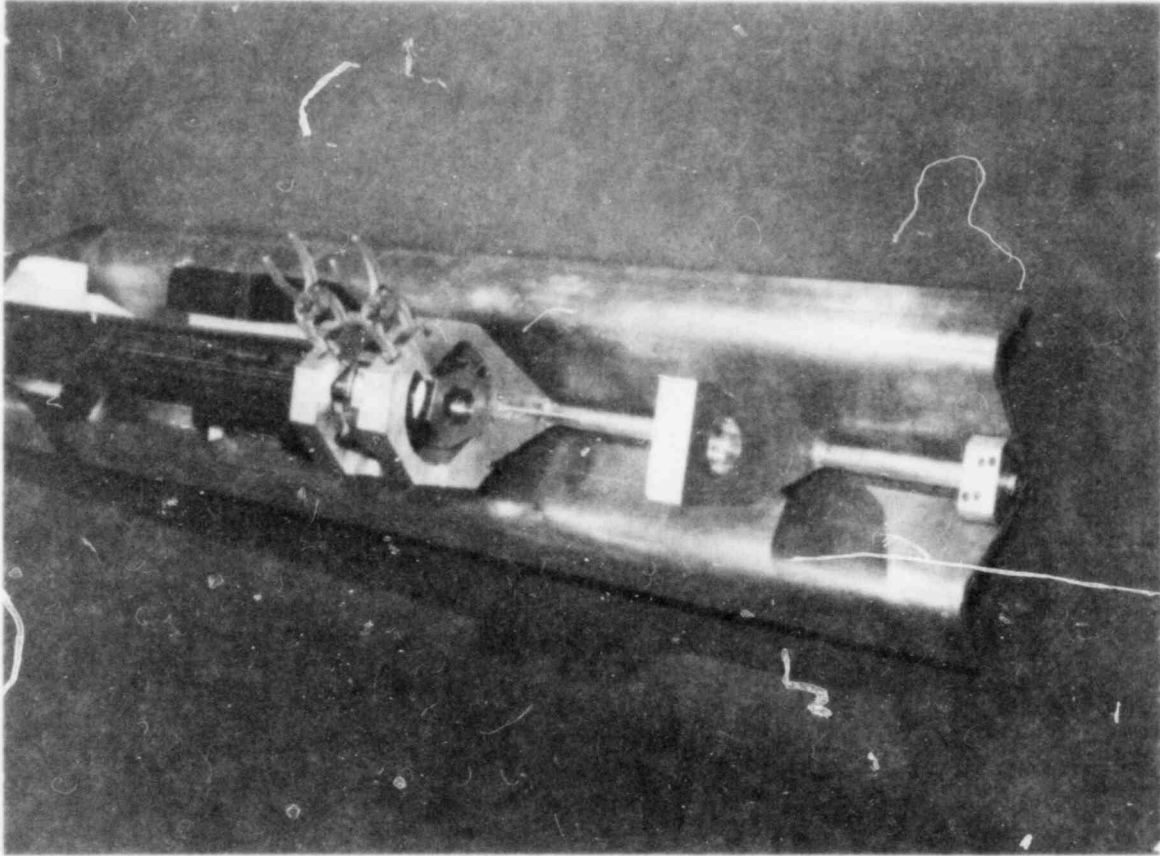


FIGURE 5. Lower End of Strongback with Partially Assembled Test Train



Figure 6 is an exploded view of the flow restrictor seal, showing four of the braze plugs that nest in the hub. The quadrant pieces clamp the braze plugs in place and support the piston rings. The piston seal rings are the last major item installed on the test train, coming up over the entire train from below.

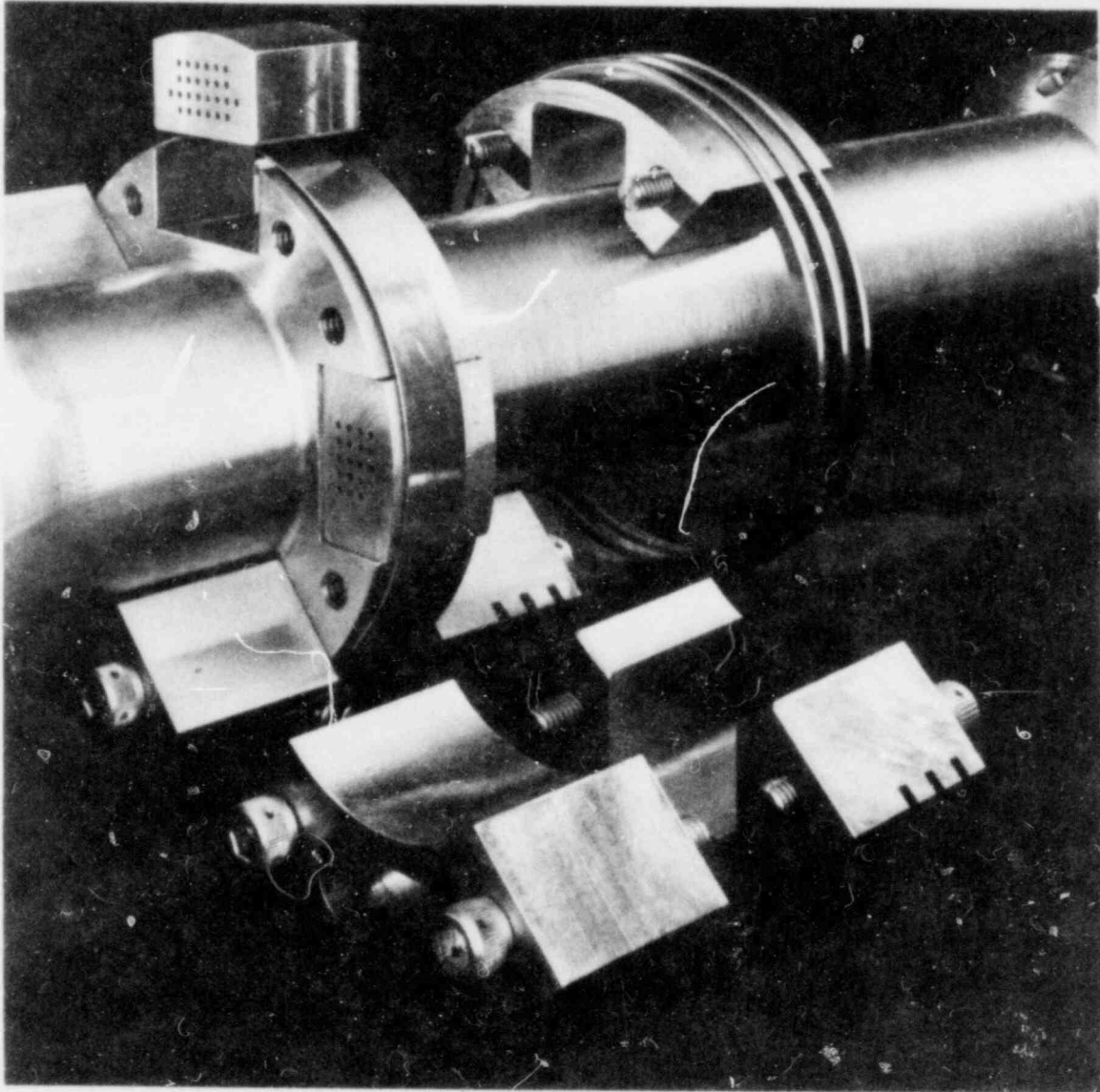


FIGURE 6. Exploded View of Flow Restrictor Seal

Figure 7 shows the Zircaloy shroud clamped into the shroud fixture. This fixture compresses the C-seals at the corners of the shroud, enabling the shroud clips to be slid over the dovetail joints. A close-up of the C-seal is shown in Figure 8.

Other important features of the test train include the retainer pins at the base of the shroud; Figure 9 shows the flat external tabs of the pins. These pins are rotated during a partial disassembly operation in the basin, allowing a single fuel rod to be replaced without dismantling the whole rod bundle. The test train is supported in the strongback during this operation. The Johnson screen, which is used to retain fuel particles that may be swept out of the bundle, is shown in position in Figure 10. Two of the hanger tubes have been removed for clarity. The screen is fabricated by winding a triangular-shaped wire, point in, around a group of ribs.

The OPTRAN 1-3 experiment involves a series of transients in the PBF. Since the instrumented fuel bundle will be composed of irradiated rods that have seen normal boiling water reactor (BWR) service, it has been necessary to develop procedures and equipment for remotely assembling the test train. The assembly work is to be done by EG&G Idaho, Inc., at INEL.

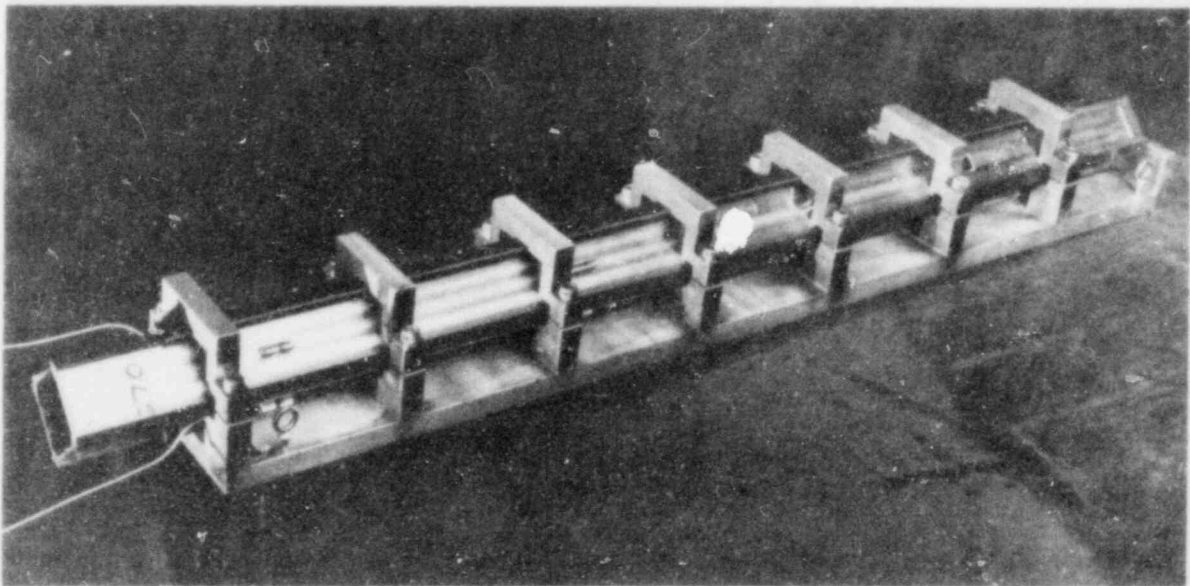


FIGURE 7. Zircaloy Shroud Clamped in Shroud Fixture

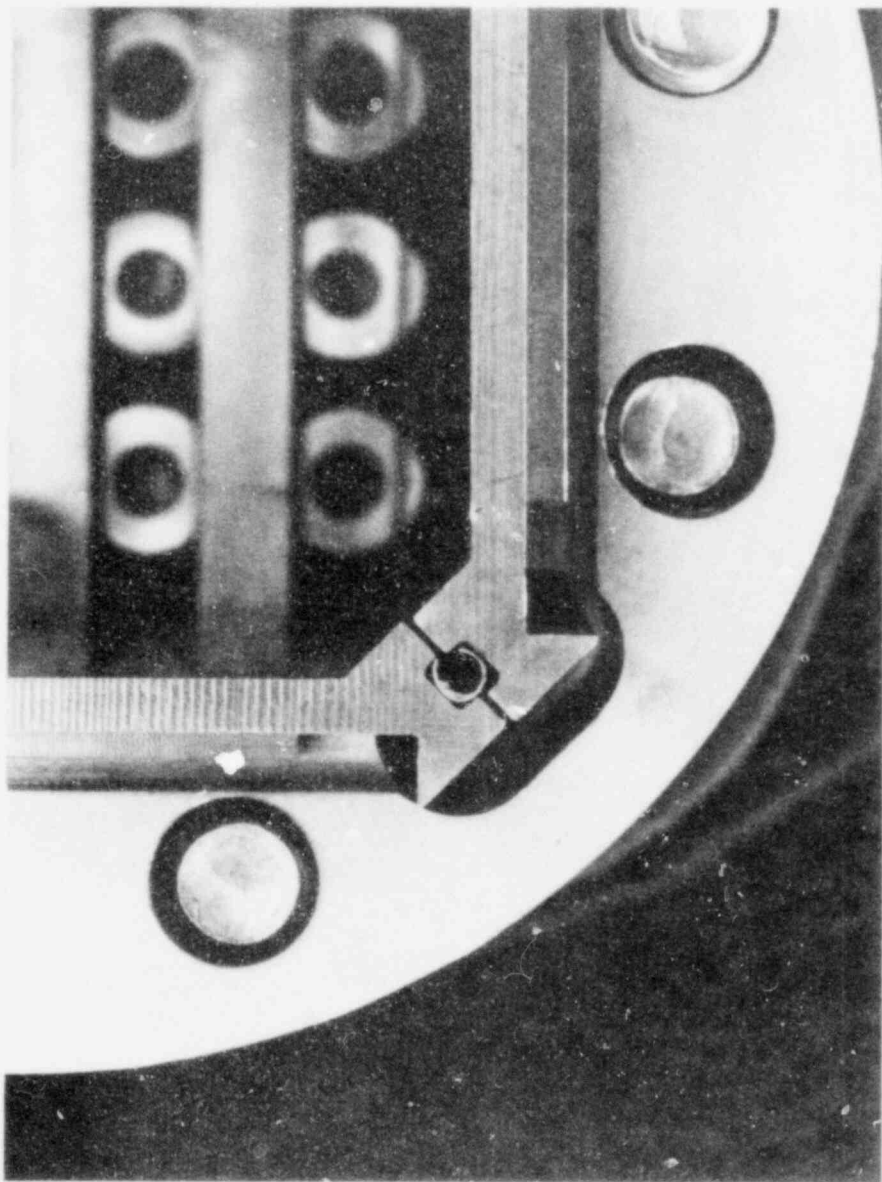


FIGURE 8. Close-Up of C-Seal in Dovetail  
Corner Joint of Shroud

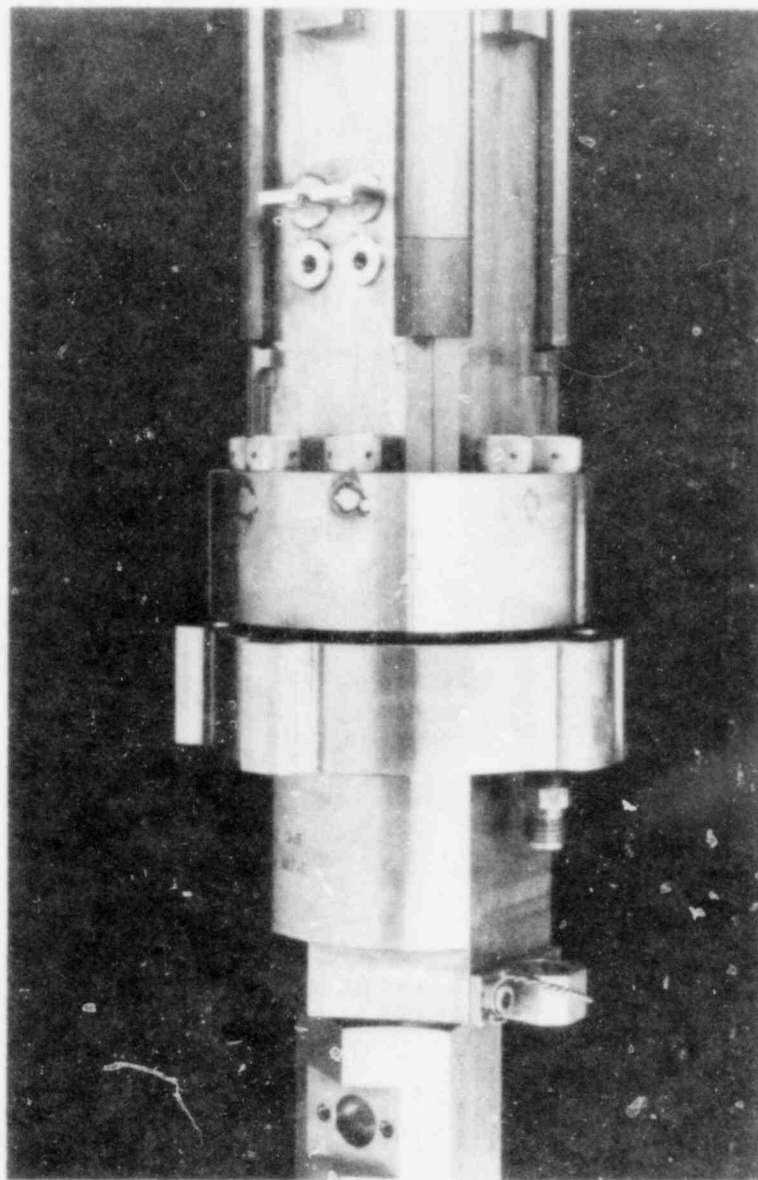


FIGURE 9. Lower End of Core Region of  
Test Train

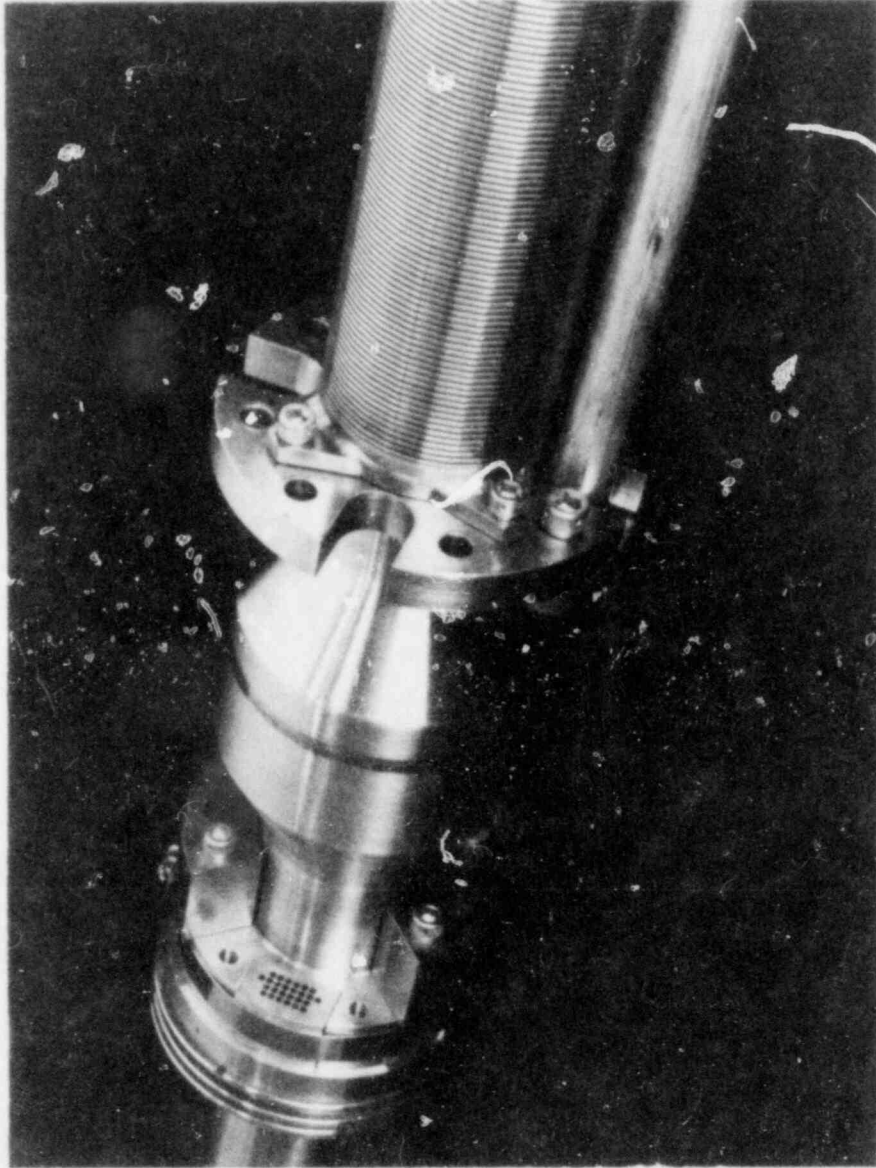


FIGURE 10. Catch Screen in Position Near Top of Test Train

#### TECHNICAL PROGRESS

Assembly and fit-up checks of test train components were completed. Modifications were made to the rod retainer pin seals where the pins penetrate the shroud. The changes brought the leak rate within specification.

Fit-up of the test train to the strongback required changes in the clamp configuration. These changes were made, and the associated drawings were scheduled for revision.

Interface dimensions were taken on the test train where it contacts the PBF in-pile tube and seal surfaces. Minor outages were handled in a Materials Review Board.

The test train hardware, instruments, and remote handling equipment were shipped to INEL on March 25, 1981.

#### FUTURE WORK

Final drawing changes will be completed in April. Remaining as-built data and other information will also be transmitted to EG&G in April. A close-out quality assurance (QA) audit will be scheduled.

The only open item on the contract is the strain gage development effort at EG&G, which is being partially supported by PNL. This work is scheduled for completion in fiscal year (FY)-1981.

PNL will provide assistance to EG&G as needed during final assembly of the OPTRAN 1-3 test train.

## CORE THERMAL MODEL DEVELOPMENT(a)

D. S. Trent, Program Manager  
M. J. Thurgood, Project Manager

T. E. Guidotti  
R. J. Kohrt  
G. A. Sly

### SUMMARY

Development assessment of the COBRA/TRAC computer code continued during the past quarter. Reasonable predictions of various two-phase flow phenomena that are important in reactor safety were made, including comparisons with reflood, transient downcomer, loop stability, and upper head drain experiments. Comparison of code predictions with experimental data is in general very good.

### INTRODUCTION

The COBRA-TF computer code is being developed as part of the U.S. Nuclear Regulatory Commission (NRC) Water Reactor Safety Research Program in the area of analysis development. The purpose of this work is to provide better digital computer codes for computing the behavior of full-scale reactor systems under postulated accident conditions. The resulting codes are being used to perform pre- and post-test analysis of light water reactor (LWR) components and system effects experiments. This Pacific Northwest Laboratory (PNL) project has two main objectives:

- to develop a hot bundle/hot channel analysis capability that will be used in evaluating the thermal-hydraulic performance of LWR fuel bundles during postulated accidents

---

(a) RSR FIN Budget No.: B2041; RSR Contact: S. Fabric.



- to develop a water reactor primary system simulation capability that can model complex internal vessel geometries such as those encountered in upper head injection (UHI)-equipped pressurized water reactors (PWRs).

COBRA-TF is formulated to model three-dimensional (3-D), two-phase flow using a three-field representation: the vapor field, the continuous liquid field, and the droplet field. The model allows thermal nonequilibrium between the liquid and vapor phases and allows each of the three fields to move with different velocities. Thus, one can mechanistically treat a continuous liquid core or film moving at a low or possibly negative velocity from which liquid drops are stripped off and carried away by the vapor phase. This is an essential feature in the treatment of the hydrodynamics encountered during the reflooding phase of a loss-of-coolant accident (LOCA). This model allows the prediction of liquid carryover in the FLECHT and FEBA<sup>(a)</sup> series of experiments. The treatment of the droplet field is also essential in predicting other phenomena such as CCFL and upper plenum deentrainment and fallback.

The code also features flexible noding, which allows modeling of the complex geometries encountered in reactor vessel internals, such as slotted control rod guide tubes, jet pumps, and core bypass regions. These geometries cannot be modeled easily in regular Cartesian or cylindrical mesh coordinates; however, since they have significant impact on the thermal-hydraulic response of the system, these geometries must be modeled with reasonable accuracy.

The fuel rod heat transfer model utilizes a rezoning mesh to reduce the rod heat transfer mesh size automatically in regions of high heat flux or steep temperature gradients and to increase the mesh size in regions of low heat flux. This model has proven very effective in resolving the boiling curve in the region of the quench front.

COBRA-TF has been implemented into TRAC-PIA as the vessel module, providing a system simulation with the capabilities described above. The resulting code, referred to as COBRA-TRAC, is being assessed by comparing its predictions

---

(a) Flooding experiment in blocked arrays experiment.

of various two-phase flow experiments with the measured data from the experiments. Several such simulations have been completed during the past quarter.

## TECHNICAL PROGRESS

### FRIGG LOOP PROJECT

The FRIGG Loop Project is an experimental investigation of the hydrodynamic and heat transfer conditions in a boiling water reactor (BWR) channel. COBRA-TRAC simulations of FRIGG tests have been done to assess the ability of the code to predict two-phase pressure drop in rod bundles, axial void distribution in the heated length, and hydrodynamic instability at high power levels.

#### Description of Experiment

The FRIGG experiments were carried out in an 8-MW loop with a uniformly heated 36-rod cluster simulating a fuel bundle for the Marviken BWR. Each rod had a heated length of 4.4 m with an outer diameter of 13.8 mm. The system pressure was maintained at 50 bar by spray nozzles in a spray condenser and an electrical heater surrounding the lower part of the condenser wall. Experiments were run in both natural and forced circulation; inlet subcooling in natural circulation was controlled by feeding water from the cooling circuit into the upper part of the downcomer.

Liquid mass velocity was measured in the downcomer using a venturi and a DP cell with fast response. Void fraction was measured by a gamma attenuation system using four gamma beams to determine the radial distribution. The device was mounted on an elevator to measure axial distribution.

#### COBRA/TRAC Model

The COBRA/TRAC model of the FRIGG loop consists of eight vessel channels; five of which model the riser and steam separator above the rod bundle. One channel models the heated length, and two channels model the inactive parts above and below the heated length. A TRAC tee component with a fill boundary condition on the secondary leg models the downcomer for the natural



circulation tests. A flow boundary condition is used for forced circulation, and a pressure boundary condition is used in both conditions at the steam exit.

### Discussion of Results

Results of COBRA simulations for several FRIGG experiments were reported in the past and showed that the COBRA code predicts the axial void fraction distribution quite well for both natural and forced circulation conditions.

To predict the liquid mass flow rate at high heat flux in natural circulation the friction factor for an unstable film has been modified. The Wallis correlation for stable films results in too little friction loss and a mass flow rate that is 8% too high. Nine times the Wallis correlation results in a mass flow rate that is 10% too low. The optimum value appears to be 5.0 times the Wallis correlation for stable films. Only the case with a heat flux of  $90 \text{ W/cm}^2$  is affected by changing the unstable film friction factor.

Hydrodynamic instability was not experimentally reached in the FRIGG loop, but the liquid mass flow variations were recorded and used to extrapolate an instability threshold at a heat flux of  $109 \text{ W/cm}^2$ . A COBRA simulation was run with similar conditions at a heat flux of  $120 \text{ W/cm}^2$ . Large fluctuations in liquid mass velocity at the inlet to the test section are shown in Figure 1 that indicate that the expected hydrodynamic instability is predicted by COBRA.

The liquid mass flow rate is affected by the hydrostatic driving head and the two-phase pressure drop through the test section. Figure 2 shows the collapsed liquid level in the test section as a function of time. The oscillations in liquid level are exactly in phase with the oscillations in liquid mass velocity. When the liquid level is at a minimum, the mass velocity is low; therefore, the hydrostatic head does not control the liquid mass flow rate. Instead the instability is driven by fluctuations in the steam generation rate that lead to a change in the two-phase pressure drop. A plot of steam generation rate versus time (see Figure 3) shows that the steam generation rate is highest when the liquid mass velocity is at a minimum. The two-phase pressure drop varies directly with the steam generation rate and therefore controls the liquid flow rate into the test section.

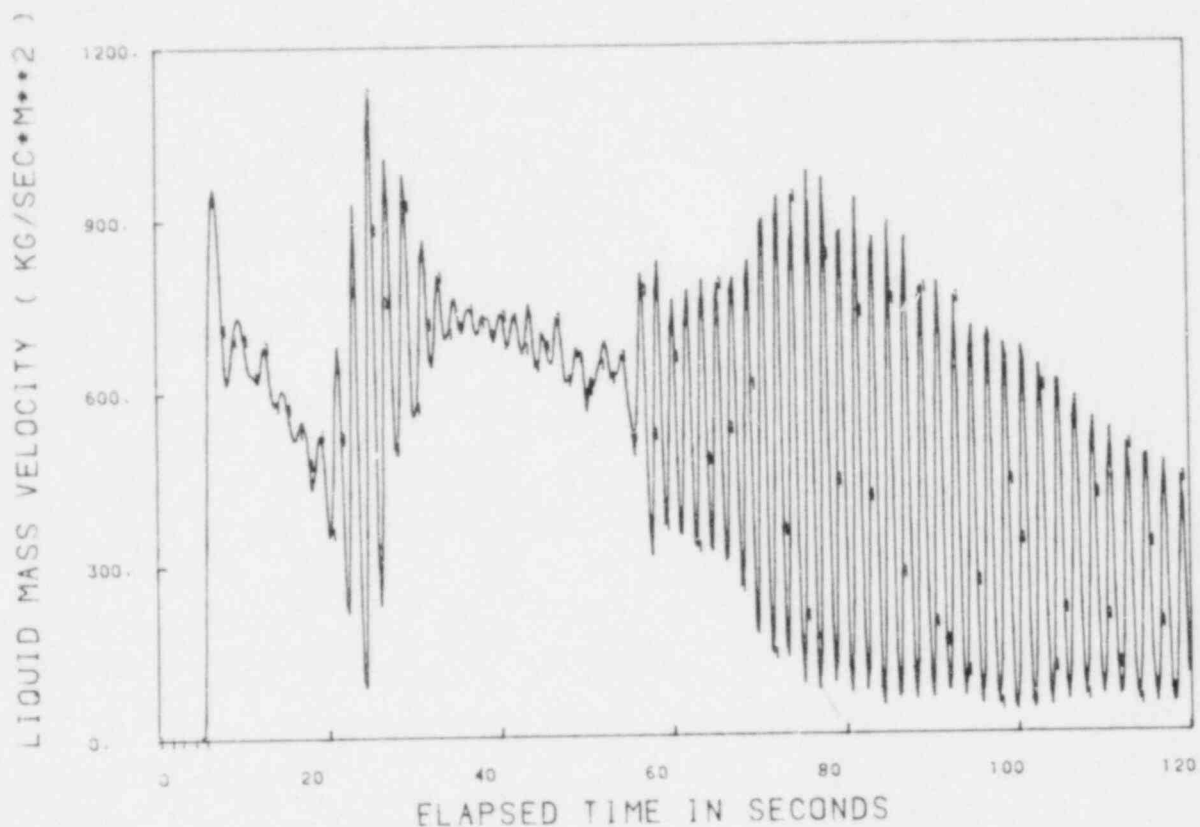


FIGURE 1. Liquid Mass Velocity Versus Time

#### WESTINGHOUSE DRAIN TEST

The Westinghouse Drain Test was run to determine the rate at which water injected into the upper head of a reactor vessel during a LOCA will drain from the upper head into the core cavity. The purpose of the COBRA-TF simulation was to determine the ability of the code to predict this drain rate.

#### Description of Experiment

The test section was designed to simulate the reactor vessel upper head on a per unit guide tube basis. A prototypical 17 x 17 rod cluster control (RCC) guide tube was used in the test and included a full-length drive rod and thermal sleeve. The support columns were simulated by two parallel pipes, but only 1-1/2 support columns are required to simulate the reactor on a per guide tube

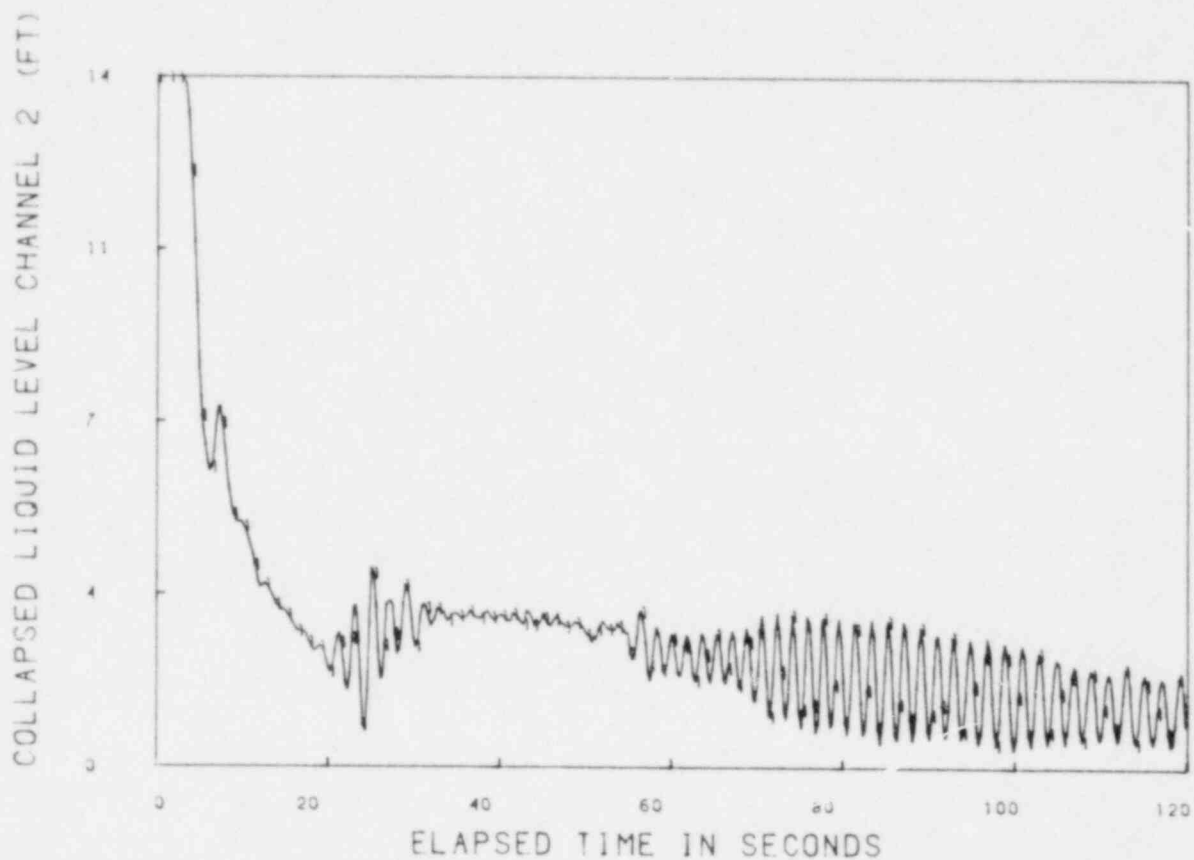


FIGURE 2. Collapsed Liquid Level Versus Time

basis. One of the support columns was orificed at the top to allow only half of the normal flow rate. Saturated steam in a specially designed steam chamber simulated the conditions in the upper plenum.

Initially the upper head and support columns were filled with water and the guide tube and upper plenum were filled with saturated steam. Steam conditions in the steam chamber, absolute pressure in the upper head, and 10 temperatures were recorded continuously throughout the test period. The time for the liquid level in the upper head to reach the top of the support column was also recorded.

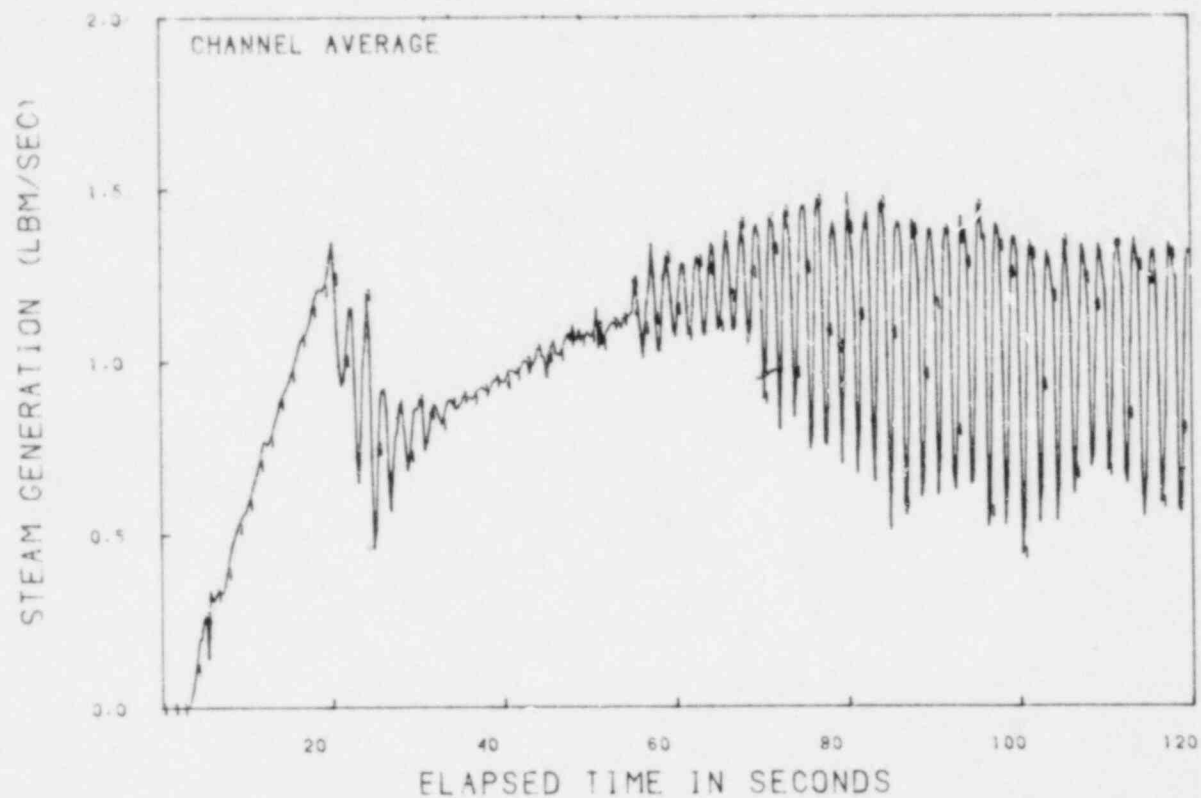


FIGURE 3. Steam Generation Rate Versus Time

#### COBRA-TF Model

The Westinghouse drain test is modeled by COBRA using five channels. Two channels with a total of 14 nodes modeled the guide tube; the two support columns are combined into one channel with 8 nodes and loss coefficients in the channel model the orifices; and the upper head is modeled by two channels with a total of 8 nodes.

A pressure, enthalpy boundary condition modeled the steam chamber at the bottom of the support columns and guide tube.

#### Data Comparisor.

Figure 4 shows the computed and experimental liquid level in the upper head; the drain time and rate are predicted well by COBRA. The largest deviations occur at the beginning and end of the transient. Toward the end of the

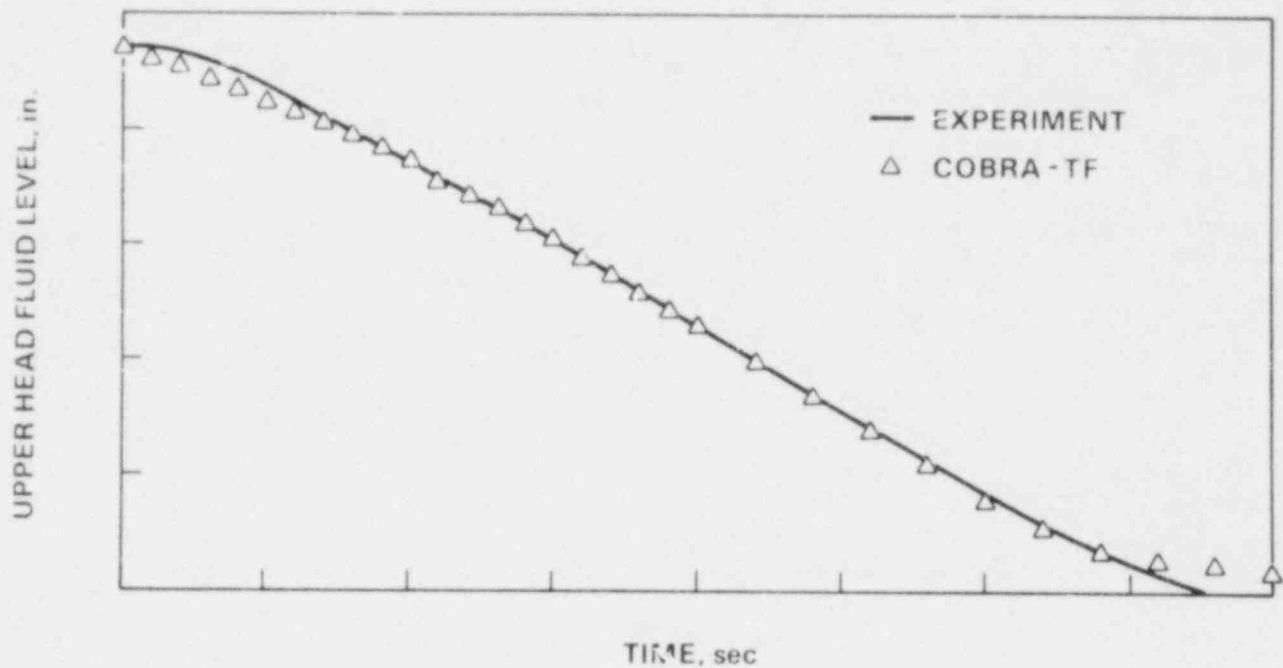


FIGURE 4. Westinghouse Drain Test No. 5, Upper Head Fluid Level Versus Time

time period a small amount of liquid was trapped in the bottom node of the upper head as liquid drains from the support column. The reason for the higher liquid penetration rate at the beginning of the transient is not clear. An outstanding data fit was obtained from 10 to 15 sec where the top of the guide tube was uncovered and the slope of the curve changed.

#### FEBA WITH AND WITHOUT GRID SPACER TEST

A COBRA-TF simulation was performed to assess the effect that grid spacers had on the desuperheating of steam during bottom reflooding of a test assembly. The simulation was modeled after experimental tests performed in Karlsruhe, West Germany, in the FEBA test assembly.

#### Experiment Description

The FEBA test facility was originally designed to simulate idealized reflood conditions in a German PWR core with constant, forced bottom reflood,

system pressure, and test section geometry. The experimental test loop consisted of five major components: the lower plenum, test section, test housing, upper plenum, and buffer tank. The test section consisted of a 5 x 5 electrical heater rod array placed in a square housing. The heater rods were held in place by a typical KWU-PWR grid spacer that was located at the test midplane and every 545 mm above and below that point.

The electrical heater rods were used to simulate nuclear fuel rods. The nuclear cosine power profile of the fuel rods was approximated by a seven-step power profile.

The test assembly was initially heated by radiation from the heater rods for about two hours prior to reflood. During this heatup phase the heater rods were surrounded by stagnant steam and had a lower power level. These test conditions were maintained until the initial peak cladding temperatures were reached. After the cladding temperatures had reached the required initial temperature, reflood was initiated. Water was injected into the lower plenum with a constant flow rate of 3.5 cm/sec, an inlet temperature of 40°C, and at a pressure of 4 bars. When the rising water reached the bottom end of the heated length, the rod power was stepped up to a decay heat level comparable to the ANS +20% value for 40 sec after shutdown and followed this curve for the remainder of the transient.

#### COBRA/TF Model

The FEBA test facility was modeled with four COBRA-TF channels: one channel for the lower plenum and three for the heated length and upper plenum. A total of 19 fluid nodes were in the four channels. The 25 heater rods were approximated by a single COBRA-TF rod with the average thermal properties of all the heater rods. The test section housing was modeled by a second COBRA-TF rod with an inside heat transfer surface and an insulated outer surface.

The system was initialized with saturated steam at 2.8 bars. A constant flow boundary of 3.5 cm/sec was specified at the bottom of the vessel and a pressure boundary of 2.8 bars was specified at the test section outlet.

The heater rod was initialized with an axial temperature profile from top to bottom with a maximum cladding temperature of 850°C and an axial step power profile with a maximum peak power of 0.8 kW/ft. The housing rod was initialized with an axial temperature profile, a peak temperature of 650°C, and zero power generation. Both rod temperature profiles were symmetric about the test section midplane.

The reflood transient was run from a standing start, with the initial parameters mentioned earlier and the ANS +20% rod power decay. The simulation continued until 75% of the heated test rod was completely quenched.

### Discussion of Results

Figures 5 and 6 show the computed and experimental temperature versus time plots at two axial levels. For data comparison purposes, the FEBA temperature data were visually extracted from the available reports and then averaged at a particular axial position. The figures show that COBRA-TF does a rather good job of predicting peak temperatures and the quench time, implying that the amount of steam desuperheating due to the existing grid spacer model is of the proper order and that the model is working properly for this particular type of experiment. Further examination of the figures shows that at higher elevations the calculated quench time becomes increasingly greater than the experimental value.

### Conclusions

Although discrepancies currently exist between the COBRA-TF prediction and the experimental results, it is felt that COBRA-TF did a very good job of predicting peak temperatures and quench times.

### TRANSIENT BATTELLE COLUMBUS DOWNCOMER SIMULATIONS

Two transient Battelle Columbus downcomer tests were simulated this quarter. These calculations assessed COBRA-TF's ability to predict the combined effects of ramped reverse core steam flow, subcooled emergency core cooling (ECC) water, and hot walls on the penetration behavior during countercurrent flow in a downcomer.

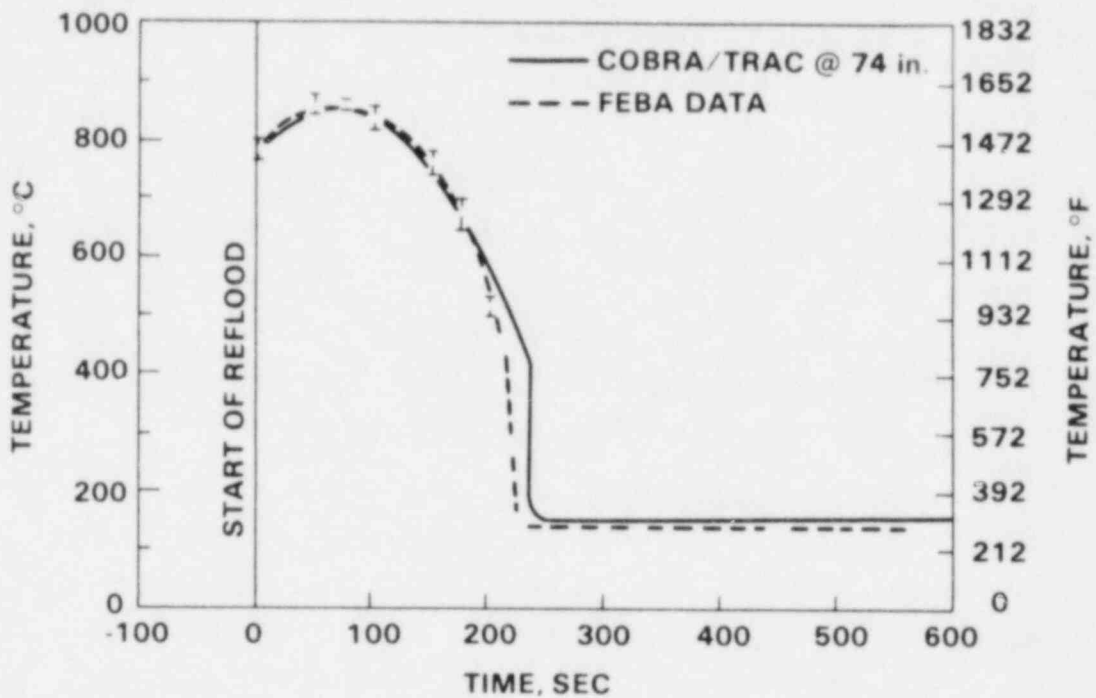


FIGURE 5. Computed and Experimental Temperature Versus Time Plot at an Axial Level of 74 in.

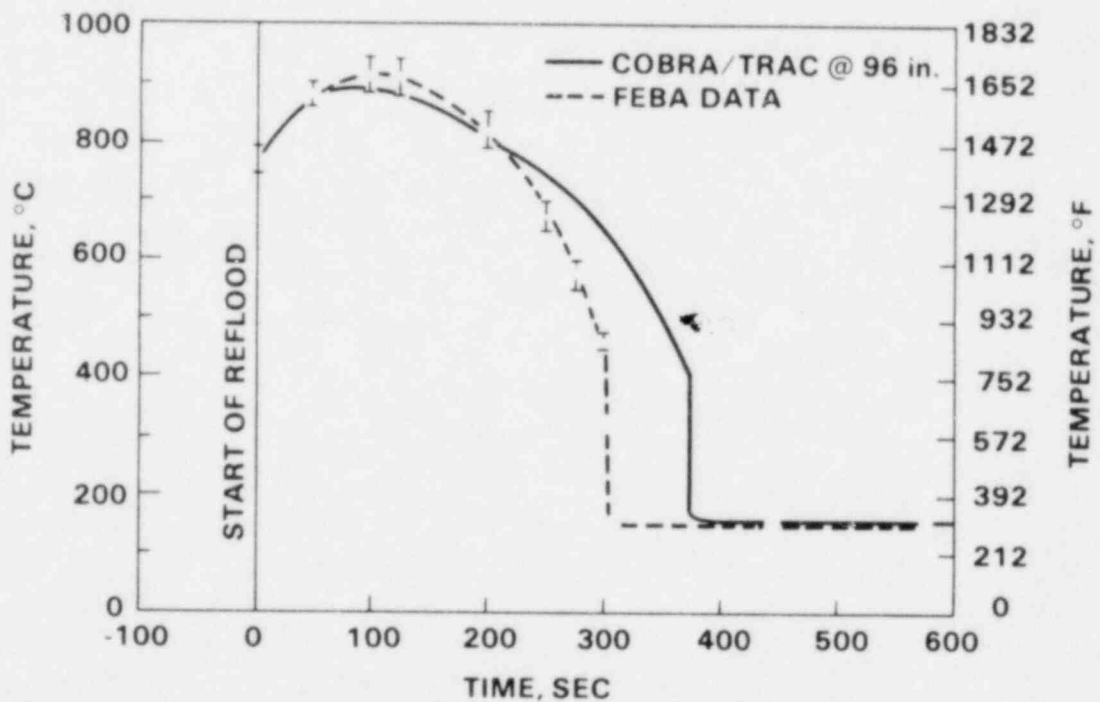


FIGURE 6. Computed and Experimental Temperature Versus Time Plot at an Axial Level of 96 in.



The test vessel was a 2/15-scale PWR downcomer with an extended lower plenum. The downcomer was 41.0 in. high with a circumference of 72.6 in. and a gap of 1.23 in. For a complete facility description, see Reference 1.

The COBRA-TF model consisted of 9 channels, 7 gaps, and 57 fluid cells. Six channels and seven axial levels were used to model the downcomer. Constant mass flow rate boundary conditions were used to represent the three cold leg ECC injection locations, and a time-dependent mass flow rate boundary condition was used to specify the reverse core steam flow rate. The break cold leg was modeled using a constant pressure boundary condition.

Figures 7 and 8 show the lower plenum liquid volume versus time (ECC started at 1 sec) for the ramped steam, hot wall tests 404 and 501.<sup>(2)</sup> The test conditions are given in Table 1. The data comparison is good: COBRA-TF predicted the initial time delays to within 1 sec; and the filling rate for test 404 is in excellent agreement. A slightly higher filling rate occurred in test 501 because the containment pressure used in COBRA-TF was too high. This data comparison would improve if the transient containment pressures were used; however, only the initial containment pressure was given in the data report.

TABLE 1. Battelle Columbus Downcomer Test Conditions

Test Number	Initial Wall Temperature, °F	Initial ECC Subcooling Temperature, °F	Initial Steam Flow Rate, lbm/sec	ECC Injection Rate, gpm	Containment Pressure, psia
404	355	121	5.55	243	28.3
501	550	105	3.28	412	81.9

#### FUTURE WORK

System simulations of semiscale, CCTF, PKL, and a UHI plant are currently being run. These simulations will complete the development assessment effort. COBRA/TRAC is expected to be released toward the end of the next quarter. Development of the hot bundle version of COBRA-TF will continue.

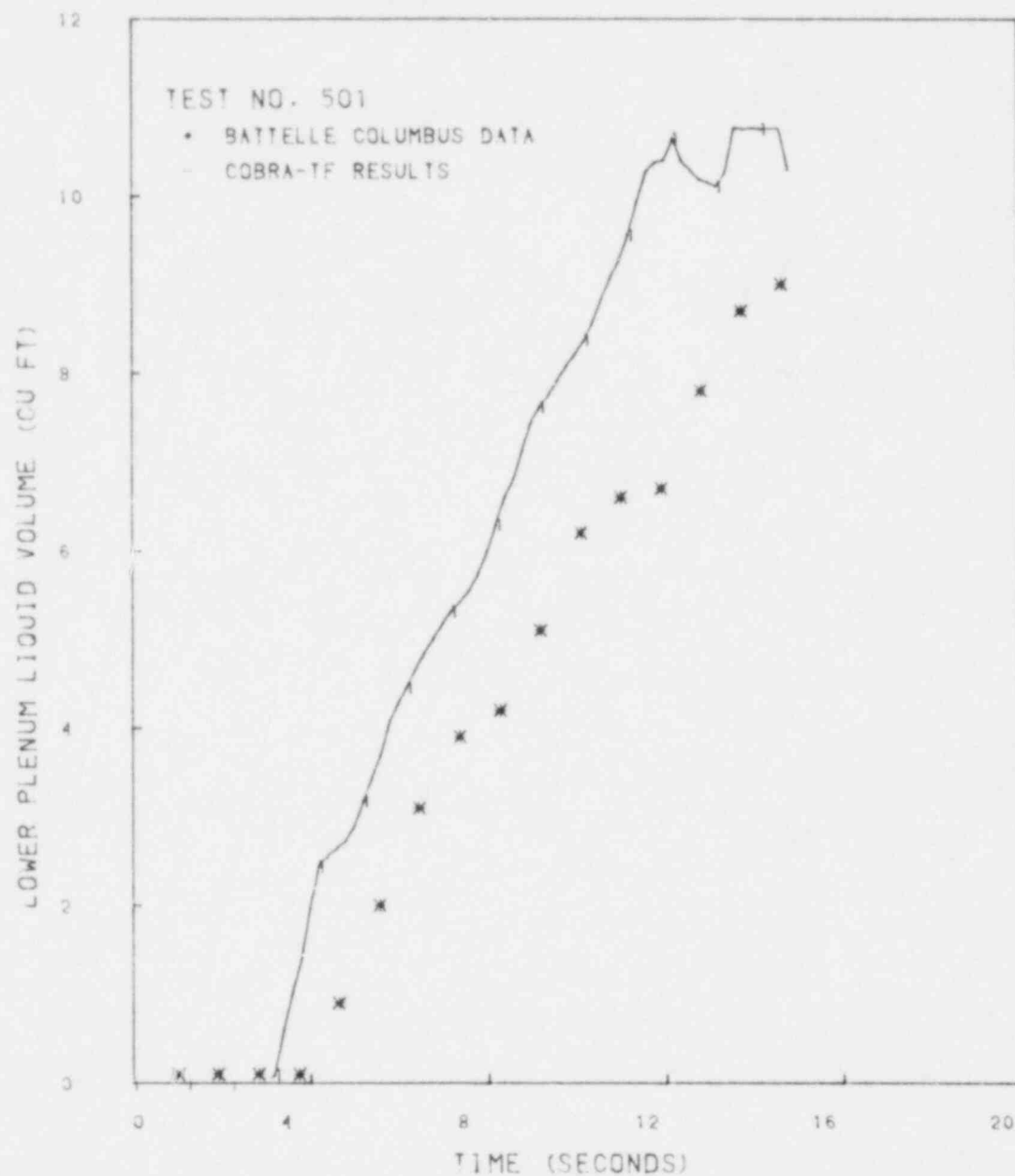


FIGURE 7. Lower Plenum Liquid Volume Versus Time Plot for Test 501

REFERENCES

1. Carbiener, W. A., et al. 1977. Steam-Water Mixing and System Hydrodynamics Program, Quarterly Progress Report, January 1 to March 31, 1977. BMI-NUREG-1972, Battelle Columbus Laboratories, Columbus, Ohio.

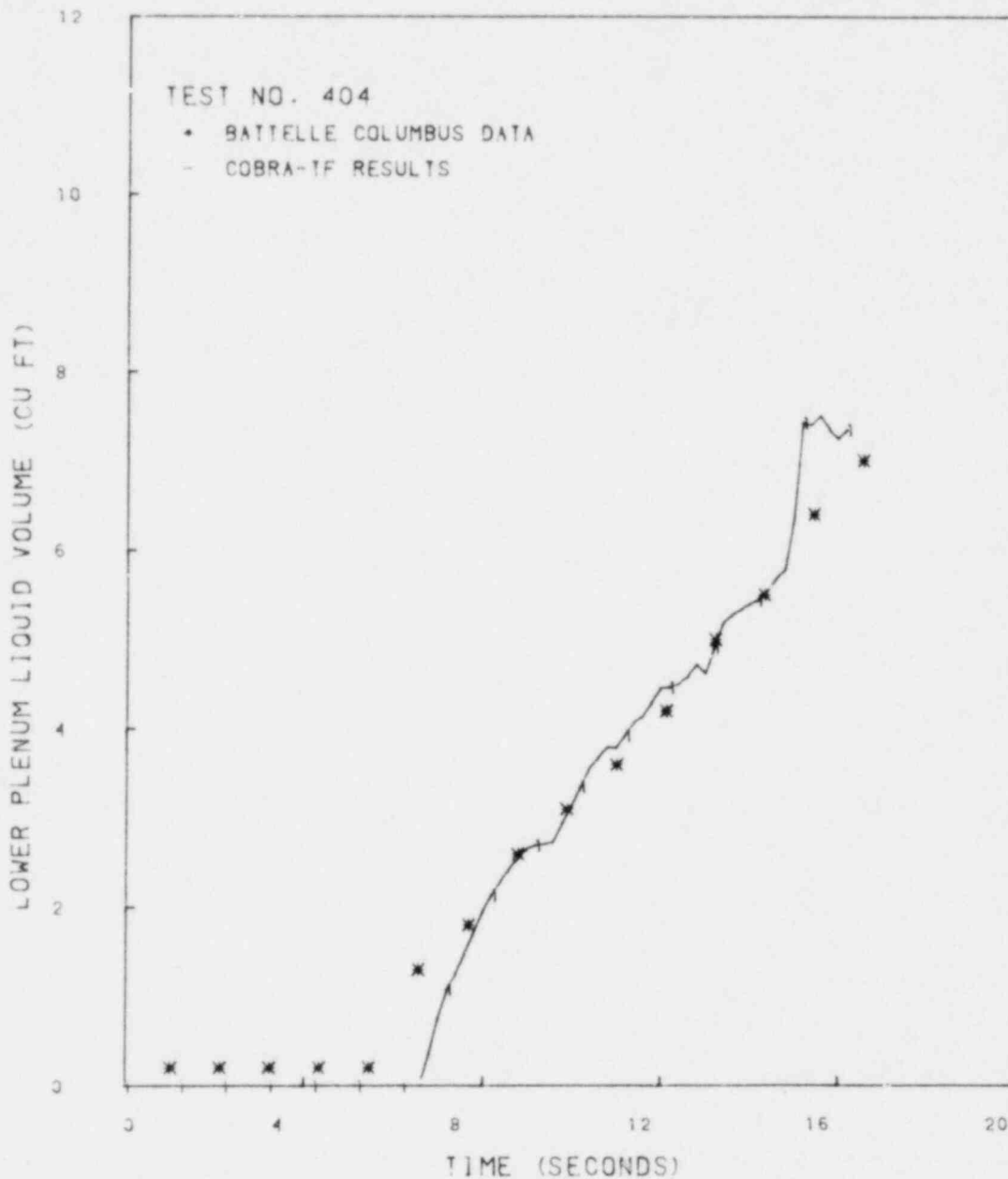


FIGURE 8. Lower Plenum Liquid Volume Versus Time Plot for Test 404

- Collier, R. P., et al. 1978. Steam-Water Mixing and System Hydrodynamics Program, Quarterly Progress Report, April 1 to June 30, 1978. NUREG/CRO526, BMI-2011, Battelle Columbus Laboratories, Columbus, Ohio.

## LOCA SIMULATION IN NRU(a)

C. L. Mohr, Project Manager

J. P. Pilger, Assistant Project Manager

P. N. McDuffie, Project Administration

### SUMMARY

The thermal-hydraulic test series review meeting was conducted in Silver Spring, Maryland, February 4 and 5, 1981. This meeting was attended by representatives from British, Japanese, and the United States nuclear industries. Test results were well received by all those in attendance, and the British expressed an interest in participating in the program. The first Materials Test (MT-1) was rescheduled to the March 30-April 3 window at Chalk River Nuclear Laboratories (CRNL).

### INTRODUCTION

The objective of the Pacific Northwest Laboratory (PNL) LOCA Simulation in NRU Program is to provide information on the heatup, reflood, and quench phases of a loss-of-coolant accident (LOCA). The tests are designed to give information on the quench-front velocities within a fuel bundle, the liquid entrainment [10 CFR 50, App. K (Sec. ID 2)], and the heat transfer coefficients [10 CFR 50, App. K (Sec. ID 5)] for full-length pressurized water reactor (PWR) fuel as a function of reflood rate and delay time before reflood starts. A total of six test trains will be prepared for the program. The first test train will be devoted to thermal-hydraulic behavior, and more than 25 tests are planned. The remaining five test trains will be used for only one test each. These test trains will have prepressurized fuel rods; and, as a result, the rods will deform and rupture during the test. These materials tests will evaluate the effects of ballooning and rupture on quench-front velocities and associated heat-transfer coefficients.

---

(a) RSR FIN Budget No.: B2277; RSR Contact: R. Van Houten.

The test loop in the NRU reactor (Chalk River, Canada) will accommodate the 12-ft long, 32-pin bundle on a 6 x 6 array with the corner pins removed. The bundle design uses commercial enrichments, cladding dimensions, and grid spacers.

#### TECHNICAL PROGRESS

Fabrication, assembly, and checkout of the MT-1 test train were completed; and the unit was shipped to CRNL for testing on April 2, 1981. Tentative test conditions selected are: peak cladding temperature = 1600<sup>0</sup>F; reflood delay = 30 sec; reflood rate = 2 in./sec.

MT-1 will be the first of a series of tests using pressurized fuel rods in the test cruciform and represents the low-temperature range of the series.

The disassembly, examination, reassembly machine (DERM) was assembled, shipped, and installed in the fuel bay at NRU. Initial examination of the thermal-hydraulic test train is scheduled to start April 3, 1981. Both optical (periscope and TV) and physical measurements are planned.

## STEAM GENERATOR TUBE INTEGRITY(a)

R. A. Clark, Project Manager  
V. F. FitzPatrick, Deputy Project Manager

J. M. Alzheimer  
R. L. Burr  
P. G. Doctor  
G. R. Hoenes  
G. H. Lyon  
C. J. Morris  
K. R. Wheeler

### SUMMARY

The Steam Generator Examination Facility (SGEF) is 14.6% complete; construction is six weeks ahead of schedule. Efforts to establish a Steam Generator Group Project proceeded on several fronts; letters of interest have been received from several potential sponsors. Programmatic tasks that precede research on the Surry generator continued per plan, the health physics task was initiated, and the data management task is progressing. Research continued on stress corrosion crack (SCC) characterization and leak rate determinations.

### INTRODUCTION

The Steam Generator Tube Integrity Program (SGTIP) is a multiphase, multi-task laboratory program conducted at Pacific Northwest Laboratory (PNL). The principal objective is to provide the U.S. Nuclear Regulatory Commission (NRC) with validated information on the remaining integrity of pressurized water reactor (PWR) steam generator tubes where service-induced degradation has been indicated. An additional objective is to evaluate nondestructive instrumentation/techniques to examine defects in piping or tubing that serves as the reactor primary system pressure boundary.

Initial program tasks included producing a matrix of steam generator tube specimens with mechanically or chemically induced flaws that simulated defects

---

(a) RSR FIN Budget No.: B2097; RSR Contact: [redacted]

found in nuclear steam generator service. These flawed specimens are then fully nondestructively characterized by means of positive replication and various nondestructive testing (NDT) techniques, mainly eddy current testing. The tube specimens are next tested to failure at PWR steam generator operating temperatures. The failure strength, actual flaw dimensions, and NDT-indicated flaw dimensions are used to derive mathematical relationships; and these relationships are subsequently plotted to provide, within a statistical certainty band, the remaining mechanical integrity of a steam generator tube as a function of its flaw type and size as indicated by eddy current testing.

Early work showed that conventional, single-frequency, eddy current evaluation of steam generator tubes as used for in-service inspections (ISIs) could be improved. Thus, program efforts were expanded to include new eddy current measurement techniques, the effects of different calibration standards, and a more complex statistical analysis of NDT data.

The first two phases of the program involved the study of mechanically (Phase I) and chemically (Phase II) defected tubing. Phase III of the original program included correlating the mathematical models developed in Phases I and II with actual service-flawed tubing. However, a lack of suitable specimens led to the redirection of Phase III into an effort to conduct extensive nondestructive and destructive evaluations on a retired-from-service nuclear steam generator. A generator<sup>(a)</sup> removed from the Surry II nuclear plant (Surry, Virginia) after six years of service was judged suitable for this research.

Initial efforts on the Surry generator were concerned with licensing and transport activities to bring the unit from Virginia to Hanford, Washington. The generator is now at Hanford and will remain on a storage pad until a specially designed containment facility (the SGEF) is completed. The SGEF will be

---

(a) The Surry II generators were among the first removed from service in the United States; they contain evidence of most of the degradation mechanisms identified in steam generators and have features that are common to many similar units.

equipped to allow both nondestructive examination (NDE) and physical sectioning of the generator. Capabilities to perform chemical cleaning and decontamination will also be included.

Research efforts on the Surry IIA generator will be initiated shortly after the generator is placed in the SGEF, which is scheduled for completion in November 1981. Research will be conducted in the following areas:

- NDT technique verification and instrument development
- defect matrix identification
- profiling of defect types, extent, and locations
- identification of deposits and sources of corrosion
- verification of tubing and secondary support structure component integrity
- health physics.

The generator will also become a source of specimens with service-induced flaws for various NRC programs. Planned future research phases include simulated operation of a portion of the generator to assess long-term effects of possible chemical cleaning or decontamination procedures on generator serviceability that may be proposed to NRC for licensing. Study of the recovery and reuse of materials in decommissioned reactor components is another potential research task.

#### TECHNICAL PROGRESS

The following paragraphs detail progress of program tasks active this past quarter.

#### SURRY GENERATOR PROJECT

The Surry IIA generator remains at an access-controlled interim storage site on the Hanford Reservation. The generator is maintained under an argon gas purge that keeps it a 1/2-psi positive pressure relative to the surrounding atmosphere.



### Steam Generator Examination Facility

Figures 1, 2, and 3 illustrate the construction status of the SGEF as of the end of this reporting period. All cast-in-place concrete structural components of the tower portion of the building are complete, and all excavation activities have been completed. Forming for the support building foundation is in place. Precast concrete wall modules have been manufactured as have the radiologic shield doors. Construction is 14.6% complete and six weeks ahead of schedule. No change orders, modifications, or work delays that would affect costs have occurred.

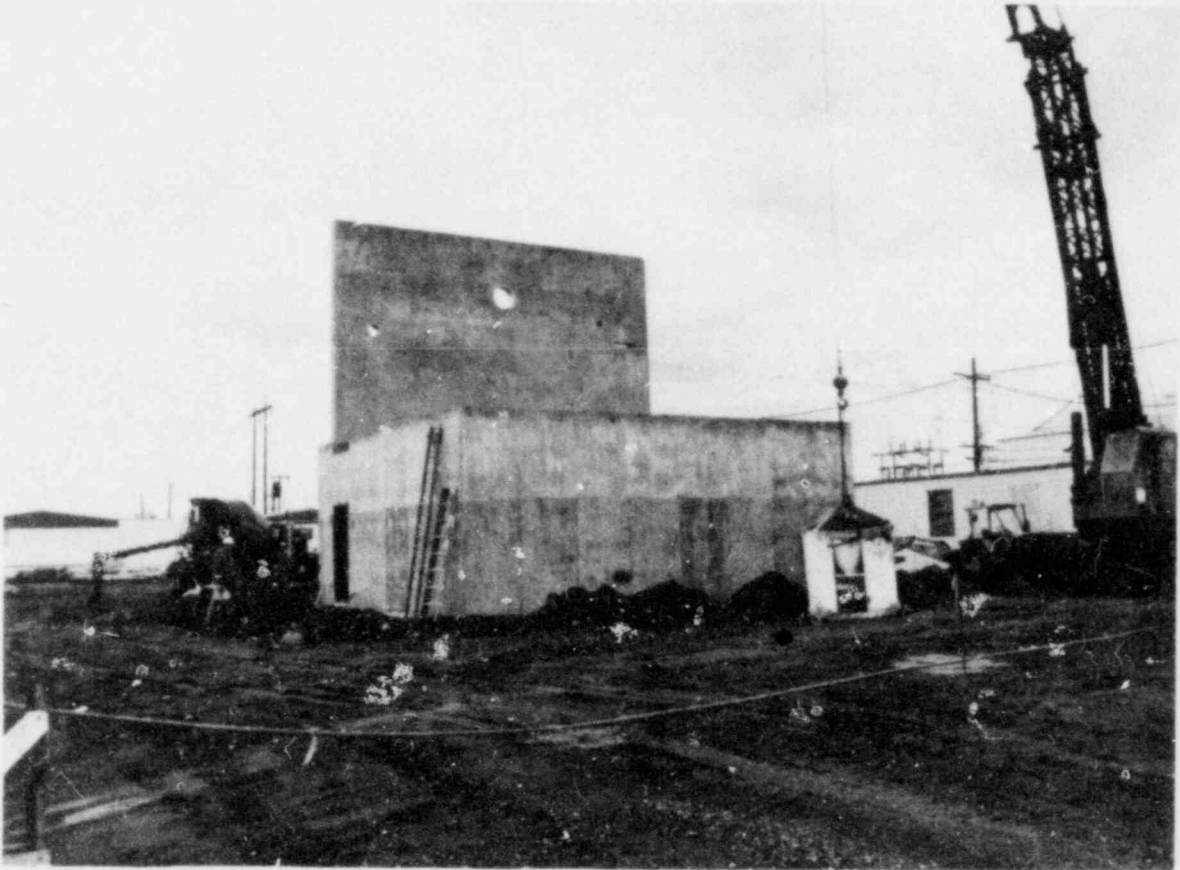


FIGURE 1. Cast-in-Place Tower Portion of Steam Generating Examination Facility

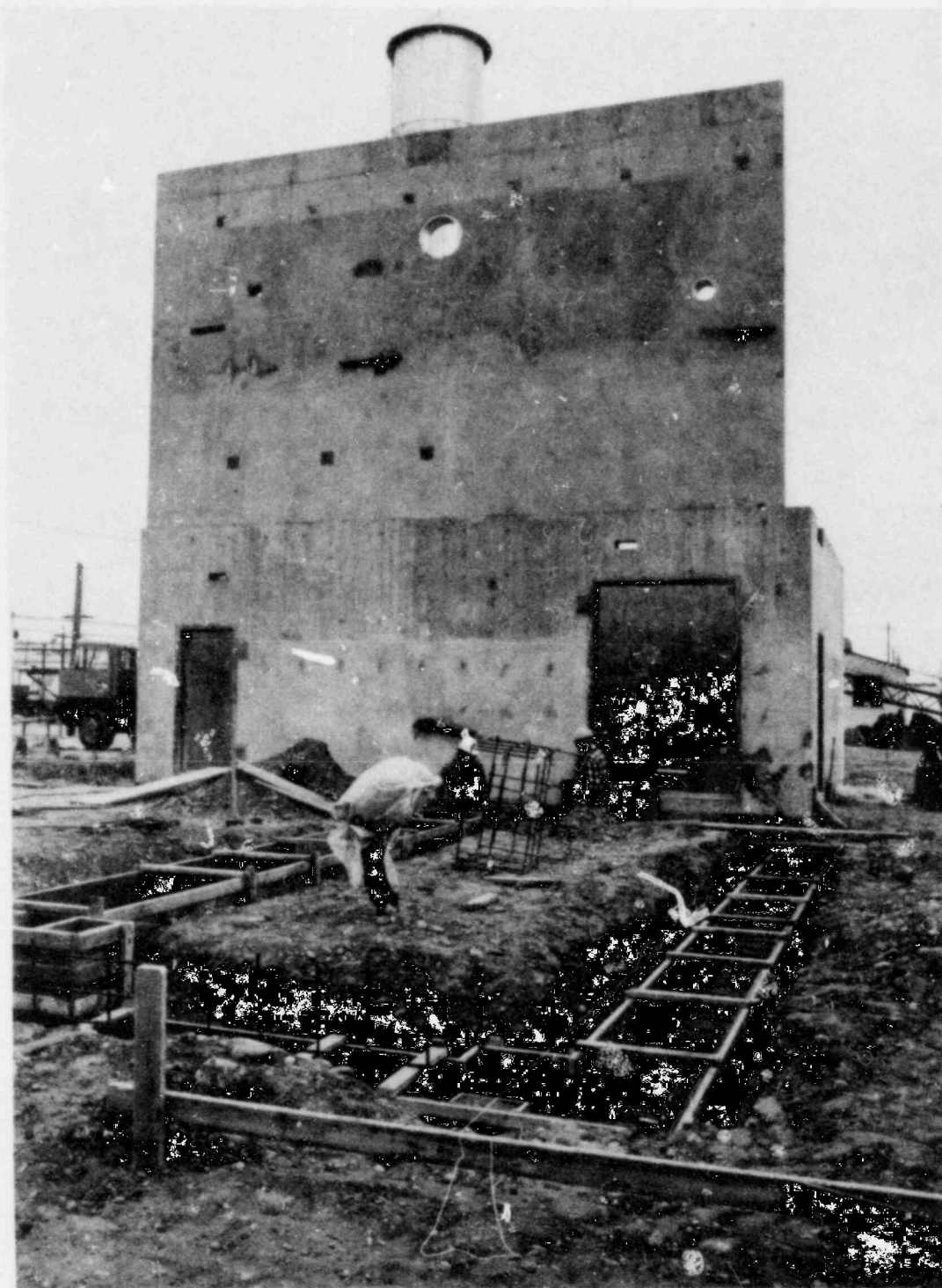


FIGURE 2. View of Tower Showing Foundation Forms for Support Building Portion of Facility



FIGURE 3. View into Tower Showing Depth of Excavation and Generator Support Pad

#### Generator Research Tasks

The data management system task will provide computer software and arrange for use of computer hardware to handle information derived from research on the Surry generator. During the past quarter a definition of the form and amount of input data has been established and an analysis has been made of computational needs as well as forms of data retrievability. Based on this background information three computer software/hardware alternatives were developed and are undergoing evaluation in terms of cost/benefits and staff availability. The alternatives basically represent tradeoffs between purchasing sophisticated hardware, software development requirements, and degree of automation in data

input and signal processing. The generalized format of data handling is based on the evaluation that approximately 750 mega-bytes of information will be stored and information will be handled in digitized form. Since most nondestructive examination (NDE) data are analog, the task is addressing questions on sampling frequency to digitize these data without loss of information.

A VAX 11/780 computer system with software for analysis of large data sets is in place at PNL and has been made available to the program. Necessary peripherals are being identified for purchase.

The health physics task was initiated this quarter. Procedures for personnel exposure monitoring, control, and documentation will be established and coordinated, including review of procedures submitted by subcontractors. Procedure guidelines will be prepared for administrative control of operations involving access to the internals of the heat exchanger. Health physics research activities will include radiologic mapping, determination of the effectiveness of decontamination efforts, and evaluation of waste and waste disposal problems associated with different operations. This quarter preparation of administrative procedures for operation of the SGEF, establishment of a personnel training program, and definition of equipment and data handling needs for research aspects of the task were begun.

Other tasks initiated this quarter associated with the Surry generator include those to move the generator into the SGEF, reopen pre-shipment examination penetrations, and decontaminate the channel head. These tasks are basically subcontracted items; efforts to date have involved preparation of statements of work.

#### Management Activities

Efforts continued to establish a Steam Generator Group Project to broaden sponsorship and technical support of research on the Surry IIA steam generator. Several favorable responses have been received from potential sponsors. A European trip is planned to discuss technical details and present contracting information to these parties. A large part of this quarter's management endeavor has involved establishing suitable operating contract provisions and seeking necessary approvals.

A midyear program review was held in Washington, D.C. Details on current tasks and schedules were presented; in addition, draft plans for FY-1982 and preliminary data for FY-1983 planning were discussed. All current activities are on schedule and within budget.

## PHASE II - STEAM GENERATOR TUBE INTEGRITY PROGRAM

### Stress Corrosion Cracking Characterization

Efforts are continuing at definitive nondestructive characterization of laboratory-produced intergranular stress corrosion cracking (IGSCC) in Inconel 600 steam generator tubes. A group of 10 round robin specimens was nondestructively characterized by J. A. Jones Applied Research and Zetec this past quarter. A confirmatory destructive assay is planned for the end of the current quarter.

### Leak Rate Tests

Production of the matrix of test specimens with through-wall SCCs of various lengths and orientations continues. Specimen fabrication is to be completed and leak rate testing will be conducted during the coming quarter.

### Milestones

- health physics task initiated
- channel head decontamination task initiated
- task to reopen preshipment examination penetrations initiated.

### Problems

There is some delay in publishing reports due to technical staff manpower limitations. The high-temperature, high-pressure flow meter purchased for leak rate testing failed during a trial run. The device was returned to the manufacturer for repair.

## FUTURE WORK

During the coming quarter the following activities will be pursued:

- travel to Europe to establish participation in the Steam Generator Group Project

- conduct leak rate tests
- conduct destructive assay of round robin SCC specimens
- initiate NDT task for Surry generator examinations
- issue a preliminary report on the data acquisition task.



DISTRIBUTION

No. of  
Copies

No. of  
Copies

OFFSITE

	A. A. Churm DOE Patent Division 9800 S. Cass Avenue Argonne, IL 60439	G. P. Marino U.S. Nuclear Regulatory Commission Reactor Safety Research Division Washington, DC 20555
788	U.S. Nuclear Regulatory Commission Division of Technical Information and Document Control 7920 Norfolk Avenue Bethesda, MD 20014	10 J. Muscara U.S. Nuclear Regulatory Commission Reactor Safety Research Division Washington, DC 20555
2	DOE Technical Information Center	M. L. Picklesimer U.S. Nuclear Regulatory Commission Reactor Safety Research Division Washington, DC 20555
	R. F. Abbey, Jr. U.S. Nuclear Regulatory Commission Reactor Safety Research Division Washington, DC 20555	M. Vagins U.S. Nuclear Regulatory Commission Reactor Safety Research Division Washington, DC 20555
	S. Fabic U.S. Nuclear Regulatory Commission Reactor Safety Research Division Washington, DC 20555	R. Van Houton U.S. Nuclear Regulatory Commission Reactor Safety Research Division Washington, DC 20555
	R. B. Foulds U.S. Nuclear Regulatory Commission Reactor Safety Research Division Washington, DC 20555	M. A. Wolf Department of Atmospheric Sciences Oregon State University Corvallis, OR 97330
	D. A. Hoatson U.S. Nuclear Regulatory Commission Reactor Safety Research Division Washington, DC 20555	L. Agee Electric Power Research Institute P.O. Box 10412 Palo Alto, CA 94304
	W. V. Johnston U.S. Nuclear Regulatory Commission Reactor Safety Research Division Washington, DC 20555	B. R. Sehgal Electric Power Research Institute P.O. Box 10412 Palo Alto, CA 94304

No. of  
Copies

F. Shakir  
Department of Metallurgy  
Association of American Railroads  
3140 S. Federal  
Chicago, IL 60616

SM-ALC/MMET  
Attn: Capt. John Rodgers  
McClellan AFB, CA 95652

Dr. Sotirios, J. Vahaviolos  
Western Electric, ERC  
P.O. Box 900  
Princeton, NJ 08540

Jerry Whittaker  
Union Carbide Company  
Oak Ridge National Laboratory  
Y-12  
Oak Ridge, TN 37830

L. J. Anderson, B2402  
Dow Chemical Company  
Texas Division  
P.O. Drawer K  
Freeport, TX 77541

M. C. Jon  
Western Electric, ERC  
P.O. Box 900  
Princeton, NJ 08540

W. L. Pearl  
Nuclear Water & Waste Technology  
P.O. Box 6406  
San Jose, CA 95150

FOREIGN

P. Caussin  
Vincotte  
1640 Rhode-Saint-Genese  
Belgium

No. of  
Copies

W. G. Cunliffe  
Building 396  
British Nuclear Fuels Ltd.  
Springfields Works  
Salwick, Preston  
Lances. PR40XJ  
U.K.

ACE Sinclair  
Research Division  
Berkeley Nuclear Laboratories  
Berkeley  
Gloucestershire, GL 13 9 PB  
U.K.

Don Birchon  
Admiralty Materials Laboratory  
Holton Heath Poole  
Dorset, England  
020-122-2711

ONSITE

50 Pacific Northwest Laboratory

J. M. Alzheimer  
M. C. Bampton  
F. L. Becker  
T. D. Chikalla  
R. A. Clark  
E. L. Courtright  
M. E. Cunningham  
J. M. Cuta  
J. F. Dawson  
R. L. Dillon  
S. K. Edler (5)  
C. E. Elderkin  
J. E. Garnier  
R. L. Goodman  
C. R. Hann (3)  
A. J. Haverfield  
P. H. Hutton  
J. M. Kelly  
R. J. Kurtz  
P. T. Langsiedel  
D. D. Lanning  
R. P. Marshall  
C. L. Mohr



No. of  
Copies

W. C. Morgan  
C. J. Morris  
R. D. Nelson  
F. E. Panisko  
L. T. Pedersen  
G. J. Posakony  
E. B. Schwenk  
F. A. Simonen  
J. R. Skorpik  
A. M. Sutey  
M. J. Thurgood  
G. L. Tingey  
D. S. Trent  
C. L. Wheeler  
Technical Information (5)  
Publishing Coordination Y0(2)

<b>NRC FORM 335</b> (7-77)		<b>U.S. NUCLEAR REGULATORY COMMISSION</b> <b>BIBLIOGRAPHIC DATA SHEET</b>		1. REPORT NUMBER (Assigned by DDC) NUREG/CR-2127, Vol. 1 PNL-3801-1	
4. TITLE AND SUBTITLE (Add Volume No., if appropriate) Reactor Safety Research Programs Quarterly Report January - March 1981		2. (Leave blank)		3. RECIPIENT'S ACCESSION NO.	
7. AUTHOR(S) S.K. Edler, Ed.		5. DATE REPORT COMPLETED MONTH   YEAR May   1981		9. PERFORMING ORGANIZATION NAME AND MAILING ADDRESS (Include Zip Code) Pacific Northwest Laboratory Richland, WA 99352	
12. SPONSORING ORGANIZATION NAME AND MAILING ADDRESS (Include Zip Code) Division of Accident Evaluation Division of Engineering Technology Office of Nuclear Regulatory Research U.S. Nuclear Regulatory Commission Washington, DC 20555		6. (Leave blank)		10. PROJECT/TASK/WORK UNIT NO.	
13. TYPE OF REPORT Quarterly Report		11. CONTRACT NO. FINs B2101, B2088, B2289, B2043, B2383, B2084, B2372, B2084, B2041, B2277, B2097		8. (Leave blank)	
15. SUPPLEMENTARY NOTES		14. (Leave blank)		PERIOD COVERED (Inclusive dates) January - March 1981	
16. ABSTRACT (200 words or less) <p>           This document summarizes the work performed by Pacific Northwest Laboratory (PNL) from January 1 through March 31, 1981 for the U.S. Nuclear Regulatory Commission (NRC). Evaluations of nondestructive examination (NDE) techniques and instrumentation are reported; areas of investigation include demonstrating the feasibility of determining the strength of structural graphite, evaluating the feasibility of detecting and analyzing flaw growth in reactor pressure boundary systems, examining NDE reliability and probabilistic fracture mechanics, and assessing the integrity of pressurized water reactor (PWR) steam generator tubes where service-induced degradation has been indicated. Experimental data and analytical models are being provided to aid in decision-making regarding pipe-to-pipe impacts following postulated breaks in high-energy fluid system piping. Core thermal models are being developed to provide better digital codes to compute the behavior of full-scale reactor systems under postulated accident conditions. Fuel assemblies and analytical support are being provided for experimental programs at other facilities. These programs include loss-of-coolant accident (LOCA) simulation tests at the NRU reactor, Chalk River, Canada; fuel rod deformation, severe fuel damage, and postaccident coolability tests for the ESSOR reactor Super Sara Test Program, Ispra, Italy; the instrumented fuel assembly irradiation program at Halden, Norway; and experimental programs at the Power Burst Facility, Idaho National Engineering Laboratory (INEL). These programs will provide data for computer modeling of reactor system and fuel performance during various abnormal operating conditions.         </p>					
17. IDENTIFIERS/OPEN ENDED 1.					
18. AVAILABILITY STATEMENT Unlimited		19. SECURITY CLASS (This report) Unclassified		21. NO. OF PAGES	
		20. SECURITY CLASS (This page) Unclassified		22. PRICE \$	